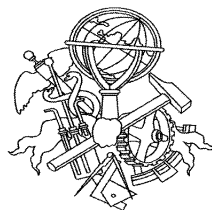


URUBU: ENERGY SCAVENGING IN WIRELESS SENSOR NETWORKS

Rui Filipe de Sá Ribeiro



Master degree in Electrical and Computer Engineering

Telecommunications

Electrical Engineering Department

Polytechnic Institute of Porto – School of Engineering

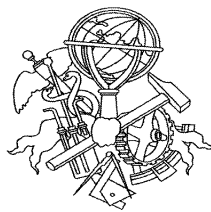
2010

A thesis submitted in partial fulfilment of the specified requirements for the degree of
Master in Electrical and Computer Engineering

Candidate: Rui Filipe de Sá Ribeiro, N° 1980168, 1980168@isep.ipp.pt

Supervisor: Mário Alves, mjf@isep.ipp.pt

Co-supervisor: Ricardo Gomes, rftg@isep.ipp.pt



Master degree in Electrical and Computer Engineering
Telecommunications

Electrical Engineering Department
Polytechnic Institute of Porto – School of Engineering
12 de Novembro de 2010

This thesis is dedicated to my beloved wife.

Andreia, thank you for your patience, support, and encouragement.

Acknowledgements

I would like to thank my supervisor, Mário Alves, for the opportunity he gave me to experience a little bit the excitement of research, and for his patience and words of encouragement during the course of this work. Special thanks goes to my co-supervisor, Ricardo Gomes, whose support and willingness to help were fundamental to finish this thesis.

I am ever grateful to my family for their constant love and confidence in me.

Abstract

For the past years wireless sensor networks (WSNs) have been coined as one of the most promising technologies for supporting a wide range of applications. However, outside the research community, few are the people who know what they are and what they can offer. Even fewer are the ones that have seen these networks used in real world applications. The main obstacle for the proliferation of these networks is energy, or the lack of it. Even though renewable energy sources are always present in the networks environment, designing devices that can efficiently scavenge that energy in order to sustain the operation of these networks is still an open challenge.

Energy scavenging, along with energy efficiency and energy conservation, are the current available means to sustain the operation of these networks, and can all be framed within the broader concept of “Energetic Sustainability”. A comprehensive study of the several issues related to the energetic sustainability of WSNs is presented in this thesis, with a special focus in today’s applicable energy harvesting techniques and devices, and in the energy consumption of commercially available WSN hardware platforms.

This work allows the understanding of the different energy concepts involving WSNs and the evaluation of the presented energy harvesting techniques for sustaining wireless sensor nodes. This survey is supported by a novel experimental analysis of the energy consumption of the most widespread commercially available WSN hardware platforms.

Keywords

Wireless Sensor Networks, Energetic Sustainability, Energy harvesting, Energy Consumption.

Resumo

Há já alguns anos que as redes de sensores sem fios (do Inglês Wireless Sensor Networks - WSNs) têm sido apontadas como uma das mais promissoras tecnologias de suporte a uma vasta gama de aplicações. No entanto, fora da comunidade científica, poucas são as pessoas que sabem o que elas são e o que têm para oferecer. Ainda menos são aquelas que já viram a sua utilização em aplicações do dia-a-dia. O principal obstáculo para a proliferação destas redes é a energia, ou a falta dela. Apesar da existência de fontes de energia renováveis no local de operação destas redes, continua a ser um desafio construir dispositivos capazes de aproveitar eficientemente essa energia para suportar a operação permanente das mesmas.

A colheita de energia juntamente com a eficiência energética e a conservação de energia, são os meios disponíveis actualmente que permitem a operação permanente destas redes e podem ser todos englobados no conceito mais amplo de “Sustentabilidade Energética”. Esta tese apresenta um estudo extensivo das várias questões relacionadas com a sustentabilidade energética das redes de sensores sem fios, com especial foco nas tecnologias e dispositivos explorados actualmente na colheita de energia e no consumo energético de algumas plataformas comerciais de redes de sensores sem fios.

Este trabalho permite compreender os diferentes conceitos energéticos relacionados com as redes de sensores sem fios e avaliar a capacidade das tecnologias apresentadas em suportar a operação permanente das redes sem fios. Este estudo é suportado por uma inovadora análise experimental do consumo energético de algumas das mais difundidas plataformas comerciais de redes de sensores sem fios.

Palavras-chave

Wireless Sensor Networks, Energetic Sustainability, Energy harvesting, Energy Consumption.

Index

ACKNOWLEDGEMENTS	I
ABSTRACT	III
RESUMO.....	V
INDEX	VII
FIGURES INDEX.....	IX
TABLES INDEX.....	XIII
ACRONYMS.....	15
1. INTRODUCTION	17
1.1. CONTEXT AND MOTIVATION	17
1.2. OBJECTIVE	19
1.3. CONTRIBUTIONS	19
1.4. STRUCTURE	20
2. ENERGETIC SUSTAINABILITY IN WSNS	21
2.1. “EFFICIENCY + CONSERVATION + SCAVENGING = SUSTAINABILITY”	21
2.2. A SNAPSHOT ON ENERGY SCAVENGING	23
3. PHOTONIC ENERGY.....	27
3.1. INTRODUCTION	27
3.2. SOLAR CELL STRUCTURE	28
3.3. SOLAR CELL OPERATION	30
3.4. SOLAR CELL MATERIALS AND EFFICIENCIES	32
3.5. SOLAR CELL CHARACTERISTICS	34
3.6. MAXIMUM POWER POINT TRACKING.....	36
3.6.1. <i>Measurement method for MPPT</i>	37
3.6.2. <i>Software vs. hardware mppt controller</i>	37
3.6.3. <i>Some literature examples</i>	38
4. KINETIC ENERGY	41
4.1. INTRODUCTION	41
4.2. ELECTROMAGNETIC TRANSDUCTION	44
4.2.1. <i>Operating principle</i>	44
4.2.2. <i>Types of microscale magnetic generators</i>	45
4.2.3. <i>Examples and application of magnetic generators</i>	46
4.3. ELECTROSTATIC TRANSDUCTION.....	49

4.3.1. <i>Operating principle</i>	49
4.3.2. <i>Types of micromachined electrostatic generators</i>	54
4.3.3. <i>Examples and application of electrostatic generators</i>	55
4.4. PIEZOELECTRIC TRANSDUCTION	57
4.4.1. <i>Piezoelectricity</i>	57
4.4.2. <i>Operating modes</i>	59
4.4.3. <i>Cantilever unimorph and bimorph</i>	60
4.4.4. <i>Examples and application of piezoelectric generators</i>	61
4.5. SUMMARY	64
5. THERMAL DIFFERENTIALS	67
5.1. INTRODUCTION	67
5.2. OPERATING PRINCIPLE	68
5.3. THERMAL CONVERSION EFFICIENCY	71
5.4. EXAMPLES AND APPLICATION OF THERMOELECTRIC GENERATORS	72
6. ENERGY CONSUMPTION OF COMMERCIAL HARDWARE PLATFORMS	77
6.1. INTRODUCTION	77
6.2. MEASUREMENT SETUP	78
6.3. HARDWARE AND SOFTWARE	80
6.3.1. <i>Hardware platforms under test</i>	80
6.3.2. <i>Operating system and programming language</i>	81
6.4. EXPERIMENTAL ANALYSIS	82
6.4.1. <i>Booting</i>	83
6.4.2. <i>Low power modes</i>	84
6.4.3. <i>LEDs test</i>	89
6.4.4. <i>Transmitting and receiving</i>	90
6.4.5. <i>Summary</i>	95
7. CONCLUSIONS AND FUTURE WORK	97
REFERENCES	99
APPENDIX A. TECHNICAL REPORT	109

Figures Index

Figure 1	Taxonomy of approaches to achieve energetic sustainability of WSNs.....	23
Figure 2	Essential features of simple solar cell structure.....	29
Figure 3	Essential features of a TFSC. [30].....	32
Figure 4	A multijunction device is a stack of individual single-junction cells in descending order of band gap [31]......	33
Figure 5	Current–voltage behavior of silicon photovoltaic cells with and without incident radiation [13]. As the cell temperature rises, I_{sc} increases and V_{oc} decreases, leading to a net decrease in output power	35
Figure 6	Operating point of a solar cell when connected to a load resistance (RL). V_p represents the operating voltage, I_p the operating current, and P_{max} the MPP [33].	36
Figure 7	Solar module characteristics of three cells in series [28].	39
Figure 8	Solar cell module used in the ZebraNet project [28].	40
Figure 9	MPPT of the AmbiMax platform using a switching regulator and comparator [25].	40
Figure 10	Generic model of – (a) direct-force generator and (b) inertial generator [16]. ..	42
Figure 11	An inertial electromechanical generator [50].	44
Figure 12	Three different types of PM power generation technologies: (a) rotational device driven by continuous rotational power, (b) oscillatory device driven in resonance by forced vibration, and (c) hybrid device that converts linear vibrations into rotational motion [46].	46
Figure 13	Exploded view of Seiko Kinetic watch. Image adapted from the operational instructions of the Seiko Kinetic watch.....	47
Figure 14	Electromagnetic generators proposed by: (a) Williams et al [52][53], and (b) Li et al [54][55].	48
Figure 15	Cantilever beam designs using a four-pole configuration from (a) Glynne-Jones et al [57], and (b) Torah et al [59].	49
Figure 16	QV diagram that describes (a) the charge-constrained cycle, and (b) the voltage-constrained cycle [60].	50
Figure 17	Energy cycles compared [60].	53
Figure 18	Three basic topologies for micromachined variable capacitors: (a) in-plane overlap varying, (b) in-plane gap closing, (c) out-of-plane gap closing [47]. ..	54
Figure 19	Examples of micromachined electrostatic generators. (a) In-plane overlap varying [63]; (b) In-plane gap closing [47].	55

Figure 20	On the left the fundamental structure of a honeycomb-type variable capacitor (capacitance decreases with expansion and increases with compression). On the right a detail of a unit cell from the honeycomb structure. Images adapted from [65].	56
Figure 21	Polarizing (poling) a piezoelectric ceramic. (a) Random orientation of electric dipoles prior to polarization; (b) Polarization in DC electric field; (c) Remanent polarization after electric field removed [68].	58
Figure 22	Illustration of 33 and 31 mode operation for piezoelectric materials [44].	59
Figure 23	(a) Schematic of a piezoelectric unimorph [71]; (b) Operation of a piezoelectric bimorph poled for series operation [72].	61
Figure 24	(a) Small bimorph cantilever generator with a 1,5 cm length constraint [72]; (b) Integrated piezoelectric vibration energy harvester and wireless temperature and humidity sensing node [78].	63
Figure 25	Schematic of a thermoelectric generator with an enlarge detail of a thermocouple [84].	69
Figure 26	Seiko Thermic, a wristwatch powered by body heat using a thermoelectric generator (Copyright by Seiko Instruments Incorporated). Cross-sectional diagram [84].	72
Figure 27	Construction of the LPTG in principle and the Thermo Life® button-type LPTG next to a penny. Image adapted from [90].	73
Figure 28	On the left the MPG-D651 and MPG-D751 proposed by Micropelt. On the right detailed view of a 2,5 mm x 2,5 mm wafer containing 578 thermoelectric couples [93].	74
Figure 29	On the left the eTEG HV14 commercialized by Nextreme Thermal Solutions [96]. On the center a photo of the surface micromachined poly-SiGe thermopile chips and on the right a photo of a wearable TEG [98].	75
Figure 30	Schematic and picture of the measurement setup	79
Figure 31	Synchronizing task execution with data collection when the chosen platform is: a) receiving a message; b) turning on a LED; c) booting.	80
Figure 32	nesC Active Message interface.	82
Figure 33	Booting implementation	83
Figure 34	Traces of current consumption for each platform when booting	84
Figure 35	<i>SleepNoInterrupt</i> implementation	85
Figure 36	Implementation of the <i>SleepPeriodicInterrupt</i> application	86
Figure 37	Traces obtained for TelosB and MicaZ for the <i>SleepPeriodicInterrupt</i> application	87
Figure 38	<i>LEDTest</i> implementation	89
Figure 39	Implementation of the <i>RadioInit</i> application	90
Figure 40	Traces of the current consumed by each of the sensor nodes when initializing the radio	91

Figure 41	Structure of the common message buffer abstraction called <i>message_t</i>	92
Figure 42	Structure used to hold the node identification and the counter value	93
Figure 43	Implementation of the <i>RadioSend</i> application	93
Figure 44	CFLAGS used to set the transmission power for different platforms.....	94
Figure 45	The <i>setRFPower</i> command for Mica2	94
Figure 46	Implementation of the <i>Receive.receive</i> event.....	95

Tables Index

Table 1	WSN hardware platforms used in the measurements	81
Table 2	Energy spent by each sensor node to boot	84
Table 3	Average power consumed by each sensor node when sleeping without the use of any timer.....	85
Table 4	Values obtained for each platform when sleeping with the use of a timer	87
Table 5	Energy increase in the energy consumption of the platforms when in a sleep state due to the use of a timer ($t = 3600$ s and $T_{tmr} = 60$ s)	88
Table 6	Consumption for each sensor node with each LED on	89
Table 7	Energy consumed by each sensor node for initializing the radio	91
Table 8	Energy consumed by each sensor node for sending a message	94
Table 9	Energy consumed by each sensor node for receiving a message.....	95
Table 10	Summary of the energy measurements for each sensor node	95
Table 11	Total energy consumption of each sensor node in a simple scenario	96

Acronyms

AC	–	Alternating Current
COTS	–	Commercial off-the-shelf
CPU	–	Central Processing Unit
DC	–	Direct Current
DSC	–	Dye-sensitized Solar Cell
DSP	–	Digital Signal Processor
LED	–	Light Emitting Diode
MAC	–	Medium Access Control
MCU	–	Microcontroller Unit
MEMS	–	Microelectromechanical systems
MPP	–	Maximum Power Point
MPPT	–	Maximum Power Point Tracking
OS	–	Operating system
RF	–	Radio Frequency
TEG	–	Thermoelectric Generator
TFSC	–	Thin Film Solar Cell
WSN	–	Wireless Sensor Network

1. INTRODUCTION

1.1. CONTEXT AND MOTIVATION

A Wireless Sensor Network (WSN) can be described as a collection of spatially distributed nodes organized into a cooperative network [1]. Each of these nodes can sense, measure, and gather information from the environment and, based on some local decision process, they can transmit the sensed data to the user. The advances in Micro-Electro-Mechanical Systems (MEMS) technology, wireless communications, and digital electronics have facilitated the development of small, low-power, multifunctional WSN platforms, labeled by some authors as “smart sensor nodes”. These sensor nodes¹ are in general equipped with one or more sensors (e.g. mechanical, thermal, biological), a microprocessor, memory, a power supply, a radio and one or more actuators [2].

A WSN typically has little or no infrastructure and is composed of possibly a large number of sensor nodes deployed in any given region of interest in order to monitor physical phenomena such as temperature, humidity, vibration, motion, and others. The data

¹ For simplicity, the term "sensor node" will be used in the context of this work to refer to a wireless sensor network platform.

gathered by each node is forwarded, probably via multiple hops, relaying to a sink (sometimes denoted as base station) that can use it locally or is connected to other networks (e.g. internet) through a gateway. Initially developed and used for military purposes, WSNs are currently recognized as one of the key technologies of the XXI century and are emerging in areas such as global scale environmental monitoring, precision agriculture, home and assisted living, medical care, smart buildings and cities, and industrial automation [3].

WSNs are commonly related to other terms such as networked embedded systems, and ubiquitous and pervasive computing. Terminology is very important, but it can also be confusing. Although these terms are all highly related each of them is represented by different research communities with different emphasis. Networked embedded systems emphasize form factor, cost and other constraints. Ubiquitous and pervasive computing emphasizes computation, while WSNs emphasize communications and sensing. In the future these fields will increasingly overlap, taking properties from each other and leading to the progression of WSNs from mostly passive sensing to sensing, actuation, and increased computation [4]. These networks are sometimes referred as WSANs (wireless sensor and actuator networks) as they can not only sense the environment but also act on it, enabling interaction between people or computers and the surrounding environment.

At present, WSNs face several design and resource constraints that include for example short communication range, low bandwidth, and limited processing and data storage capabilities. Most constraints (if not all) are correlated with the limited amount of available energy. The most common energy source used by sensor nodes consists of a battery, which is usually the largest contributor to the sensor node in terms of both dimensions, weight and maintenance costs. To reduce both dimensions and weight, batteries are kept as small as possible. However, without energy, a sensor node is useless and cannot contribute to the utility of the network as a whole. In other words, the lifetime of WSNs is limited by the energy budget of their nodes [5].

In a battery-powered sensor node, typical power management design goals are to minimize the energy consumption or to maximize the lifetime achieved while meeting the required performance constraints [6]. For some applications, a limited lifetime is sufficient and battery power is the logical choice. On the other hand, emerging applications like for example long-term structural health monitoring of civil engineering infrastructures (e.g.

buildings, bridges and tunnels), require sensor nodes to operate for years or even decades after they are deployed. Moreover, in such scenarios it is impossible or unaffordable to replace or recharge batteries. Therefore, the crucial question still is “how to prolong the network lifetime to such a long time?” [7].

Exploiting renewable energy resources in the sensor nodes environment offers an energy source limited only by the nodes physical survival. A key distinction of this energy from that stored in a battery is that this one is potentially infinite, though there may be a limit on the rate at which it can be used [6]. While the use of renewable energy to generate electricity is not new (e.g. solar, wind, water, and thermal), existing systems are unsuitable for WSNs. There are complex tradeoffs to be considered when designing energy scavenging devices for WSNs arising from the interaction of various factors like the characteristics of the energy sources and energy storage devices (if any), the system energy consumption, the application behavior, etc. Additionally, the energy-scavenging device should be comparable in size (i.e. small enough) with the sensor nodes [8].

1.2. OBJECTIVE

The large reductions in energy consumption achieved in electronics, along with the eagerness to eliminate the need of batteries to power mobile and other autonomous devices are continuously increasing the attractiveness of scavenging techniques. *The goal of the work presented in this Thesis is to present a comprehensive study of the several issues related to energetic sustainability in the scope of WSNs, specially focusing in applicable energy scavenging techniques and devices, and energy consumption of commercial off-the-shelf (COTS) wireless sensor nodes. In summary, provide a baseline of knowledge to answer the question “are current energy scavenging technologies able to sustain the operation of current wireless sensor nodes?”.*

1.3. CONTRIBUTIONS

The work carried out in the context of this thesis lead to the co-authorship of a Technical Report published by the CISTER Research Unit, where the author of this thesis contributed to sections 2.7, 3.7 and 4.7. This Technical Report is presented in Appendix A.

Importantly, the experimental study on the energy consumption of popular hardware platforms is being used for updating the OPNET simulation model of the IEEE 802.15.4

protocol. This model, available as an open-source at <http://www.open-ZB.net> is being used worldwide both by academics and companies. This work will enable to achieve more realistic simulations results, resulting from more accurate energy consumption models.

1.4. STRUCTURE

The remainder of this Thesis is structured as follows:

- Section 2 introduces the concept of “Energetic Sustainability” and presents several terms regarding energy and their role in the pursue of long-lasting operation in WSNs;
- Sections 3 to 5 introduce the fundamentals of several energy scavenging techniques that transform light, kinetic and thermal energy ubiquitously available in environment into electrical energy;
- Section 6 presents a study regarding the overall energy consumption of a set of WSN hardware platforms, that represent the most widespread COTS chipsets, when performing pre-established common tasks, like sleeping or transmitting data;
- Section 7 presents the main conclusions regarding energy scavenging in WSNs. Finally, the major contributions of this Thesis and the related future work are discussed.

2. ENERGETIC SUSTAINABILITY IN WSNs

2.1. “EFFICIENCY + CONSERVATION + SCAVENGING = SUSTAINABILITY”

Particularly in larger-scale WSNs, most of the sensor nodes must be energetically self-sustainable, as maintenance actions, such as battery recharge/replacement, may not be feasible or at least not convenient. Current sensor nodes rely on small batteries with a very restricted energy budget. Moreover, batteries with reasonable form factor and cost do not yield the lifetime required by most applications, despite recent technological advances [9].

Energy efficiency has been a major focus of research since the dawn of the WSN paradigm and witnessed significant advancements over the last decade. **Energy efficiency** can be defined as the ratio of the amount of work done to the amount of energy consumed. Thus, using less energy to perform the same amount of work or performing more work from the same energy input can be defined as an efficiency gain.

Efficiency is one way of reducing the energy consumption of sensor nodes. Another way is to use several different techniques proposed in literature to maximize the lifetime of battery-powered wireless sensor nodes. These techniques aim at **energy conservation**, which can be defined as reducing energy consumption through a reduction in the amount

of work done. Conservation schemes leave the ratio of the amount of work done to the amount of energy consumed unchanged and so they do not affect efficiency.

In [7] the authors identify three main enabling techniques used for energy conservation in wireless sensor networks: duty cycling, data driven, and mobility. The design principles behind them and their features are presented in the referred survey, however for a complete set of networking protocols the reader is referred to [3]. While all these techniques optimize and adapt energy usage to maximize the lifetime of energy reservoirs, the lifetime remains bounded and finite.

Efficiency and conservation techniques, even in combination, can prolong the lifetime of a WSN system, but cannot turn it “perpetual”. To realize such WSNs, it is crucial to collect energy from the surrounding environment in order to supplement or even replace batteries [10]. The process of extracting energy from the surrounding environment and converting it into consumable electrical energy is generally known as **energy scavenging** or **energy harvesting**. For the purpose of this work both terms will be used interchangeably. Energy harvesting, along with energy efficiency and energy conservation, are the current available means to enable sensor nodes self-sustainability and achieve perpetual WSNs, and can all be framed within the broader concept of “Energetic Sustainability” [11].

A systematic and comprehensive taxonomy of the energetic sustainability techniques is presented in Figure 1, which are subsequently discussed in depth in the remainder of this thesis.

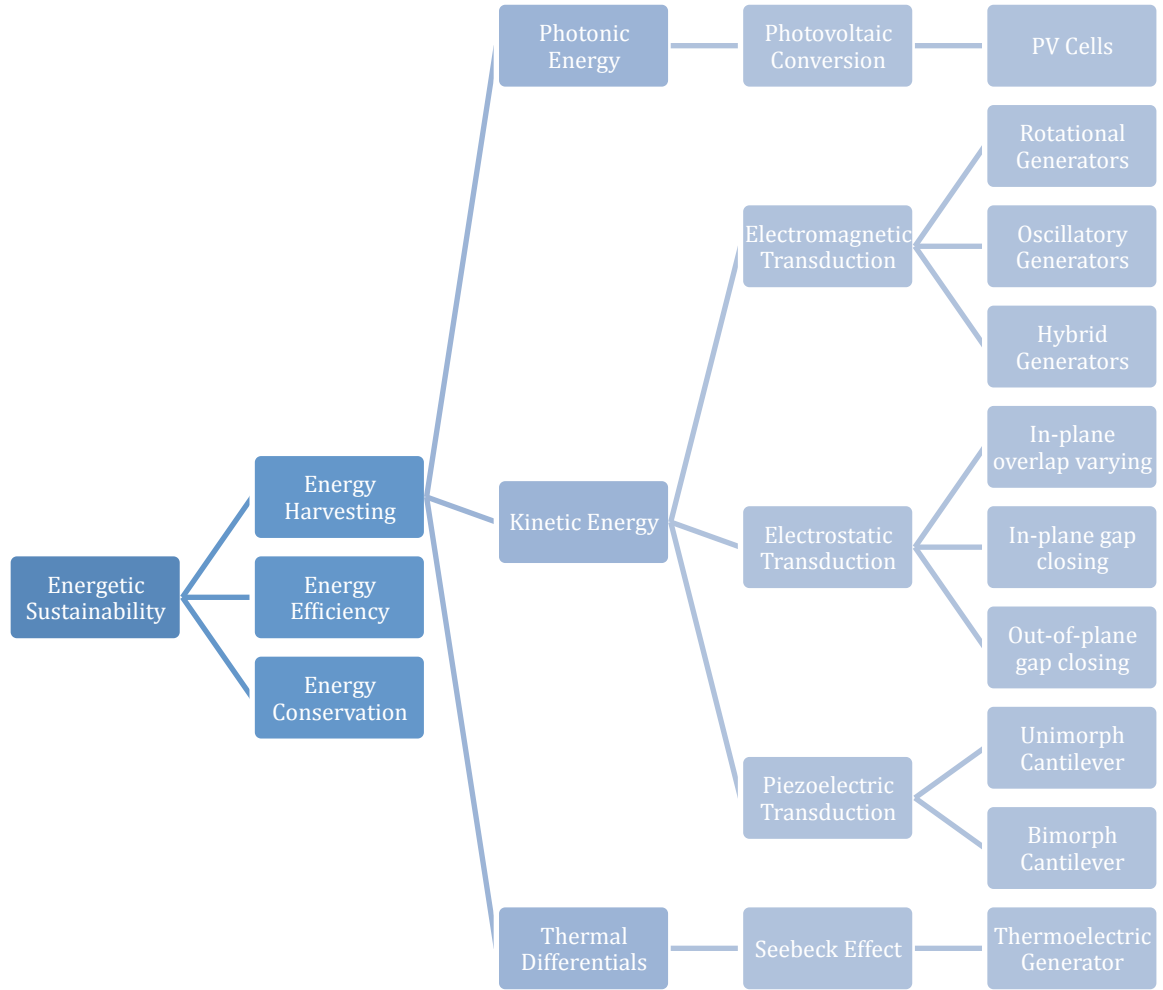


Figure 1 Taxonomy of approaches to achieve energetic sustainability of WSNs.

2.2. A SNAPSHOT ON ENERGY SCAVENGING

A comprehensive review of the many possible sources of energy that could potentially be scavenged is given in [12]. Among the currently most feasible are photonic, kinetic and thermal differentials. Solar-energy harvesting is based on the well-known principle of photovoltaic conversion, which provides high power densities, making it the best-suited choice to power wireless outdoors applications [13]. Solutions to power wireless indoor applications have also been implemented [14][15] revealing several weaknesses that dictate the need for further research on this area.

Kinetic energy from vibrations or movements is present almost everywhere and it can be transformed into useful electrical energy by any kind of electromechanical transduction. Electromagnetic, electrostatic, and piezoelectric devices have been widely investigated and several companies now offer commercially miniature mechanical harvesters delivering sufficient power for sensor nodes operating in an industrial environment [16]. However, researchers have not yet overcome difficulties encountered for body-powered applications [17] (particularly body sensor networks), which demand for true MEMS devices.

Temperature differences between various objects (in natural and industrial environments) are also freely available. Manufacturing applications, where heat is a by-product of the manufacturing process, are typically ideal applications for thermal energy harvesting. A few companies are already commercializing thermoelectric generators that can exploit those scenarios. Despite their low efficiency, due to their reliability and absence of moving parts (compared with other types of generators), there has been a growing interest in the generation of power from body heat [18], as a mean to power wearable devices. In spite of that, further researches are needed on nanostructured materials and multilayer arrangements, in order to optimize thermoelectric properties, as well as on miniaturization using micromachining [19].

The need for multiple power sources is mentioned in [20] and a well successful approach is exploited in the multi-powered platform for precision agriculture proposed in [21]. In the cited example, besides a solar panel and a wind turbine, a small size hydrogenerator has been introduced as a way to harvest the energy of water-flow in irrigation pipes.

Energy sources are ubiquitous in the environment [10], so it is reasonable to consider that the energy required to permanently operate a WSN can be obtained through energy harvesting. There are currently several methods to collect energy from some of those sources. Nevertheless, some others are neglected, mostly due to challenges raised by the low energy density or today's feasibility of the energy harvesting method (*e.g.*, ambient RF energy [22][23] or ambient air-flow energy [24]). All those sources have in common their random nature, a characteristic that still dictates the undesirable use of energy reservoirs, typically rechargeable batteries or, more recently, ultracapacitors [25]. As a consequence, several approaches have to be exploited simultaneously, so that a system continues to operate perennially.

As the power levels achieved by miniature harvesters are usually low, sensor nodes should be prepared to harvest energy from all the available energy sources surrounding it, in order to suffice its power requirements. Moreover, in contrast to approaches that only attempt to minimize the energy consumption of each sensor node, software (*e.g.*, algorithms, protocols) design must also concern on adapting node-level system parameters (*e.g.*, duty-cycling, transmission power, sensing reliability, etc) such that the energetic sustainability of the sensor node is maintained [26].

Finally, another important issue is that sensor nodes deployed in different places will probably have different harvesting opportunities. This means that it is absolutely necessary to align the workload allocation with the energy availability of each individual node [6]. For that, network solutions and protocols, at MAC and routing level, will have to be redesigned so they can deal with such changeable nodes and maintain the desired quality of service (QoS).

Based on the above remarks it is clear that further enhancements still have to be done, especially regarding energy harvesting, to accomplish perpetual operation in WSNs.

3. PHOTONIC ENERGY

3.1. INTRODUCTION

Light energy harvesting is a relatively mature technology and photonic energy (photon radiation) is readily available outdoors and in artificially lighted indoor locations. Photonic energy can be converted directly to electricity using photovoltaic (PV) cells made from semiconductor materials.

A PV cell or solar cell is a device that converts light energy into electrical energy. Some authors employ the term “solar cell” when referring to devices intended specifically to capture energy from sunlight, while the term “PV cell” is used when the light source is unspecified. In the context of this work, such distinction is not made and both terms apply to any type of light source.

Fundamentally, solar cells are quite simple devices that need to fulfill only two functions: photogeneration of charge carriers (electrons and holes) in a light-absorbing material, and separation of the charge carriers to a conductive contact that will conduct the electric energy (simply put carrying electrons off through a metal contact into a wire or other circuit). This conversion is called the PV effect, and the field of research related to solar cells is known as photovoltaics [27].

Solar cells can be used in many individual ways. They have long been used in situations where electrical energy from the grid is unavailable, such as in remote area energy systems, Earth orbiting satellites and space probes. More recently, solar powered remote fixed devices have seen increasing use in locations where significant connection cost makes grid energy usage prohibitively expensive, or at least less cost-effective. Such applications include parking meters, emergency telephones, traffic signs, remote guard posts and signals, among others. Even so, the majority of solar modules are used today for grid connected energy generation.

Compared to those well-studied macro-solar systems, solar energy harvesting for micro-solar systems is much more constrained in energy budget and energy use, and is still under active research. Typical WSNs applications using solar energy as a energy source are focussed in the outdoor environment, where the variation of the ambient light energy source is regular and relatively predictable. Examples of this kind of applications are the Princeton ZebraNet Project [28] designed for wildlife tracking and the MPWiNodeX platform [21] designed for precision agriculture.

As for indoor applications, it is important to note that indoor light energy has limited overall energy irradiance (usually less than 1 mWcm^{-2}) compared to outdoor light energy (10 to 100 mWcm^{-2}). Since the conversion efficiency of the solar panel also decreases with decreasing irradiance in low illuminance level, this results in an even lower converted energy. Nevertheless, recent studies [14][15] indicate the feasibility of indoor light energy harvesting for WSN applications.

While the price of solar cells continues to fall, mostly due to government incentives for clean energy technologies and policies to reduce greenhouse gases emissions, solar energy harvesting becomes a real possibility not only for sensor nodes but also for consumer products, such as electronic toys, portable radios, battery chargers and cell phones. Solar cells used in these kinds of devices may utilize artificial light (e.g. from incandescent and fluorescent lamps) as well as sunlight to assist, recharge, or replace batteries.

3.2. SOLAR CELL STRUCTURE

Solar cells, whether used in a central power station, a satellite, or a sensor node, have the same basic structure (see Figure 2). Light enters the device through an optical coating, or antireflection layer that minimizes the loss of light by reflection. This layer effectively

traps the light falling on the solar cell by promoting its transmission to the energy-conversion layers below. The antireflection layer is typically an oxide of silicon, tantalum, or titanium that is formed on the cell surface by spin coating or a vacuum deposition techniques.

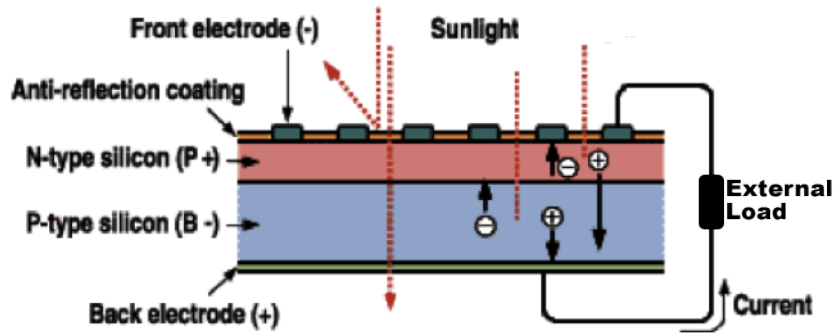


Figure 2 Essential features of simple solar cell structure.

Below the antireflection layer are the energy-conversion layers, which constitute the core of the device. Two additional electrical contact layers are needed to allow electric current to flow out to an external load and back into the cell, thus completing an electric circuit. The electrical contact layer on the face of the cell where light enters is generally present in some grid pattern and is composed of a good conductor such as a metal. Since metal blocks light, the grid lines are as thin and widely spaced as possible without impairing collection of the current produced by the cell. The back electrical contact layer has no such diametrically opposed restrictions. It simply needs to function as an electrical contact and thus usually covers the entire back surface of the solar cell structure. Because the back layer must also be a very good electrical conductor, it is always made of metal.

All electromagnetic radiation is composed of particles called photons, which carry specific amounts of energy determined by the spectral properties of their source. As most of the energy in sunlight is in the visible and infrared range, a solar cell absorber should be efficient in absorbing radiation at those wavelengths. Materials that strongly absorb visible radiation belong to a class of substances known as semiconductors. Semiconductors in thicknesses of about 100 micron or less can absorb all incident visible light; since the junction-forming and contact layers are much thinner, the thickness of a solar cell is essentially that of the absorber. Examples of semiconductor materials employed in solar

cells include silicon (Si), gallium arsenide (GaAs), indium phosphide (InP), and copper indium selenide (CuInSe₂ or CIS).

3.3. SOLAR CELL OPERATION

All solar cells work in essentially the same way. They contain a junction between two different materials across which there is a ‘built-in’ electric field. When the cell absorbs light, mobile electrons and holes are created. These flow in opposite directions across the junction. In this way the flow of absorbed photons is converted into a flow of direct current (DC) power from the illuminated cell.

The crystalline silicon cell has a simple junction structure (previously presented in Figure 2), and provides a good model in which to explore the PV effect. The energy-conversion layers of this type of cell are made up of a thin wafer of silicon pn-junction. The n-type silicon at the top (the n-side) is created by doping² the silicon with phosphorous atoms (i.e. adding a small amount of phosphorous atoms to the silicon). The thickness of the n-side is about 0,5 micron for a conventional solar cell. The p-type silicon at the bottom (the p-side) is created by doping the silicon with boron atoms and its thickness is about 100 – 300 microns for a conventional silicon solar cell.

A space-charge region with a built-in electric field develops at the interface where the n-type and p-type materials meet. The direction of the built-in electric field is from the n-side to the p-side. The development of such a built-in electric field is characteristic of a pn-junction, which is important for the performance of the solar cell.

The back metal contact covers the whole area of the bottom of the pn-junction. Some solar cells are designed such that the back metal contact reflects the solar radiation that has passed right through the pn-junction back into it for a further chance of absorption. The front and back metal contacts connect the solar cell to an external circuit.

² Doping is the process of intentionally introducing impurities into an extremely pure (also referred to as intrinsic) semiconductor to change its electrical properties. The impurities are dependent upon the type of semiconductor.

In the operation of the solar cell, light enters the pn-junction and is absorbed by the silicon atoms. Some electrons take up enough energy to leave the atoms and become mobile electrons. When an electron leaves the atom, a vacancy (called a hole) is created in the atom's electron site. As the atom is then missing an electron, it carries a net positive charge. Under the influence of the built in electric field, the electron, being negatively charged, will move in the direction opposite to that of the electric field. As the electric field points to the p-side, the electron moves towards the n-side.

On the other hand, the positively charged hole attracts the electron from a surrounding atom to fill up the vacancy. The electrons on the p-side are preferentially attracted to the positive ion (hole) because of the influence of the built-in electric field. So the hole appears to move towards the p-side. As a result, the electrons and the holes drift in opposite directions.

The drifting of the holes towards the p-side and the drifting of the electrons towards the n-side separate the charges. As the negative free electrons and the positive ions (holes) are at different sides of the pn-junction, a potential difference is set up between the two sides of the junction with the free electrons on the n-side and the positive ions (holes) on the p-side. Due to this potential difference, electrons leave the pn-junction and enter the external circuit at the front contact, and enter the pn-junction from the external circuit at the back contact to neutralize the hole. A current is created and the electrical energy is delivered to the external circuit.

From an electrical point of view, all solar cells look pretty much the same: a light-controlled current source in parallel with a diode. Output current is a function of the physical size and conversion efficiency of the cell. Output voltage per cell is essentially one diode drop, roughly 0,5 to 0,6 V. Higher voltage cells are composed of stacks of series cells.

A number of solar cells electrically connected to each other and mounted in a support structure or frame is called a PV module. Modules are design to supply electricity at a certain voltage and can be wired together to form an array. In general, the larger the area of a module or array the more electrical energy will be produced. Modules and arrays can be connected in both series and parallel electrical arrangements to produce any required voltage and current combination.

3.4. SOLAR CELL MATERIALS AND EFFICIENCIES

Today's most common PV devices use a single junction, or interface, to create an electric field within a semiconductor such as a solar cell. In a single band gap solar cell, efficiency is limited due to the inability to efficiently convert the broad range of energy that photons possess in the solar spectrum. Photons below the band gap of the cell material are lost; they either pass through the cell or are converted to only heat within the material. Energy in the photons above the band gap energy is also lost, since only the energy necessary to generate the hole-electron pair is utilized, and the remaining energy is converted into heat.

The most common material used in these first generation cells is crystalline silicon (c-Si), also called wafer silicon. It's a material consisting of one (single crystal) or multiple (multicrystalline) small silicon crystals. Single junction silicon devices are approaching the theoretical limiting efficiency of 31% [29]. Second generation materials have been developed to address energy requirements and production costs of solar cells. A Thin-Film Solar Cell (TFSC) is a solar cell that is made by depositing one or more thin layers of PV material on a substrate such as glass or ceramics (Figure 3).

Polycrystalline thin-film cells are made of many tiny crystalline grains of semiconductor materials. The materials used in these cells have properties that are different from those of silicon. As a result, it seems to work better to create the electric field with an interface between two different semiconductor materials. This type of interface is called a heterojunction because it is formed from two different materials, in comparison to the single junction formed by two doped layers of the same material, such as the one in silicon solar cells.

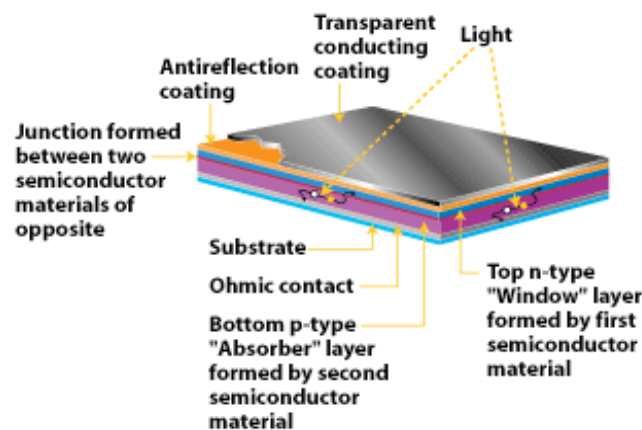


Figure 3 Essential features of a TFSC. [30]

The typical polycrystalline thin film has a very thin (less than 0,1 micron) layer on top called the "window" layer. The window layer's role is to absorb light energy from only the high-energy end of the spectrum. It must be thin enough and have a wide enough band gap (2,8 eV or more) to let all available light through the interface (heterojunction) to the absorbing layer. The absorbing layer under the window, usually doped p-type must have a high absorptivity (i.e. the ability to absorb photons) for high current and a suitable band gap to provide a good voltage. Still, it is typically just 1 to 2 microns thick.

The most successful second-generation materials have been cadmium telluride (CdTe), copper indium gallium selenide (CIGS), and thin-film silicon (TF-Si), which uses amorphous (a-Si or a-Si:H), protocrystalline, nanocrystalline (nc-Si or nc-Si:H) or black silicon. Dye-sensitized solar cell (DSC) and Organic solar cell are still in the development or pilot-plant phase. Solar cells made from these materials tend to have lower energy conversion efficiency than crystalline silicon, but are also less expensive to produce.

Third generation technologies aim to enhance poor electrical performance of thin-film technologies while maintaining very low production costs. One approach to achieve high efficiencies is the use of multijunction devices. This structure, also called a cascade or tandem cell, can achieve higher total conversion efficiency by capturing a larger portion of the solar spectrum.

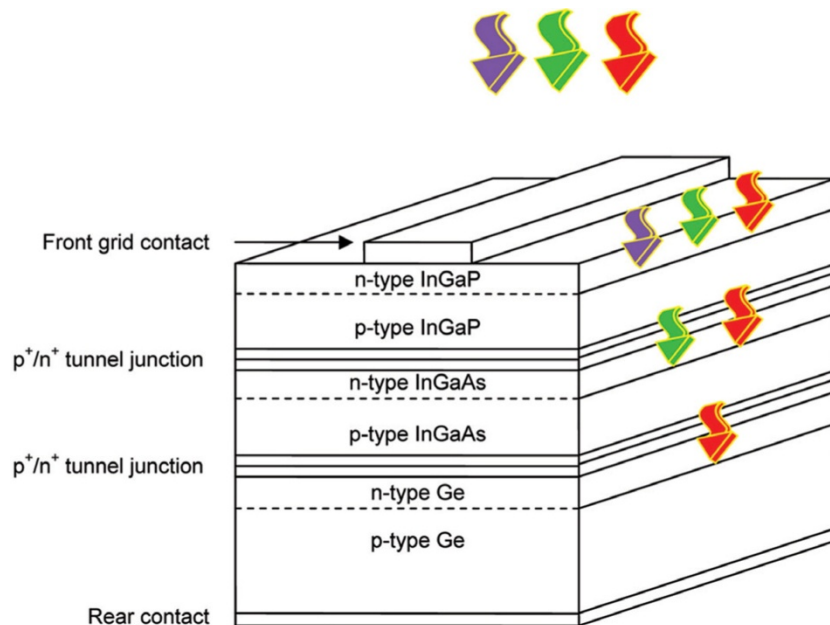


Figure 4 A multijunction device is a stack of individual single-junction cells in descending order of band gap [31].

In the typical multijunction cell, individual cells with different band gaps are stacked on top of one another. The individual cells are stacked in such a way that sunlight falls first on the material having the largest band gap (see Figure 4). Photons not absorbed in the first cell are transmitted to the second cell, which then absorbs the higher-energy portion of the remaining solar radiation while remaining transparent to the lower-energy photons. These selective absorption processes continue through to the final cell, which has the smallest band gap.

A multijunction cell can be made in two different ways. In the mechanical stack approach, two individual solar cells are made independently, one with a high band gap and one with a lower band gap. Then the two cells are mechanically stacked, one on top of the other. In the monolithic approach, one complete solar cell is made first, and then the layers for the second cell are grown or deposited directly on the first. Much of today's research in multijunction cells focuses on gallium arsenide (GaAs) as one (or all) of the component cells. Other materials studied for multijunction devices are amorphous silicon and copper indium diselenide.

Other approaches for achieving high efficiencies include modifying incident spectrum (concentrator systems or up/down converters), the use of excess thermal generation caused by ultraviolet (UV) light to enhance voltage or carrier collection (hot carrier cells), and the use of the infrared spectrum for nighttime operation (nantennas) [31] [32].

3.5. SOLAR CELL CHARACTERISTICS

The output characteristics of solar cells are expressed in the form of a current-voltage (I-V) curve and, in particular, three points: the open-circuit voltage (V_{oc}), the short-circuit current (I_{sc}) also known as the short circuit voltage, and its maximum power point (MPP).

The I_{sc} corresponds to the short circuit condition when the impedance is low and the voltage equals zero. I_{sc} occurs at the beginning of the forward-bias sweep and is the maximum current value in the power quadrant. For an ideal cell, this maximum current value is the total current produced in the solar cell by photon excitation. The V_{oc} occurs when there is no current passing through the cell. V_{oc} is also the maximum voltage difference across the cell for a forward-bias sweep in the power quadrant.

The power produced by the cell in Watt can be easily calculated along the I-V curve by the equation $P = I \cdot V$. At the I_{sc} and V_{oc} points, the power will be zero and the maximum value for power (i.e. MPP) will occur between the two. This point is shown as P_{max} in Figure 5, where a typical I-V curve for pn-type solar cells is represented. These three defining characteristics of a solar cell are used to define the fill factor, FF [13]:

$$FF = \frac{P_{max}}{I_{sc} \cdot V_{oc}} \quad (1)$$

The fill factor is a measure of cell quality ranging from 0 (poor) to 100% (excellent). Values in the range of 70 to 80% are common for commercial cells.

Increasing the light-sensing area or the illuminance level per single solar cell produces a proportionate increase in the I_{sc} . The V_{oc} remains constant regardless of the light-sensing surface area, and is hardly changed at all even by the illuminance level. However, this voltage will drop drastically if the intensity of the incident light is reduced in the extreme.

Like in all semiconductors, the crystals used to make solar cells are sensitive to temperature. The performance of solar cells is such that I_{sc} increases and V_{oc} decreases as the temperature rises. Since the rate at which V_{oc} decreases is higher than the rate at which I_{sc} increases, the maximum output is also reduced. The power of crystalline silicon solar cells drops about 0,4 - 0,5 %/Kelvin and the power of amorphous silicon solar modules drops about 0,2 - 0,25 %/Kelvin (1 Kelvin corresponds to a temperature difference of 1° C).

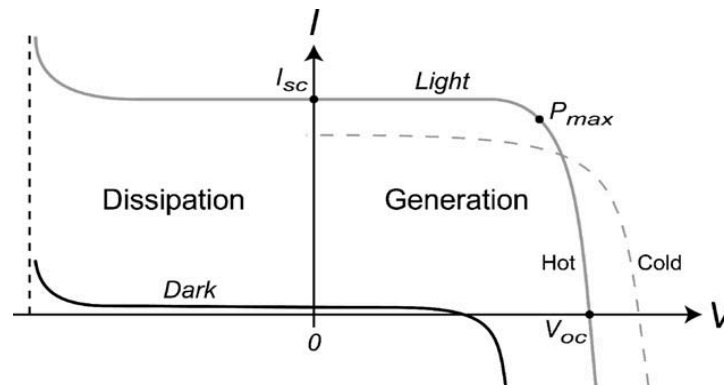


Figure 5 Current–voltage behavior of silicon photovoltaic cells with and without incident radiation [13]. As the cell temperature rises, I_{sc} increases and V_{oc} decreases, leading to a net decrease in output power

3.6. MAXIMUM POWER POINT TRACKING

As seen before, solar cells show large variations of electrical power depending on the environmental conditions. Moreover, when connected to a load other problems arise that cause the energy transferred to the load to rarely correspond to the maximum energy produced by the harvester.

Maximum Power Point Tracking (MPPT) controllers were developed after 1968, in order to improve the performance of systems consisting of a nonlinear source and an arbitrary load. These types of controllers are particularly suitable for regulating non-linear sources and force them to work at the point of maximum power, thereby improving overall efficiency.

When connecting a power source to a load, the point of operation is determined by the intersection of electrical current-voltage (I-V) characteristic of the source, with the corresponding characteristic of the load, as shown in Figure 6. This operating point changes whenever the characteristics of the source or the load change. That is why very often the system is not operating at Maximum Power Point (MPP) and the energy supplied to the load is less than the maximum that could be provided.

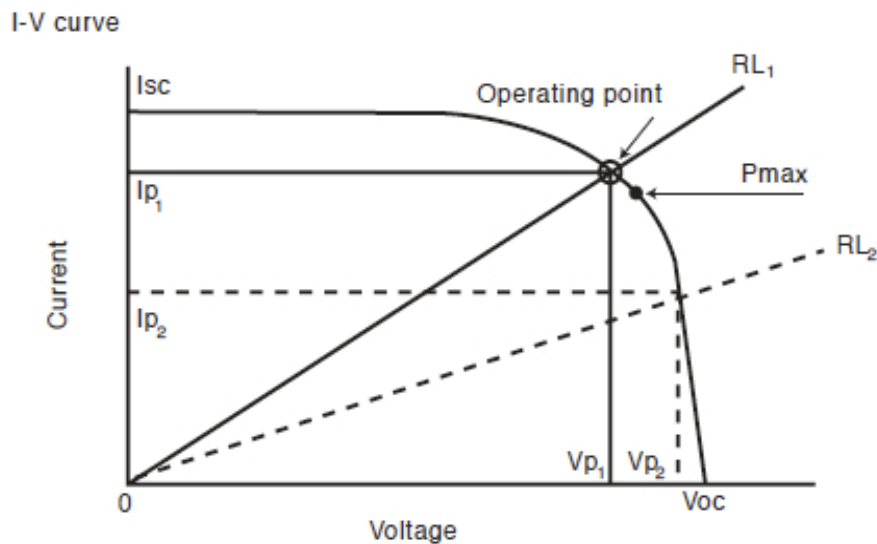


Figure 6 Operating point of a solar cell when connected to a load resistance (RL). V_p represents the operating voltage, I_p the operating current, and P_{max} the MPP [33].

The principle of operation of MPPT controllers is based in the pursuit of the MPP and is applicable to not only direct current (DC) sources such as solar cells but also to alternating current (AC) sources such as wind generators, and virtually to all other ambient power sources as well. Although MPPT is not strictly required for energy harvesting to work, because of the wide dynamic range of ambient sources, the efficiency loss can be tremendous that 65% to 90% of the available power may simply be discarded [34].

3.6.1. MEASUREMENT METHOD FOR MPPT

To perform MPPT the input intensity must be known, so that the MPP can be determined in terms of voltage and current. This can be done by measuring either before or after conversion to electricity. For instance, the MPP for solar panels is determined mainly by the light intensity and secondarily by temperature. One may perform direct measurement of sunlight before conversion by including a light intensity sensor and possibly a temperature sensor, so that the MPP can be looked up or computed.

An alternative is to sense the input intensity after conversion, which means measuring the voltage and current from the solar panel. One may measure either the open-circuit voltage (V_{oc}) or short-circuit current (I_{sc}). A drawback is that both require the load to be temporarily disconnected from the supply during its measurement. This implies having an energy storage device such as a battery or a capacitor to continue powering the system while the measurement is being taken. An alternative to avoid the transient drop of power caused by the temporary disconnection is to exploit an additional small solar module, which matches the characteristics of the principal module, acting as a pilot cell [35]. Sensing the input intensity after conversion can better track the entire area of exposure, although discrete sampling assumes the input level does not alter rapidly.

Several methods and algorithms have been suggested over the past few decades to analyze and find the MPP. The relative merits of the most common MPPT methods for solar panels are discussed in [36].

3.6.2. SOFTWARE VS. HARDWARE MPPT CONTROLLER

The control for MPPT can be implemented either in hardware or software. A hardware implementation usually means an exclusive designed circuit. It requires taking the output of a sensor, usually before conversion to electricity, and controlling a DC-DC converter or

a programmable regulator, all without additional computation. The AmbiMax platform [25] uses this kind of implementation usually called autonomous. This is due to the fact that MPPT can be performed with low overhead and be part of the power subsystem in a modular way, without the involvement from the microcontroller or DSP.

On the other hand, a software implementation entails sampling the voltage level, usually after conversion to electricity, either performing a table look-up or running a DSP algorithm, and then controlling the power circuitry accordingly. This requires running MPPT as a low duty task on the same MCU that also performs the sensing control and power management functions. The wireless sensor node named Everlast [37] is an example of this kind of system. However, this implementation has several downsides: first it doesn't work when the MCU is asleep; second it takes up precious I/O resources; and third the MPPT can only be performed in synchrony with the application's duty cycle, which will only work well if the supply condition does not change abruptly.

In wireless sensor networks powered by ambient power sources the MPPT controller must be designed for very low power consumption. This usually translates into very simple hardware implementations that keep the overhead low, but tend to track the MPP with a hysteresis band.

3.6.3. SOME LITERATURE EXAMPLES

Basic prototypes of solar energy harvesters presented in literature do not perform any MPPT. They use a solar cell panel directly connected to a primary buffer whose terminal voltage determines the panel's operating point along its I-V curve. By choosing a battery connected through a diode (or a supercapacitor), whose voltage is close to the maximum power point voltage of the solar cell panel (V_{Pmax}), operation at MPP is intended while avoiding the use and overhead of an MPPT circuit. However, as the solar cell operates at a voltage that follows the battery characteristics and not the panel characteristics, maximum power is not delivered.

The plug-and-play solar harvesting module known as Heliomote [38], is an example of this kind of system. Because the V_{Pmax} of the used solar cell panel lies at around 3 V, the authors chose two NiMH batteries whose voltage varied between 2,2 V and 2,8 V to operate the module. This way, they tried to ensure that the voltage across the solar cell

panel terminals remained close to the V_{Pmax} . An identical approach was also used in the Prometheus design [39].

It is clear that these types of designs cannot respond to sudden changes in the supply condition. Furthermore, even if the battery's voltage would slightly differed most of the times from the V_{Pmax} , which is unlikely, precious power would still be wasted, reducing the transfer efficiency of the system.

In the ZebraNet project [28], a solar cell array of fourteen solar cells along with a rechargeable battery were used to power the sensor nodes built into collars on zebras. The input voltage characteristics of each module are shown in Figure 7. Maximum power is produced at the corner where the cells change from constant voltage to constant current (shaded area).

In order to keep the solar cell array operating at the maximum power corner the authors designed the circuit shown in Figure 8. By using a simple comparator to control a boost converter the circuit maintains the three-cell series operating near the maximum power corner voltages, between 1,0 V and 1,3 V.

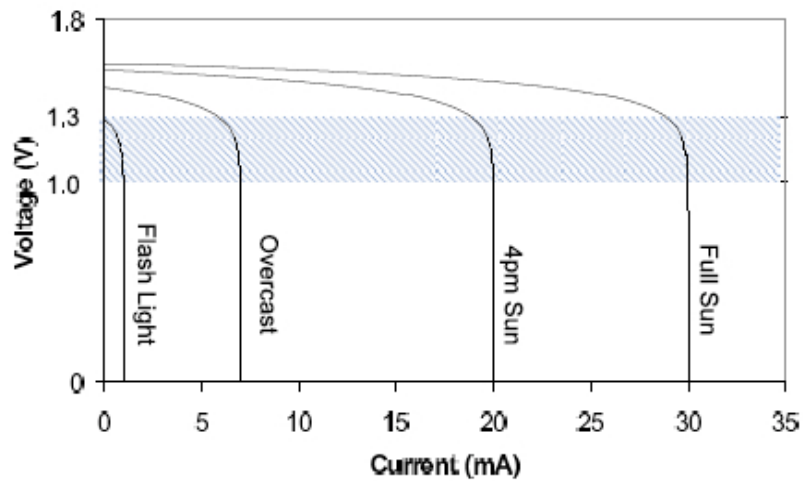


Figure 7 Solar module characteristics of three cells in series [28].

The principle of operation used is similar to the one of an MPPT method. The difference is that this circuit considers a maximum power gap instead of a maximum power point. As a result, the harvesting efficiency of such a system will increase (decrease) in accordance with a more (less) precise determination of the power gap voltages of the used solar cells. Whatever the case is, precious power is still wasted, though in a smaller proportion than in Heliomote and Prometheus.

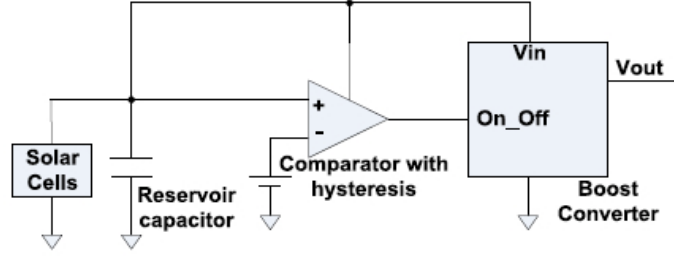


Figure 8 Solar cell module used in the ZebraNet project [28].

On the AmbiMax platform [25] a comparator is also used to control the operation of a switching regulator. However, this one compares the short circuit voltage (V_{ambi}) of an ambient power source and an output signal of a sensing device (V_{sensor}) that is generated based on the status of the ambient power source. Once V_{ambi} drops below $V_{sensor} - V_{Hysteresis}$, which means the ambient power source is out of the maximum power point, the comparator turns off the regulator. Also, when V_{ambi} increases so that it is higher than $V_{sensor} + V_{Hysteresis}$, the comparator turns on the regulator again. Figure 9 summarizes how MPPT works on the AmbiMax platform.

For solar power harvesting the authors used a light intensity sensor to control the on/off-switching regulator. While straightforward, it was not take into account that the light sensor covers a much smaller area than the solar panel and might not yield a representative reading, if dust or shadow on the panel does not cover the light sensor in the same proportion (and *vice-versa*).

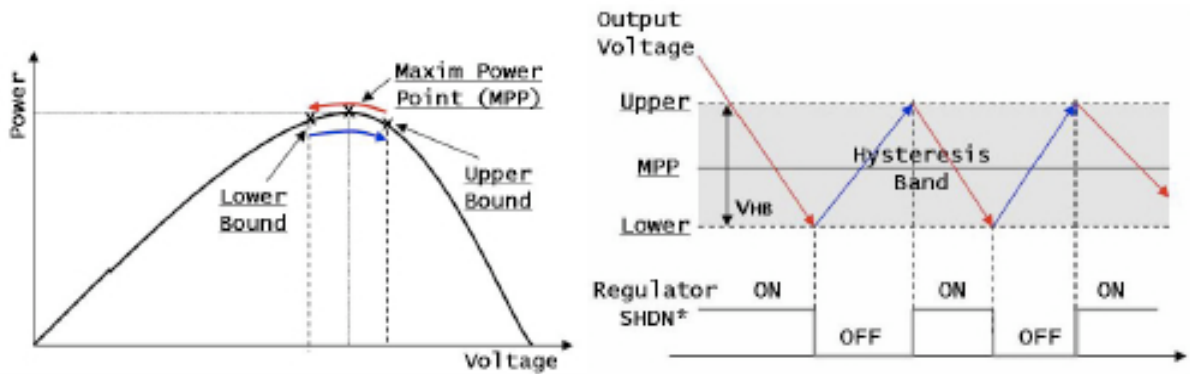


Figure 9 MPPT of the AmbiMax platform using a switching regulator and comparator [25].

4. KINETIC ENERGY

4.1. INTRODUCTION

Solar cells offer an excellent and technologically mature solution for energy harvesting, especially for outdoors applications of WSNs. However, they have the constraint of being able to generate energy only when there is sufficient light.

The general opinion from the literature is that while each application should be evaluated individually with regards to finding the best energy-harvesting method, kinetic energy in the form of motion or vibration is generally the most versatile and ubiquitous ambient energy source available. Suitable vibrations can be found in numerous applications including common household goods (fridges, washing machines, microwave ovens, etc), industrial plant equipment, moving structures and transport vehicles (automobiles, airplanes, ships, trains), structures such as buildings and bridges [40] and also in human-based applications [41].

Kinetic energy harvesting requires a transduction mechanism to generate electrical energy from motion and the generator will require a mechanical system that couples environmental displacements to the transduction mechanism. The design of the mechanical system should maximize the coupling between the kinetic energy source and the

transduction mechanism and will depend entirely upon the characteristics of the environmental motion [42].

The authors in [16] divide motion-driven microgenerators into two categories: those that utilize direct application of force and those that make use of inertial forces acting on a proof mass. The operating principle of each of these generators is depicted in Figure 10.

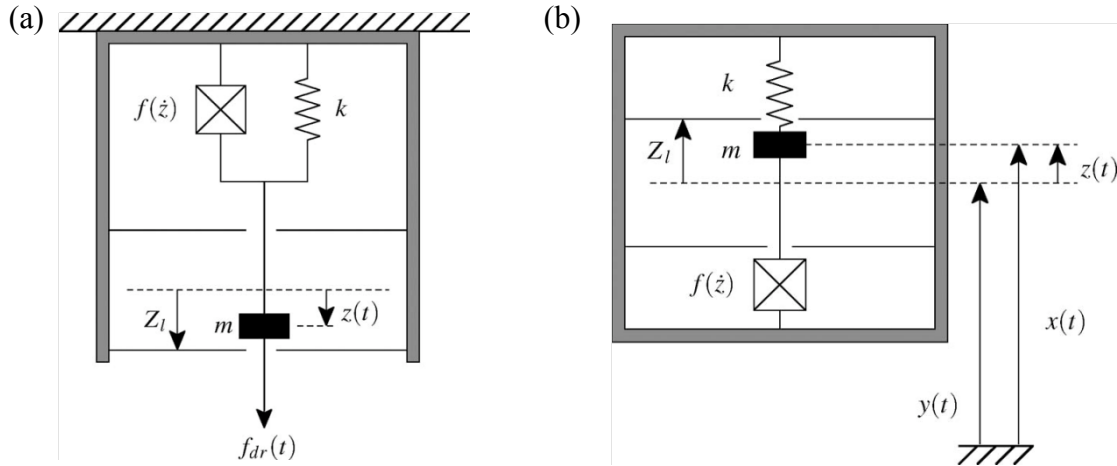


Figure 10 Generic model of – (a) direct-force generator and (b) inertial generator [16].

In the case of a direct-force generator (Figure 10a), the driving force $f_{dr}(t)$ acts on a proof mass m supported on a suspension with spring constant k , with a damping element present to provide a force $f(z)$ opposing the motion. If the damper is implemented using a suitable transduction mechanism, then in opposing the motion, energy is converted from mechanical to electrical form. There are limits of $\pm Z_l$ on the displacement of the mass, imposed by device size.

Direct-force generators must make mechanical contact with two structures that move relative to each other, and can thus apply a force on the damper. As this leads to very specific application scenarios, particularly for miniature devices, they won't be addressed in this work, but the reader can refer to [16] for further study on this type of generators.

Vibration energy is best suited to inertial microgenerators (Figure 10b). In this case the mechanical component is attached to an inertial frame with absolute displacement $y(t)$, which acts as the fixed reference. The inertial frame transmits the vibrations to a suspended inertial mass m , producing a relative displacement $z(t)$ between them. The range of $z(t)$ is again $\pm Z_l$. Energy is converted when work is done against the damping force $f(z)$, which

opposes the relative motion. As has been shown in [43], the amount of energy that can be generated under specific operating conditions (i.e. the amplitude and frequency of the input vibration), is heavily dependent on the strength of the electrical damping force.

Inertial generators require only one point of attachment to a moving structure, which gives much more flexibility in mounting than direct-force devices and allows a greater degree of miniaturization. In order to generate electricity the damper must be implemented by a suitable transduction mechanism that will exploit the mechanical strain or relative displacement occurring within the system.

In the case of relative displacement, either the velocity or position can be coupled to a transduction mechanism. Velocity is typically associated with electromagnetic transduction, which is the base of most conventional, macroscale electrical generators. Relative position is associated with electrostatic transduction, which although impractical and inefficient for large machines, becomes more functional at small size scales. The strain effect utilizes the deformation within the mechanical system and typically employs active materials like piezoelectric. Piezoelectric transduction is generally impractical for rotating systems but is well suited to the reciprocating nature of the motions typically used for harvesting (i.e. vibration). Each transduction mechanism (i.e. electromagnetic, electrostatic and piezoelectric) exhibits different damping characteristics and this should be taken into consideration while modeling the generators [42].

Several devices and applications have been studied and reported by a large number of research groups, which are still active in the field of motion-energy harvesting. General reviews of this work can be found in publications such as [44], [42], [16], and [45]. A comprehensive summary and comparative review of the different types of small magnetic power generators is presented in [46]. A work focusing in the design of electrostatic generators using MEMS fabrications technology and in the development of detailed models of different design concepts is presented in [47]. A review of energy harvesting using piezoelectric materials is presented in [48]. A more specific review focusing on vibration-based MEMS piezoelectric energy harvesters is given in [49].

In the following sub-sections, the operating principle of those devices is described along with a report of several examples proposed in the literature. These examples were chosen based on their relevance to the development of the different types of kinetic generators,

their exploitation in specific applications (with occurring vibrations from 1 Hz to 1 kHz) or due to the relevance of reported measurements.

4.2. ELECTROMAGNETIC TRANSDUCTION

4.2.1. OPERATING PRINCIPLE

Electromagnetic induction, first noticed and investigated by Faraday in 1831, can be defined as the process of generating an electric current in a circuit located within a magnetic field. The circuit typically takes the form of a wire coil and electricity is generated because of changes in the magnetic flux. Faraday's law is valid regardless of the process that causes the magnetic flux to change. It may be that a magnet is moved closer to a circuit or that a circuit is moved closer to a magnet. Figure 11 depicts an example of a device that employs this type of conversion.

The device consists of a spring connected in one end to a mass and in the other end to a rigid housing. As the housing is vibrated, the mass moves relative to the housing and energy is stored in the mass-spring system. A wire coil is attached to the mass and moves through the field of a permanent magnet (PM) as the mass vibrates. The moving coil cuts a varying amount of magnetic flux, which in turn induces a voltage on the coil determined by Faraday's Law,

$$V = -\frac{d\phi}{dt} \quad (2)$$

Where V is the generated voltage or induced electromotive force (*emf*) and ϕ is the magnetic flux.

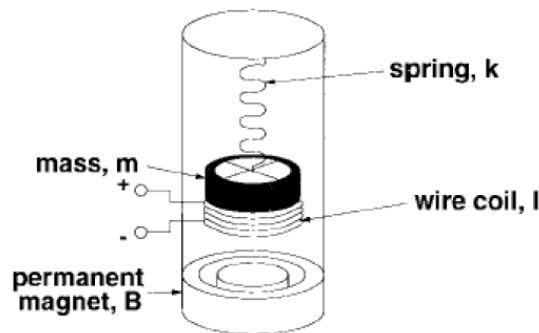


Figure 11 An inertial electromechanical generator [50].

In the simple case of the generator depicted in Figure 11, the coil moves through a perpendicular magnetic field of constant strength, as a result, the maximum open circuit voltage across the coil can be calculated by the following equation,

$$V_{oc} = NBl \frac{dy}{dt} \quad (3)$$

where:

N is the number of turns in the coil;

B is the strength of the magnetic field;

l is the length of one coil ($2\pi r$);

and y is the distance the coil moves through the magnetic field.

In this kind of devices the amount of electricity generated depends upon the strength of the magnetic field, the velocity of the relative motion and the number of turns of the coil [42]. In [44] was estimated that output voltages above 100 mV were highly improbable for this type of generator considering a maximum device size of 1 cm^3 and using vibrations of $2,25 \text{ ms}^{-2}$ at 120 Hz (typical of a small microwave oven powered from a 60 Hz electric grid).

4.2.2. TYPES OF MICROSCALE MAGNETIC GENERATORS

Microscale magnetic generator technologies can be broadly classified into three categories: rotational, oscillatory, and hybrid devices, as shown in Figure 12. Rotational generators rely on a constant source of rotational mechanical energy (*e.g.*, from miniature turbines or heat engines). Because of their small size they usually operate at high rotational speeds and thus high electrical frequencies. These higher speeds enable the generators to meet or exceed the power density of their macroscale counterparts. However, they cannot create power without the need for prime mover source, which causes them to be very application-specific.

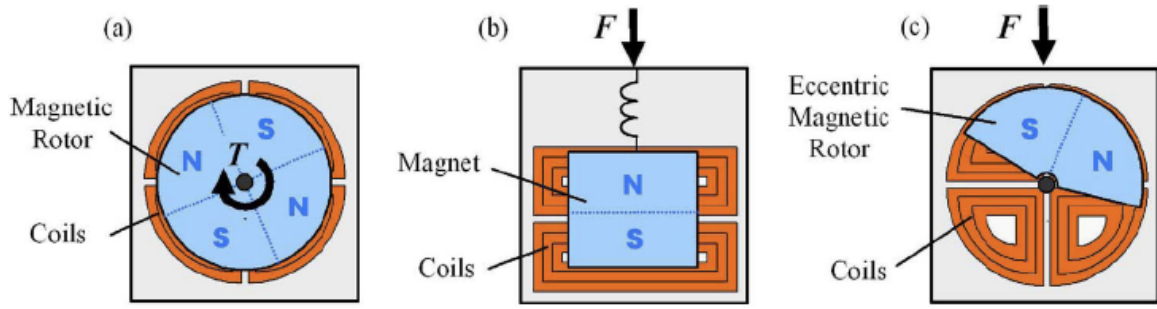


Figure 12 Three different types of PM power generation technologies: (a) rotational device driven by continuous rotational power, (b) oscillatory device driven in resonance by forced vibration, and (c) hybrid device that converts linear vibrations into rotational motion [46].

In comparison to rotational generators, oscillatory generators operate at lower electrical frequencies and lower power densities, usually relying on relatively small displacements between a PM and coil to harness power from environmental vibrations. The basic design utilizes a mass-spring-damper system such as the ones presented in Figures 11 and 12b. These types of devices generate maximum power when the resonant frequency of the generator matches the frequency of the input vibration [46], and thus cannot easily track a time-varying vibration frequency.

As the mechanical resonance of small MEMS resonators may be well above the range of naturally occurring vibrations (1 Hz to 1 kHz), nonresonant generator technologies are needed that respond to linear vibrations over a broad frequency spectrum. “Hybrid” generators [46] can convert linear motion into rotational motion by using an eccentric rotor, which rotates under forced acceleration of the pivot point (Figure 12c). Depending on the operating conditions, the rotation (and hence power generation) from these devices may be continuous, oscillatory, or chaotic.

4.2.3. EXAMPLES AND APPLICATION OF MAGNETIC GENERATORS

The first description of a small inertial energy harvester is a patent filed in 1989 by Hayakawa [51], and describes the ideas behind the commercially available Seiko Kinetic watch. The movement of the wearer rotates the oscillating weight (i.e. proof mass), which is then amplified by the high ratio gears and transferred to the permanent magnet electrical generator as depicted in Figure 13. The generator consists of a small disc-like PM that rotates in a magnetic armature to induce current in a coil winding. The current is rectified and stored in a capacitor, which supplies the electricity to drive the watch circuitry.

Estimates indicate 5 to 10 μW of average power generation during normal human activity [10].

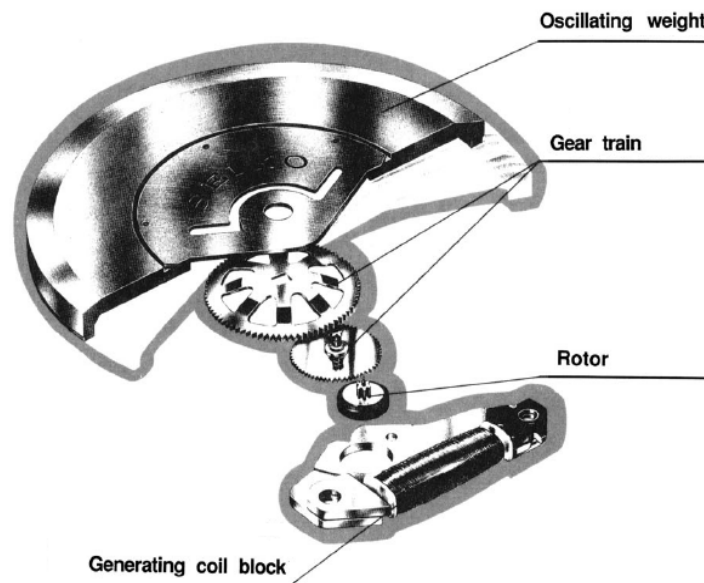


Figure 13 Exploded view of Seiko Kinetic watch. Image adapted from the operational instructions of the Seiko Kinetic watch.

In the research literature, the first description of an inertial microgenerator was of an electromagnetic type driven by reciprocating vibration, presented by Williams and Yates in 1995 [52]. Significant contributions of this work are the application of the model of Figure 10b to inertial microgenerators, and the development of an equation for power generation for linear inertial generators. Power levels from 1 to 100 μW were calculated for generators with a 15 mg mass operating between 70 Hz and 3,3 kHz. The authors also present some basic insights into the choice of generator design parameters. Based on this work Shearwood and Yates [53] developed two years later a 25 mm³ device consisting on a planar coil and a flexible polyimide membrane with attached magnet of mass 2,4 mg. The device shown in Figure 14a was tested and a peak power of 0,3 μW was obtained for 0,5 μm vibrations at 4,4 kHz.

A few years later a group of researchers from the Chinese University of Hong Kong reported a 1 cm³ electromagnetic generator capable of producing 40 μW of power, after rectification, when driven from an input vibration of between 60 and 120 Hz [54][54]. They used a small rare-earth magnet supported by a laser-micromachined copper spring structure (Figure 14b) to successfully drive a commercial infrared transmitter at a duty

cycle of 1%. The same generator is also presented in [55], which describes the integration of a microcontroller, temperature sensor, and FM transmitter into the self-powered system. The transmission of temperature data over a distance of 25 m is demonstrated.

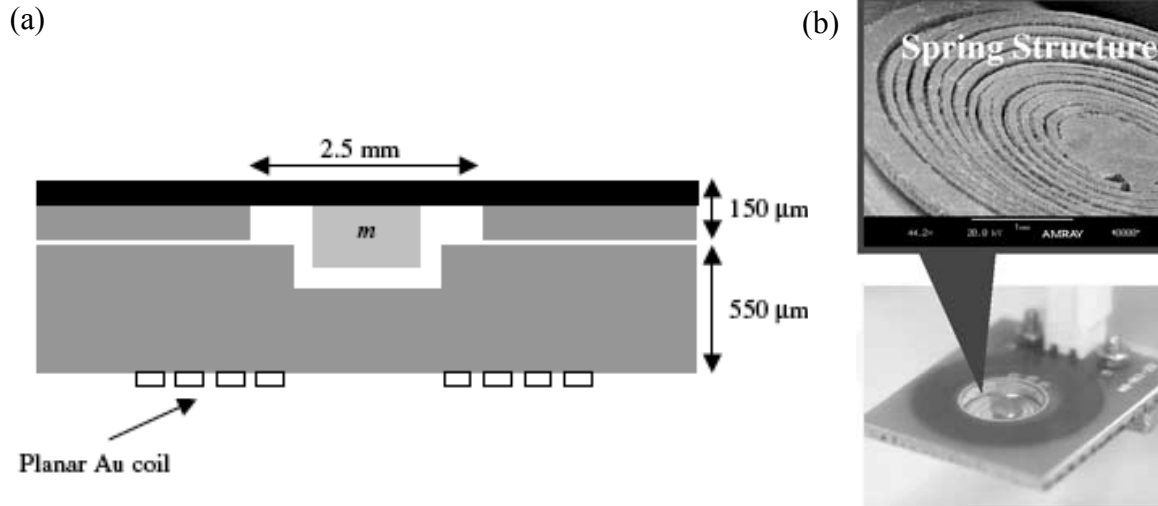


Figure 14 Electromagnetic generators proposed by: (a) Williams et al [52][53], and (b) Li et al [54][55].

In [56], a group from the University of Southampton demonstrated a conventionally manufactured resonant cantilever beam design. The mass on the beam is made up of a pair of PMs mounted on a u-shaped iron core to provide a constant field across an air gap. A copper coil is placed in the air-gap between the poles of the magnets. The 0,24 cm³ device demonstrated 0,53 mW of useful electrical power generation for vibration amplitude of 25 μm at the resonant frequency of 322 Hz. Another slightly larger design (3,15 cm³) utilized four PMs and demonstrated 157 μW of average power output (with a peak value of 3.9 mW) when attached to an automobile engine [57]. In [58] the group reported a condition monitoring system powered from this four PMs design (Figure 15a), tuned to 102 Hz and generating 2,5 mW for a source displacement amplitude of 0,4 mm.

In a European collaborative project called VIBES, the 0,15 cm³ cantilever beam device shown in Figure 15b was developed to harvest energy from an air compressor producing large vibration amplitudes at 50 and 60 Hz [59]. The device, also using the four-pole configuration, generated 17,8 μW at 89 mV, for a frequency of 60 Hz and input acceleration of 0,6 ms⁻².

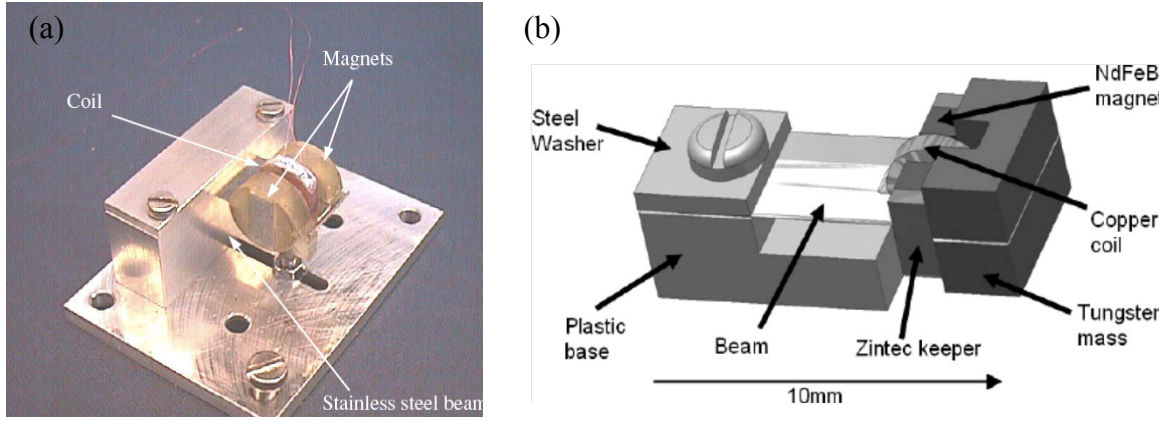


Figure 15 Cantilever beam designs using a four-pole configuration from (a) Glynne-Jones et al [57], and (b) Torah et al [59].

4.3. ELECTROSTATIC TRANSDUCTION

4.3.1. OPERATING PRINCIPLE

A capacitor is a passive electronic component consisting of a pair of electrodes that are electrically isolated from each other typically by air, vacuum or an insulator. The charging of the electrodes by a battery of a certain voltage creates equal but opposite charges on the electrodes, leading to the storage of a charge when the voltage source is disconnected. The fundamental definition of the capacitance of such a capacitor is given by,

$$C = \frac{Q}{V} \quad (4)$$

where C is the capacitance in farads (F), Q is the charge on the electrode in coulombs (C) and V is the voltage on the electrodes in volts (V).

Capacitance can be defined as the ability of a body to hold an electrical charge. It is also a measure of the amount of electrical energy stored for a given voltage. A common form of energy storage device is a parallel-plate capacitor. The energy stored in such a capacitor, with plate charge Q and potential difference V , is given by,

$$E = \frac{1}{2} QV = \frac{1}{2} CV^2 = \frac{1}{2} Q^2 / C \quad (5)$$

Note that in a variable parallel-plate capacitor, capacitance is a function of the geometry of the plates and the characteristics of the materials surrounding them, and is given by,

$$C = \varepsilon \frac{A}{d} \quad (6)$$

where ε is the permittivity of the material between the plates in farads per meter (Fm^{-1}), A is the overlap area of the plates in square meters (m^2), and d is the separation between the plates in meters (m).

An electrostatic transducer can be implemented using a resonant mechanical system and a variable capacitor. Ambient vibration will excite the resonant mechanical system that supports a variable capacitor. Changes in the geometry of the resonant system will alter the capacitance (equation 6) and thus the energy stored in the variable capacitor (equation 5). The mechanical energy induced in the variable capacitor by the vibration can then be extracted by proper electronic circuitry [60].

Electric energy is introduced into the system when the variable capacitance is at a maximum, and is extracted when the capacitance reaches a minimum. The extracted energy is delivered to a reservoir, which stores it and can then power a load. There are two possible energy conversion cycles [61]: charge constrained and voltage constrained. The QV diagrams that describe each cycle are represented in Figure 16. Note that one basic constraint for both cycles is that the maximum allowable voltage V_{high} , and it might be limited by the maximum voltage the electronic circuitry can sustain, or by electric breakdown.

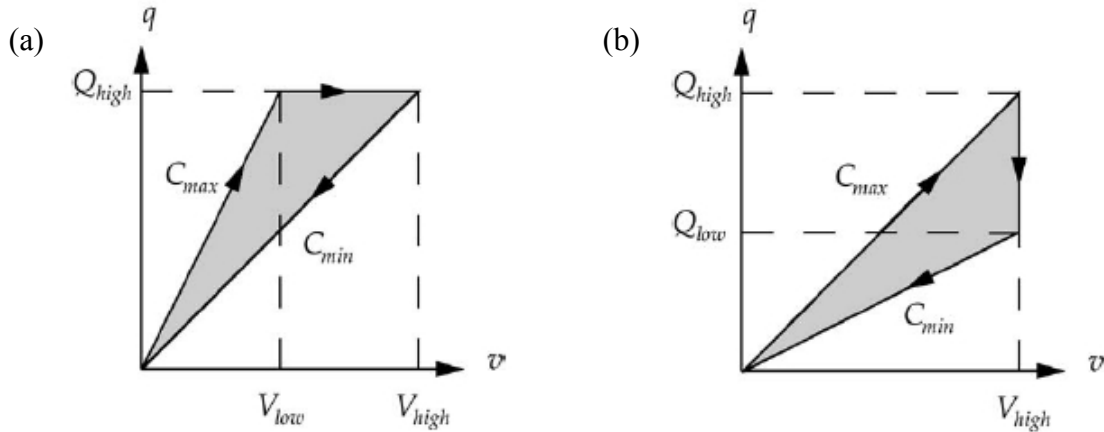


Figure 16 QV diagram that describes (a) the charge-constrained cycle, and (b) the voltage-constrained cycle [60].

A very comprehensive explanation of the conversion cycles is given by [60]. Given the importance of these cycles to understand the operation of electrostatic transducers that explanation is presented in the next sub-sections.

4.3.1.1. CHARGE-CONSTRAINED ENERGY CONVERSION CYCLE

The energy conversion cycle represented in Figure 16a, is termed a constant-charge cycle in QV plane since the charge remains constant as the capacitance varies. For any capacitor, a fixed geometry implies a fixed capacitance. As that capacitor is charged, its charge grows along the straight line defined by that capacitance. Thus, if an initially uncharged capacitor of capacitance C_{\max} is brought to some voltage V_{low} , it will trace the first line segment from the origin to the point $(V_{\text{low}}, Q_{\text{high}})$, where $Q_{\text{high}} = C_{\max} V_{\text{low}}$. A reservoir must provide the capacitor with an amount of energy equal to $\frac{1}{2} C_{\max} V_{\text{low}}^2 = \frac{1}{2} Q_{\text{high}}^2 / C_{\max}$. If the capacitor is disconnected so that no charge may flow in or out, the system will now be constrained to move along the horizontal line Q_{high} . Since the capacitor is charge-constrained, lowering the capacitance will result in a voltage increase according to

$$Q_{\text{high}} = C_{\max} V_{\text{low}} = C_{\min} V_{\text{high}} \Rightarrow \frac{C_{\max}}{C_{\min}} = \frac{V_{\text{high}}}{V_{\text{low}}} \quad (7)$$

This corresponds to tracing the horizontal segment from V_{low} to V_{high} in the QV plane. The energy content in the capacitor will increase to $\frac{1}{2} C_{\min} V_{\text{high}}^2 = \frac{1}{2} Q_{\text{high}}^2 / C_{\min}$. Note that the reservoir does not provide or receive any energy during this path segment. All the energy gained comes from the mechanical source through the force required to change the capacitance. Derivation of these forces can also be found in [60]. By substituting the relationship between V_{low} and V_{high} of equation (7), the energy inside the capacitor can be compared to its initial energy $\frac{1}{2} C_{\max} V_{\text{low}}^2$:

$$\frac{1}{2} C_{\min} V_{\text{high}}^2 = \frac{1}{2} C_{\max} V_{\text{low}}^2 \frac{C_{\max}}{C_{\min}} \quad (8)$$

Thus, the energy content has increased by the factor C_{\max}/C_{\min} . If the energy is then returned to a reservoir from the capacitor, which corresponds to moving on to the origin in the QV plane, now through the C_{\min} line, the amount of energy gained by the reservoir will be

$$\begin{aligned}
\Delta E_{chargeconstrained} &= \frac{1}{2} C_{\max} V_{low}^2 \frac{C_{\max}}{C_{\min}} - \frac{1}{2} C_{\max} V_{low}^2 \\
&= \frac{1}{2} \Delta C V_{low}^2 \frac{C_{\max}}{C_{\min}} = \frac{1}{2} \Delta C V_{high}^2 \frac{C_{\min}}{C_{\max}} = \frac{1}{2} \Delta C V_{low} V_{high}
\end{aligned} \tag{9}$$

where $\Delta C = C_{\max} - C_{\min}$ and all the alternate forms can be derived from equation (7). This quantity is equal to the shaded area in Figure 16a.

4.3.1.2. VOLTAGE-CONSTRAINED ENERGY CONVERSION CYCLE

An alternative energy conversion cycle is represented in Figure 16b. In this cycle, aptly named a voltage-constraint cycle, a capacitor is charged up to some high voltage V_{high} when the capacitor plates are close and the capacitance is again at some C_{\max} . The charge at this point will be $Q_{high} = C_{\max} V_{high}$, and the energy content provided by the reservoir will be $\frac{1}{2} C_{\max} V_{high}^2 = \frac{1}{2} Q_{high}^2 / C_{\max}$. However, in this case, the plates are connected to the reservoir at constant voltage V_{high} . Thus, when the plates are separated, and the capacitance is decreased, the capacitor will trace the line from Q_{high} to Q_{low} . In order to maintain the same voltage V_{high} , the capacitor will have to return the change in charge $Q_{high} - Q_{low}$ to the reservoir. Since the reservoir and the capacitor are held at a constant voltage V_{high} , this implies that the capacitor will provide the reservoir with an amount of energy equal to $(Q_{high} - Q_{low}) V_{high}$. Again, the energy comes from the mechanical source through the force required for this capacitance to change. If the capacitor is then discharged into the reservoir, it will trace the line back to the origin in the QV plane and return to the reservoir an additional amount of energy $\frac{1}{2} C_{\min} V_{high}^2$. Thus, at the end of the cycle, the total amount of energy gained by the reservoir will be

$$\begin{aligned}
\Delta E_{voltageconstrained} &= \frac{1}{2} C_{\min} V_{high}^2 + (Q_{high} - Q_{low}) V_{high} - \frac{1}{2} C_{\max} V_{high}^2 \\
&= \frac{1}{2} \Delta C V_{high}^2
\end{aligned} \tag{10}$$

where $\Delta C = C_{\max} - C_{\min}$. Again, this is the shaded area enclosed by the cycle in Figure 16b. Note that the converted energy given by equations (9) and (10) will eventually be reduced by any losses incurred in the power electronics that exercise each cycle.

4.3.1.3. COMPARISON BETWEEN CYCLES

Figure 17 shows three superimposed energy cycles. The smallest and darkest triangle corresponds to a voltage-constrained cycle where the maximum voltage is V_{low} . This triangle together with the medium-shaded triangle corresponds to a charge-constrained cycle where the capacitor is first charged to V_{low} , but the decrease of the capacitance increases the voltage to V_{high} . The energy gained in this cycle is given by equation (9). All triangles together correspond to another voltage-constrained cycle where the maximum voltage in this case is V_{high} . The energy gained in this case is given by equation (10). From the figure or from equations (9) and (10) it is clear that, for the same values of C_{max} and C_{min} , a voltage-constrained cycle where the maximum voltage is V_{high} will be the one to convert the most amount of energy.

The V_{high} voltage-constrained cycle requires a reservoir at voltage V_{high} , whereas the charge-constrained cycle only needs to be charged to V_{low} , as it will reach a maximum voltage V_{high} by virtue of charge conservation. The levels of energy to be harvested by this type of generators are likely to be useful only in very-low-power applications (like WSNs), where the voltage levels are typically low. Therefore, a system where the harvesting occurred at some voltage V_{high} would need a DC-DC converter to bring this voltage down to a useful level. Such an overhead in efficiency would have to be counted against the system. The net result is that a system with one reservoir voltage at some voltage less than V_{low} is probably preferable. In this case, it is easy to see from Figure 17 that the charge-constrained cycle converts far more energy than the voltage-constrained cycle.

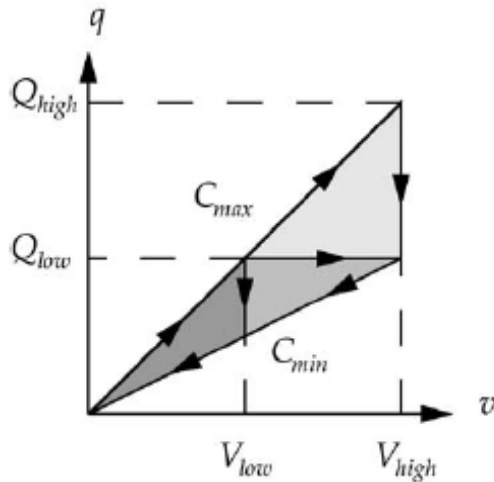


Figure 17 Energy cycles compared [60].

The pros and cons of such choice are further investigated in [60], along with solutions to approach the energy gain of a V_{high} voltage-constrained system [61]. The electronic circuitries used to implement the energy conversion cycles are also presented and discussed in both works.

4.3.2. TYPES OF MICROMACHINED ELECTROSTATIC GENERATORS

According to [47] there are three basic topologies for micromachined variable capacitors: in-plane overlap varying, in-plane gap closing, and out-of-plane gap closing. A top view of the first two devices and a side view of the third device is depicted in Figure 18. Although these illustrations are not to scale, a few representative dimensions are shown in the figure. Anchors to the substrate fix are represented by dark areas, while the light areas are released structures that are free to move.

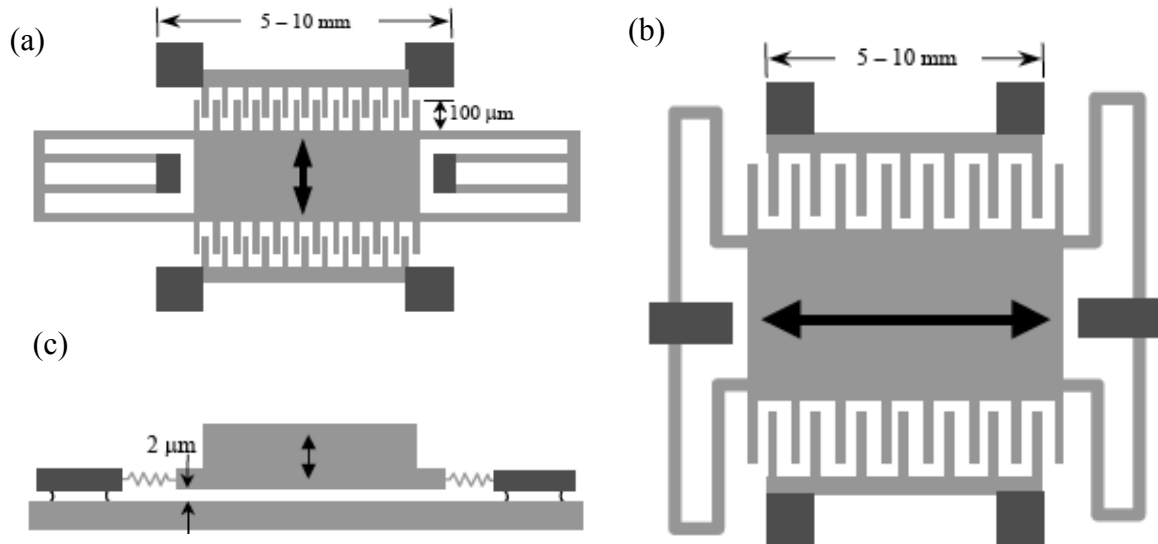


Figure 18 Three basic topologies for micromachined variable capacitors: (a) in-plane overlap varying, (b) in-plane gap closing, and (c) out-of-plane gap closing [47].

The device shown in Figure 18a is referred to as an in-plane overlap converter because the change in capacitance arises from the changing overlap area of the many interdigitated fingers. As the center plate moves in the direction indicated by the arrow, the overlap area A of the fingers changes, and thus the capacitance. The device in Figure 18b is referred to as an in-plane gap closing converter because the capacitance changes due to the changing dielectric gap d between the fingers. Recall equation (6) on how to determine the

capacitance of a variable capacitor. Note both in-plane configurations create two variable capacitors with the capacitances 180° out of phase.

Figure 18c shows a device referred to as an out-of-plane gap closing converter. This device oscillates out of the plane of the wafer, and changes its capacitance by changing the dielectric distance d between two large plates.

The three approaches can be operated either in charge constrained or voltage constrained cycles. Simulations presented in [47] indicate that the highest power density is available from in-plane gap closing converters, followed by out-of-plane gap closing converters, and finally by in-plane overlap converters. In [44] it is stated that in-plane gap closing offers the highest power output with an optimized design producing $100 \mu\text{Wcm}^{-3}$. Maximum power generation occurs for very small dielectric gaps [42].

4.3.3. EXAMPLES AND APPLICATION OF ELECTROSTATIC GENERATORS

A group at MIT was the first to report an electrostatic microgenerator work in the literature [62][61]. These papers describe a comparison between both energy conversion cycles considering both the generator and the associated control circuitry. Simulations of the device show that the proposed generator should produce $8,6 \mu\text{W}$, with approximately $5,6 \mu\text{W}$ being available for driving a load and the rest being used by the control scheme. This generator (shown in Figure 19a) was used later to power an ultra-low-power programmable DSP for sensor applications [63].

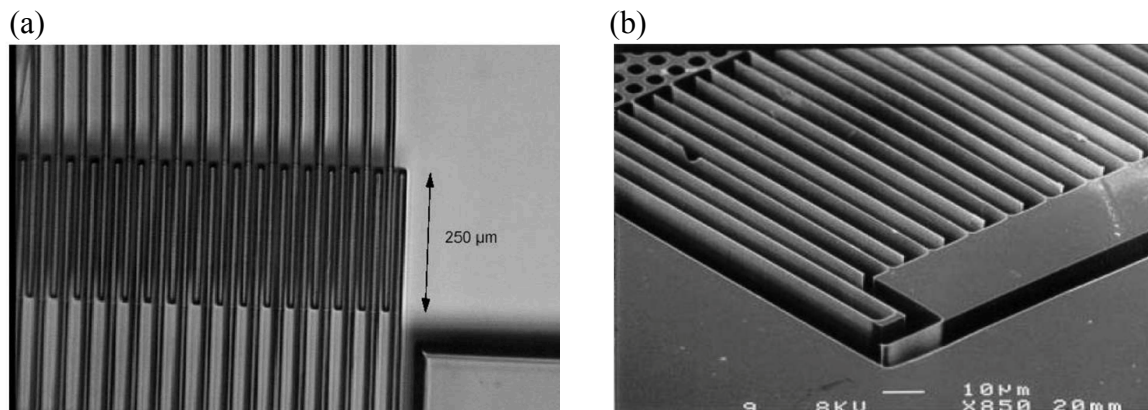


Figure 19 Examples of micromachined electrostatic generators. (a) In-plane overlap varying [63]; (b) In-plane gap closing [47].

Tashiro and his team proposed and developed an electrostatic generator that exploits the motion of a living body [64]. Their aim was to permanently supply electrical energy to an

apparatus for *in vivo* use such as a cardiac pacemaker. The proposed system consisted of a battery for initial charge supply, a honeycomb-type variable capacitor for energy conversion, a capacitor for energy storage and two rectifiers. The variable capacitor, shown in Figure 20, consisted in a honeycomb structure (with 50 layers, each with 20 unit capacitors, for a total of 1000 units), whose capacitance varied from approximately 200 to 32 nF and was resonant at 4,76 Hz. It was reported the generation of 58 μW from the simulated heart movements of a goat after an initial charging voltage of 24 V.

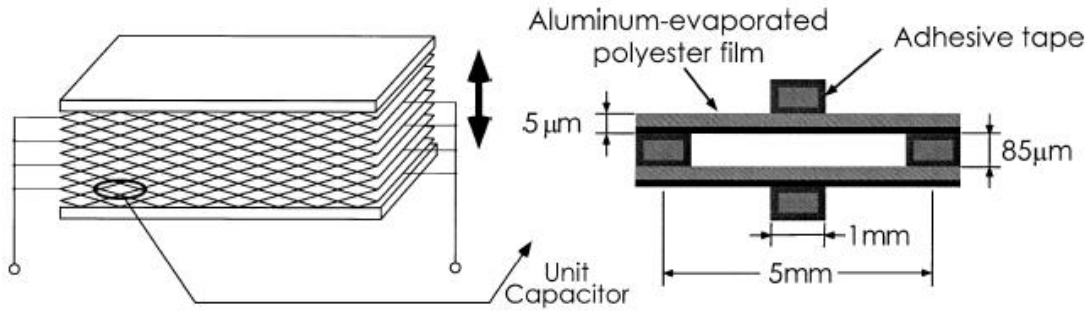


Figure 20 On the left the fundamental structure of a honeycomb-type variable capacitor (capacitance decreases with expansion and increases with compression). On the right a detail of a unit cell from the honeycomb structure. Images adapted from [65].

To certify the feasibility of the generator, the left ventricular free wall motion of a canine heart was reproduced by a vibration mode simulator in real time [65]. After initially charging the capacitor to 45 V, electric power of approximately 36 μW (15 μA at 2,4 V) was supplied to the pacemaker with peak powers as high as 500 μW . Continuous electrostatic generation and cardiac pacing were performed successfully for more than two hours in the animal experiment.

The three design concepts of electrostatic vibration-to-electricity converters using MEMS fabrications technology were evaluated and compared based on simulations and practical considerations in [47]. The preferred design concept (in-plane gap closing) was then optimized and a final design was produced using the optimal design parameters. Simulations of that design show that an output power density of 116 μWcm^{-3} is possible from input vibrations of 2,25 ms^{-2} at 120 Hz.

In [66] is presented an out-of-plane cantilever-based generator with a base capacitance of 1 nF and a variable capacitance of between 30 pF and 350 pF. The device resonated at

45 Hz and was tested on a wall with a 1 μm displacement up to 100 Hz. 120 nW was harvested for the wall acceleration of $0,08 \text{ ms}^{-2}$.

An electrostatic generator designed to operate over a wide low frequency range ($<100 \text{ Hz}$) is described in [67]. An in-plane gap closing topology was used along with a charge-constrained cycle in order to achieve high electrical damping. A fabricated macroscale device of volume $18 \text{ cm}^2 \times 1 \text{ cm}$ with a 104 g inertial mass produced a scavenged power of $1052 \mu\text{W}$ for a vibration amplitude of $90 \mu\text{m}$ at 50 Hz (corresponding to an acceleration of $8,8 \text{ ms}^{-2}$). This represents a scavenged efficiency of 60% with the losses being accounted for by charge/discharge losses and transduction losses. *In situ* measurements have also been performed and up to $250 \mu\text{W}$ have been scavenged on a car engine. A similar geometry silicon microstructure of volume $81 \text{ mm}^2 \times 0,4 \text{ mm}$ with a 2 g inertial mass excited by a vibration amplitude of $95 \mu\text{m}$ at 50 Hz was predicted to produce a scavenged power of $70 \mu\text{W}$.

4.4. PIEZOELECTRIC TRANSDUCTION

4.4.1. PIEZOELECTRICITY

In 1880, Jacques and Pierre Curie discovered an unusual characteristic of certain crystalline minerals: when subjected to a mechanical force, the crystals became electrically polarized. Tension and compression generated voltages of opposite polarity, and in proportion to the applied force. Subsequently, the converse of this relationship was confirmed: if one of these voltage-generating crystals was exposed to an electric field it lengthened or shortened according to the polarity of the field, and in proportion to the strength of the field. These behaviors were labeled the piezoelectric effect and the inverse piezoelectric effect, respectively, from the Greek word “piezein”, meaning to press or squeeze [68].

A material is considered piezoelectric when it has this ability to transform mechanical strain energy into electrical charge, and likewise to transform electrical energy into mechanical strain. Piezoelectric materials belong to a larger class of materials called ferroelectrics. A defining characteristic of a ferroelectric material is that the molecular structure is oriented such that the material exhibits a local charge separation, known as an electric dipole. Throughout the material composition the electric dipoles are orientated randomly as shown in Figure 21a, but when the material is heated above a certain point

(the Curie temperature) and a very strong electric field is applied (on the order of 2 kV/mm), the electric dipoles reorient themselves relative to the electric field. This process, depicted in Figure 21b, is termed poling. Once the material is cooled, the dipoles are locked into a configuration of near alignment and the material is then said to be poled. After the poling process is completed the material will exhibit the piezoelectric effect [69].

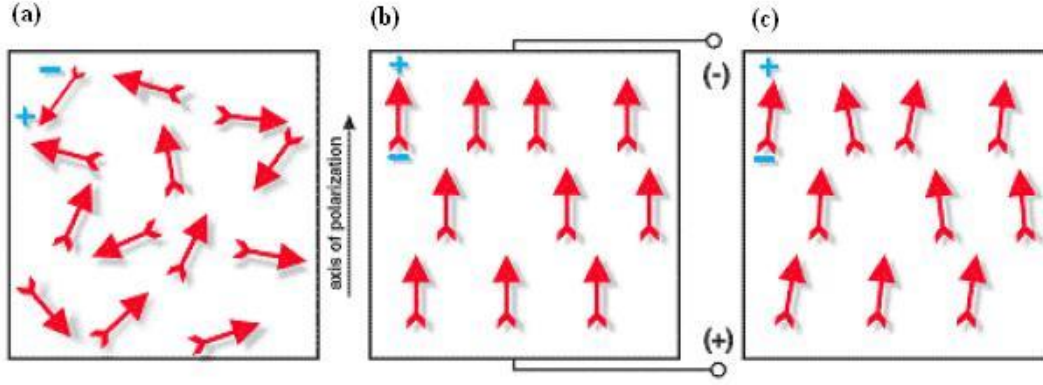


Figure 21 Polarizing (poling) a piezoelectric ceramic. (a) Random orientation of electric dipoles prior to polarization; (b) Polarization in DC electric field; (c) Remanent polarization after electric field removed [68].

To date, a number of different piezoelectric materials have been developed. The most common type of piezoelectric used in energy harvesting applications is lead zirconate titanate, a piezoelectric ceramic (or piezoceramic) known as PZT. Despite its wide use, piezoceramic's extremely brittle nature causes limitations in the strain that it can safely absorb without being damaged. This led researchers to develop and test other, more flexible, piezoelectric materials. Polyvinylidene fluoride (PVDF) for instance, is a common piezoelectric material that exhibits considerable flexibility when compared to PZT [48].

In comparing different materials a few fundamental material properties are important. The piezoelectric strain coefficient d relates strain to electric field. The electro-mechanical coupling coefficient k is an indication of the material's ability to convert mechanical energy to electrical energy (or *vice-versa*). It is functionally related to the strain coefficient by equation 11

$$k = \sqrt{\frac{Y}{\epsilon}} d \quad (11)$$

The dielectric constant ϵ , the Young's modulus Y , and the tensile strength of the material are also important material properties that should be analyzed when choosing between different piezoelectric materials [44].

Note that piezoelectric materials typically exhibit anisotropic characteristics, thus, the properties of the material differ depending upon the direction of forces and orientation of the polarization and electrodes. A full description of the piezoelectric effect and the methods used to model the behavior of these materials is beyond the scope of this work. References to a significant number of journal papers, conference proceedings, and books that develop accurate models and discuss the fundamentals of these materials in great detail are presented in [69].

4.4.2. OPERATING MODES

From equation (11) it is clear that materials with larger strain and coupling coefficients have a higher potential for energy conversion. Thus, by selecting a proper coupling mode of operation the amount of energy harvested from a chosen piezoelectric material can be increased. Figure 22 illustrates the two different modes in which piezoelectric material is generally used. The x, y, and z axes are labeled 1, 2, and 3 respectively.

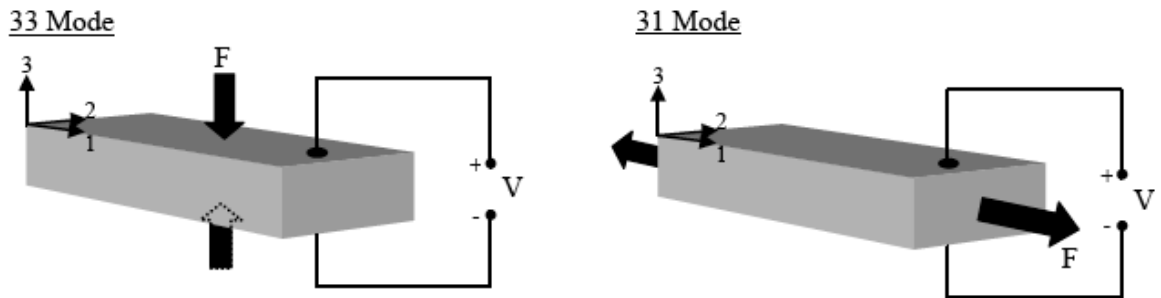


Figure 22 Illustration of 33 mode and 31 mode operation for piezoelectric materials [44].

In the 33 mode, a force is applied in the same direction as the poling direction, such as the compression of a piezoelectric block that is poled on its top and bottom surfaces. The 31 mode involves the excited vibration force being applied in the direction perpendicular to the poling direction, an example of which is a bending beam that is also poled on its top and bottom surfaces.

Between the two modes, the 31 mode produces a lower coupling coefficient k , when compared to the 33 mode. However, when comparing a piezoelectric stack operating in the 33 mode to a cantilever beam operating in the 31 mode of equal volumes, it was observed that the cantilever produced two orders of magnitude more power when subjected to the same force [70]. The authors concluded that in a small force, low vibration level environment, the 31 mode configuration cantilever proved most efficient. On the contrary, the stack configuration would be more suitable for generating energy in a high force environment (*e.g.*, heavy manufacturing facility or large operating machinery) due to its high mechanical stiffness. These results are consistent with the work presented in [40], where it was concluded that the resonant frequency of a system operating in the 31 mode is much lower, making the system more likely to be driven at resonance in a natural environment, thus providing more power.

4.4.3. CANTILEVER UNIMORPH AND BIMORPH

A bending element can be mounted in many ways to produce a generator. A cantilever structure with piezoelectric material attached to its surface (or surfaces) is the most common used geometry for harvesting energy from vibrations. The structure is designed to operate in a bending mode thereby straining the piezoelectric layer (or layers) and generating a charge from the d_{31} effect. A cantilever provides low resonant frequencies (reduced further by the addition of a mass on the end of the beam) in a low volume structure and high levels of strain in the piezoelectric layer or layers [40].

The simplest example of such a structure is the piezoelectric unimorph, which is shown in Figure 23a. The unimorph consists in a flexible cantilever supporting one piezoelectric layer sandwiched between metallic electrodes and thus acting as a capacitor. An additional mass is also attached to the tip of the cantilever. When the piezoelectric layer is stretched a voltage is generated at the terminals of the piezoelectric capacitor. Electrical power is generated when an electrical load is connected to the device [71].

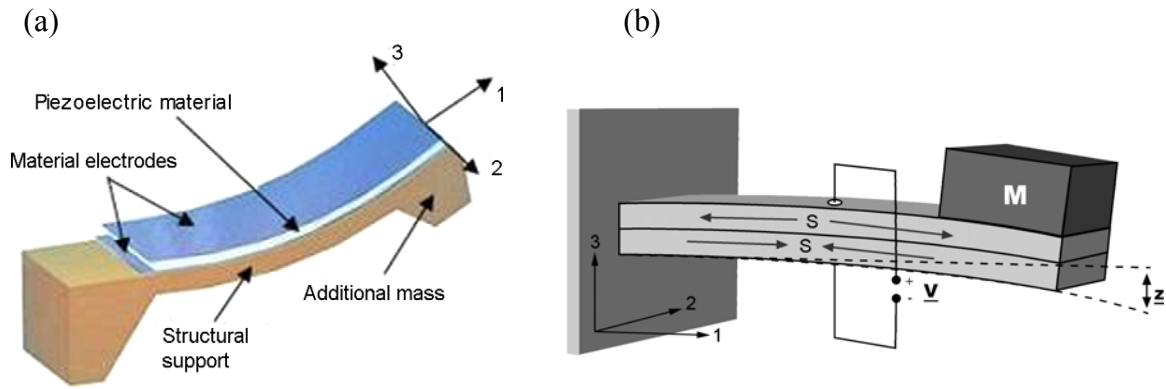


Figure 23 (a) Schematic of a piezoelectric unimorph [71]; (b) Operation of a piezoelectric bimorph poled for series operation [72].

Another common structure is the piezoelectric bimorph, in which two separate layers are bonded together, sometimes with a center shim in between them. An example of such structure is shown in Figure 23b where S represents the strain, V is voltage, M is mass, and z is the vertical displacement. As the element bends, the top layer of the element is in tension and the bottom layer is in compression or *vice-versa*. Bimorphs can be poled such that the voltage across the two layers adds (series operation), or such that the charge adds (parallel operation). Bending elements with multiple layers (more than two) can also be made, with internal electrodes providing the proper wiring between layers. In all cases, the potential for power conversion is the same. In theory, the poling and number of layers only affects the voltage to current ratio [44].

The merits of unimorph versus bimorph cantilevers have been studied in [73][74]. Findings showed that under low load resistances and excitation frequencies the unimorph generated the highest power, under medium load resistances and frequencies the bimorph arrangement with the piezo layers in parallel had the highest power output, and under high load resistances and frequencies the bimorph connected in series produced the greatest power. This result is due to the concept that maximum power transfer from the piezoelectric device occurs when the load resistance is matched to the impedance of the piezoelectric device.

4.4.4. EXAMPLES AND APPLICATION OF PIEZOELECTRIC GENERATORS

The first instance of reported piezoelectric generators occurs in the patent literature in 1983 [75], in which is described the use of a piezoelectric generator embedded in the wheel of a car to power a tire pressure sensor. The generator would be powered from wheel vibration

during driving, and abnormal tire pressure could be reported to driver using a low-power radio link.

Much research has been made for piezoelectric generators since the first piezoelectric inertial generator was reported in the research literature in 1997 [76]. However, there is a lack of experimentally validated models in the literature for these kinds of harvesters. The first exploitation of this type of generator in the context of WSNs occurs just in 2003, with the use of a fiber-based piezoelectric harvester to supply power to an adaptable wireless sensor node, capable of recording signals from different transducers and transmitting data wirelessly to a receiver [77]. When subjected to a 180 Hz vibration, the generator was capable of harvesting 7,5 mW of power, allowing the use of a microcontroller with onboard analog-to-digital conversion and wireless transmission capabilities for 250 ms. This proved to be enough time for the microcontroller to collect valid data from several sensors and transmit it four to seven times to ensure reliability. The microcontroller was activated only after the generator charged a storage capacitor to a voltage of 9,5 V, which for moderate strain levels of $150 \mu\epsilon$, took around 30 to 160 s, depending on the frequency of excitation (180 to 60 Hz). Once the voltage level across the capacitor dropped to 2,5 V the microcontroller was deactivated.

A similar approach was used in [72] to develop a small bimorph cantilever generator (see Figure 24a) used to power a custom radio transceiver, which consumed 10 mA of current at 1,2 V and was capable of transmitting a 1,9 GHz signal to a distance of 10 m. Two designs have been optimized within an overall space constraint of 1 cm^3 , taking into consideration the size of most wireless sensor nodes. Experimental results have demonstrated power transfer of $375 \mu\text{W}$ and $190 \mu\text{W}$ to a resistive and a capacitive load respectively, from driving vibrations of $2,5 \text{ ms}^{-2}$ at 120 Hz. As the radio transceiver demanded more energy than the bimorph could generate, it has been powered at a duty cycle of 1,6%.

The work presented in [78] demonstrated smart wireless sensing nodes capable of operating at extremely low power levels and driven by an energy harvesting system using piezoelectric materials. The wireless sensing nodes included a microprocessor, on-board memory, sensing means, sensor signal conditioning, 2,4 GHz radio transceiver, and rechargeable battery. The used generator was comprised of a tapered flexure element with PZT mounted on the top and bottom of a 50 mm cantilever beam. A proof mass of 250 g

was affixed to the end of the beam, which resonated at a frequency of ~ 60 Hz. The resonant cantilever flexure element harvester generated a relatively high amount of output power (around 2 to 3 mW) at low input vibration levels (1 to $1,3 \text{ ms}^{-2}$) and modest strain levels (150 to $200 \mu\epsilon$). Figure 24b presents a picture of the vibration energy harvesting wireless sensor node. The authors concluded that vibration energy harvesting systems can support wireless sensor nodes at data sampling rates that are suitable for many smart structure health monitoring systems, particularly larger structures, which often utilize sample rates of 1 to 10 Hz.

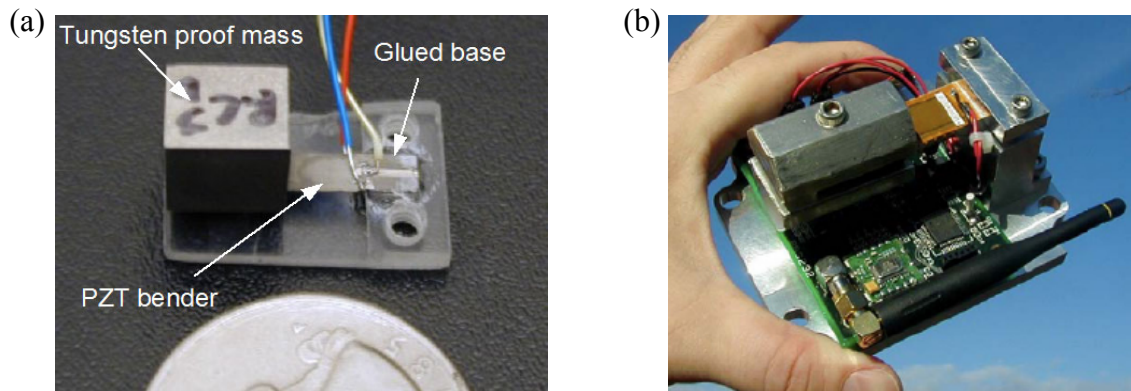


Figure 24 (a) Small bimorph cantilever generator with a 1,5 cm length constraint [72]; (b) Integrated piezoelectric vibration energy harvester and wireless temperature and humidity sensing node [78].

Harvesting energy from machinery vibrations to power a wireless sensor node was investigated in [79]. The research involved analyzing an oil pump, which was to be assessed using a health-monitoring wireless sensor node. A piezoelectric cantilever was fabricated and tested near the natural frequency of the pump, which was found to be 130 Hz. Under an excitation producing a strain of $700 \mu\epsilon$ at 100 Hz, the cantilever was able to produce 2,8 mW of power and withstand 1×10^8 cycles at which the test was terminated. This research led to the development of a self-powered sensor node designed to scavenge energy from an oil pump in an oil tanker ship [80]. The sensor node was programmed to hibernate for one hour while collecting energy from the piezoelectric cantilever (tuned to match the 130 Hz operational frequency of the oil pump), then turn on, collect data, and transmit the data collected. After four months of operation, the sensor node captured over 8000 data files. This study has demonstrated the significant benefits provided by wireless sensor nodes for shipboard machinery monitoring. The potential benefits can be

generalized to any kind of heavy machinery monitoring and include increased machinery reliability, reduced maintenance cost and effort, and enhanced safety.

4.5. SUMMARY

The three main techniques of harvesting energy from ambient vibrations have been shown to be capable of generating usable output power levels in the range of μW to mW . Nevertheless, each of the technologies has their own pros and cons and these are summarized [44][42].

The electromagnetic approach utilizes the relative motion between a coil and a magnetic field to generate a current in a coil. Relatively high output current levels are achievable at the expense of low voltages (typically $< 1\text{ V}$). These low AC voltages need to be rectified so they can be used as a power source for microelectronics (a transformer might be required to first amplify the voltage value). Wafer-scale electromagnetic generators are quite difficult to achieve due to the relatively poor properties of planar magnets, the limitations on the number of turns achievable with planar coils and the restricted amplitude of vibration (hence magnet/coil velocity). Inevitably, there are also problems associated with the assembly and alignment of micro scale electromagnetic systems.

The electrostatic concept is easily realizable as a MEMS and much processing know-how exists on the realization of in-plane and out-of-plane capacitors. Decreasing the capacitor spacing increases the energy density of the generator and facilitates its miniaturization. In addition, appropriate voltages for microelectronics, on the order of two to several volts, can be directly generated. One downside is the need of a separate voltage source to initiate the conversion process. Note however that this is not an issue in applications that use the generator to charge a battery, as this can be used to provide the necessary initial excitation level. Another disadvantage is that for many design configurations there is the risk of capacitor electrodes shorting or of stiction.

Piezoelectric generators offer the simplest approach, whereby structural vibrations are directly converted into an appropriate voltage output by using an electroded piezoelectric material. Therefore they are the simplest type of generator to fabricate. The piezoelectric materials are required to be strained directly and therefore their mechanical properties will limit overall performance and lifetime. Also the transduction efficiency is ultimately limited by piezoelectric properties of materials employed. While it is true that piezoelectric

films (thin and thick) can be integrated into MEMS processing, the piezoelectric coupling is greatly reduced.

One of the main limitations of the vast majority of reported kinetic harvesters is the necessity to ensure that the natural frequency of the mass–spring system matches with the main frequency of the input vibration [81]. Moreover, electromagnetic and electrostatic transducers require moving parts, which makes them more vulnerable to faults and breakages and subjected to sporadic maintenance. These weaknesses do not apply to the generators presented in the following section.

5. THERMAL DIFFERENTIALS

5.1. INTRODUCTION

Temperature gradients and heat flow are also found everywhere in natural and human-made settings and have the potential to generate electrical energy using thermal-to-electric energy conversion. The temperature difference provides the potential for efficient energy conversion, while heat flow provides the power. Thermoelectric energy harvesting may one day eliminate the need for replacing batteries in applications such as remote sensor networks or mobile devices [82].

Manufacturing applications, where heat is a consequence of the manufacturing process, are typically ideal applications for thermal energy harvesting, as they tend to maintain a constant temperature. Likewise, in automotive applications even a relatively inefficient thermoelectric generator (TEG) can be competitive for use with waste heat sources (~ 1 kW range) such as an automobile exhaust [83]. Additionally, in both cases, if the units are not operating, there is no need to harvest energy.

Even with large heat flow, however, the extractable power is typically low due to low Carnot³ and material efficiencies. In addition, limited heat availability will also limit the power produced. Nevertheless, the ability to fabricate exceedingly small semiconducting thermo elements has enabled the possibility of harvesting very small amounts of heat for low power applications such as wireless sensor networks, mobile devices, and even medical applications. In such applications, TEGs are also becoming competitive because they are compact, simple (inexpensive) and scalable [84]. Companies like for example Marlow Industries, Micropelt, Nextreme, Perpetua, Tellurex or Thermo Life are already commercializing thermoelectric generators that can exploit previous mentioned scenarios.

Human beings and, more generally speaking, warm-blooded animals (e.g., dangerous and endangered animals, cattle, and pets), can also be a heat source for the devices attached to their skin. In such cases the effectiveness of the thermoelectric conversion dramatically decreases due to the relative low temperature difference (in the range of 5 to 10° C) and also the low thermal conductivity of the heat source and the heat sink. As a result useful generators become too bulky [18]. The practical limit of energy production on man is approximately $30 \pm 2 \mu\text{Wcm}^{-2}$; an increased heat flow would cause the skin to cool down which is in most cases unacceptable [85]. Even so, practical applications of TEGs on human body have already been achieved [86].

Literature and information on specific design of thermoelectric generator based on micromachined thermopile is scarce. Still in the following sub-sections thermoelectric theory is briefly summarized along with a review of a few examples. Note that once again these examples were chosen based on their relevance to the development of TEGs and their applicability in WSNs.

5.2. OPERATING PRINCIPLE

In a thermoelectric material there are free electrons or holes that carry both charge and heat. When a temperature gradient is applied to such a material, the mobile charge carriers

³ Carnot efficiency is the maximum theoretical efficiency with which heat engines can convert thermal energy into useful power.

at the hot end diffuse to the cold end. Positive free charges (h^+) will produce a positive potential whereas negative free charges (e^-) will produce a negative potential. The buildup of charge carriers results in a net charge at the cold end, producing an electrostatic potential (voltage). This property, known as the Seebeck effect, is the basis of thermoelectric power generation [82].

The simplest voltage generator based on the Seebeck effect is the thermocouple. An enlarge detail in Figure 25 presents such a device, where one can distinguish two pillars, or legs, made of two different materials joined at one junction by a metal conductor. When a temperature difference is established between the top and the bottom of the pillars a voltage V develops between them at the unconnected end. This voltage is given by $V = \alpha \Delta T_{TEG}$, where α is the Seebeck coefficient between the two materials and ΔT_{TEG} is the effective temperature difference across the junctions. Semiconductors are typically used as pillars, as their Seebeck coefficient is large. Furthermore, since the sign of the Seebeck coefficient is positive for p-type and negative for n-type semiconductors, the contribution of the two pillars to the voltage adds up when semiconductors of opposite doping are used [45].

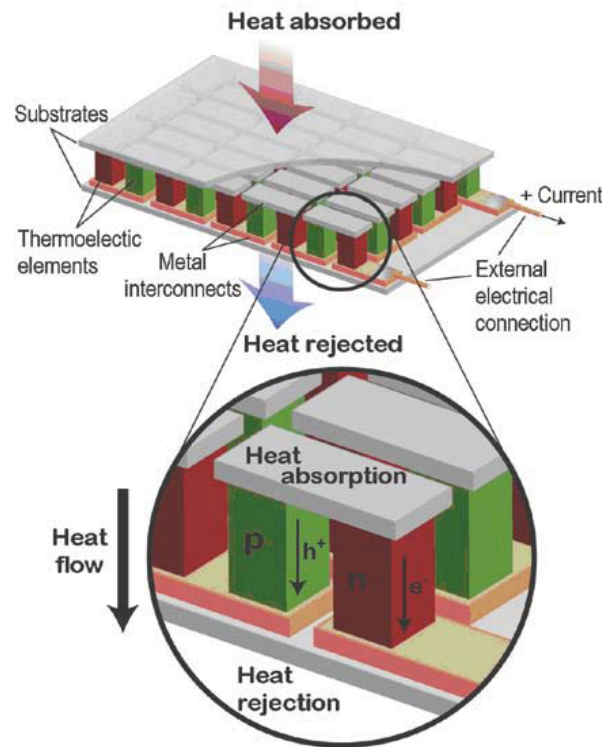


Figure 25 Schematic of a thermoelectric generator with an enlarge detail of a thermocouple [84].

A good thermoelectric material has a Seebeck coefficient between $100 \mu\text{VK}^{-1}$ and $300 \mu\text{VK}^{-1}$, which implies a very small voltage induced over a thermocouple. Thus, in order to make a thermoelectric generator (TEG) that can achieve a few volts at the load a thermopile is used. A thermopile is formed by a large number of thermocouples connected electrically in series by metal interconnects and sandwiched between two electrically insulating but thermally conducting ceramic plates (i.e. connected thermally in parallel) [84]. Besides the thermopile the thermal energy harvester may include (i) a radiator for efficient dissipation of heat in the ambient and (ii) specific structures (thermal shunts) aimed to direct the heat passing between the hot and cold plate into the thermocouple legs [45].

As it can be seen in Figure 25 a TEG uses the flow of heat across a temperature gradient to power an electric load through an external circuit. The temperature difference ΔT provides the voltage from the Seebeck effect, while the heat flow drives the electrical current and therefore determines the power output. It is important to notice that in a TEG, the effective temperature difference is always less than the external temperature difference ΔT across the ceramic plates.

If n is the total number of thermocouples, and α_p and α_n are the Seebeck coefficients for p-type and n-type material, respectively, the voltage developed by the TEG is given by (12).

$$V = n (\alpha_p - \alpha_n) (T_H - T_C) = n (\alpha_p - \alpha_n) \Delta T \quad (12)$$

The output power P is dependent on both the TEG electrical resistance R_{TEG} and the external load electrical resistance R_L :

$$P = \frac{V^2}{(R_{TEG} + R_L)^2} R_L = \frac{n^2 (\alpha_p - \alpha_n)^2 \Delta T^2}{(R_{TEG} + R_L)^2} R_L \quad (13)$$

The maximum electrical power is generated when the load R_L is matched to the electrical resistance of the generator R_{TEG} and when the thermal conductance of the thermocouples equals the one of the air between the plates. This is exactly true if considered that the TEG does not influence the heat flow.

$$P_{\max} = \frac{n^2(\alpha_p - \alpha_n)^2 \Delta T^2}{4R_{TEG}} \quad (14)$$

For a more detailed explanation on this subject, which takes into account the relationship between the effective temperature difference ΔT_{TEG} and the temperature difference applied externally ΔT , the reader is referred to [87].

5.3. THERMAL CONVERSION EFFICIENCY

A TEG converts heat Q into electrical power P with efficiency η .

$$P = \eta Q \quad (15)$$

Larger devices that use more heat will produce more energy. Similarly, the use of twice as many TEGs will naturally produce twice the energy given that they can capture twice the heat. Without a specific constraint on heat flux and system geometry, it is convenient to focus on power per unit area (P/A) produced and heat flux density (Q/A) rather than absolute power and heat consumed. This is particularly convenient for thermoelectric energy generation because as mentioned before these devices are so easily scalable that a large device can simply be an array of smaller modules [88].

The conversion efficiency depends heavily on the temperature difference ΔT across the device. This is because the TEG, like all heat engines that convert thermal energy into mechanical work, cannot have conversion efficiency greater than that of a Carnot cycle. The Carnot equation for the maximum theoretical efficiency of a heat engine connected to thermal reservoirs maintained at hot, T_{hot} , and cold, T_{cold} , temperatures is given by

$$\eta_{Carnot} = \frac{T_{hot} - T_{cold}}{T_{hot}} = \frac{\Delta T}{T_{hot}} \quad (16)$$

This equation is founded on the first and second laws of thermodynamics and serves as a “Gold Standard” for thermal-to-electric energy conversion [13].

While the exact thermoelectric materials’ efficiency is complex [89], the constant properties approximation (Seebeck coefficient, electrical conductivity, and thermal conductivity independent of temperature) leads to a simple expression for efficiency:

$$\eta = \frac{\Delta T}{T_{hot}} \cdot \frac{\sqrt{1+ZT}-1}{\sqrt{1+ZT}+T_{cold}/T_{hot}} \quad (17)$$

where the first term is the Carnot efficiency and ZT represents the relative magnitudes of electrical and thermal cross-effect transport in the used materials (i.e. the device figure of merit). A larger ZT indicates more efficient conversion of thermal to electric energy.

The efficiency of a thermoelectric generator increases nearly linearly with temperature difference. In energy harvesting applications where the temperature difference ΔT is small, the efficiency is, to a good approximation, directly proportional to the ΔT across the device. For good bismuth telluride (Bi_2Te_3) devices, the efficiency is approximately 0,04% for each 1 K of ΔT [82].

5.4. EXAMPLES AND APPLICATION OF THERMOELECTRIC GENERATORS

In a similar way to the evolution of microscale magnetic generators, the first applications of thermoelectric power generation for portable devices are found in the watch industry. The “Seiko Thermic” (Figure 26), a wristwatch powered by body heat was presented in December 1998. A thermoelectric generator with an overall size of 2 x 2 x 1,3 mm consisting of 52 pairs of elements was capable of producing under normal operation 22 μW of electrical power [86]. With only a 1,5 K temperature drop across the intricately machined thermoelectric modules, an output voltage of about 300 mV is generated and up converted to 1,5 V in order to power electronics. The conversion efficiency is about 0,1%.

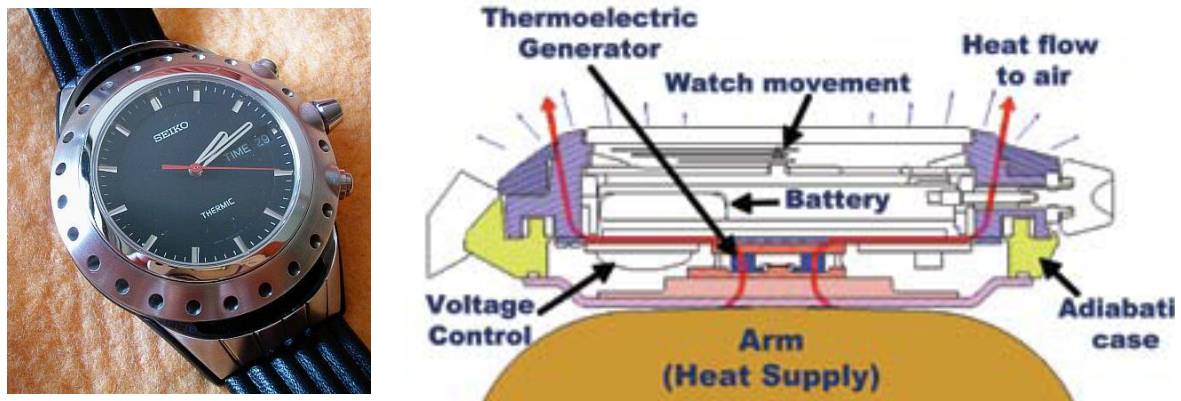


Figure 26 Seiko Thermic, a wristwatch powered by body heat using a thermoelectric generator (Copyright by Seiko Instruments Incorporated). Cross-sectional diagram [84].

Achieving miniaturized thermoelectric devices from bulk material was very complicated and represented high production costs and consequently very expensive final products. The problem of the handling limitations imposed by the semiconductor material properties lead to the development of a cost saving thin thermoelectric film technology in order to overcome these difficulties.

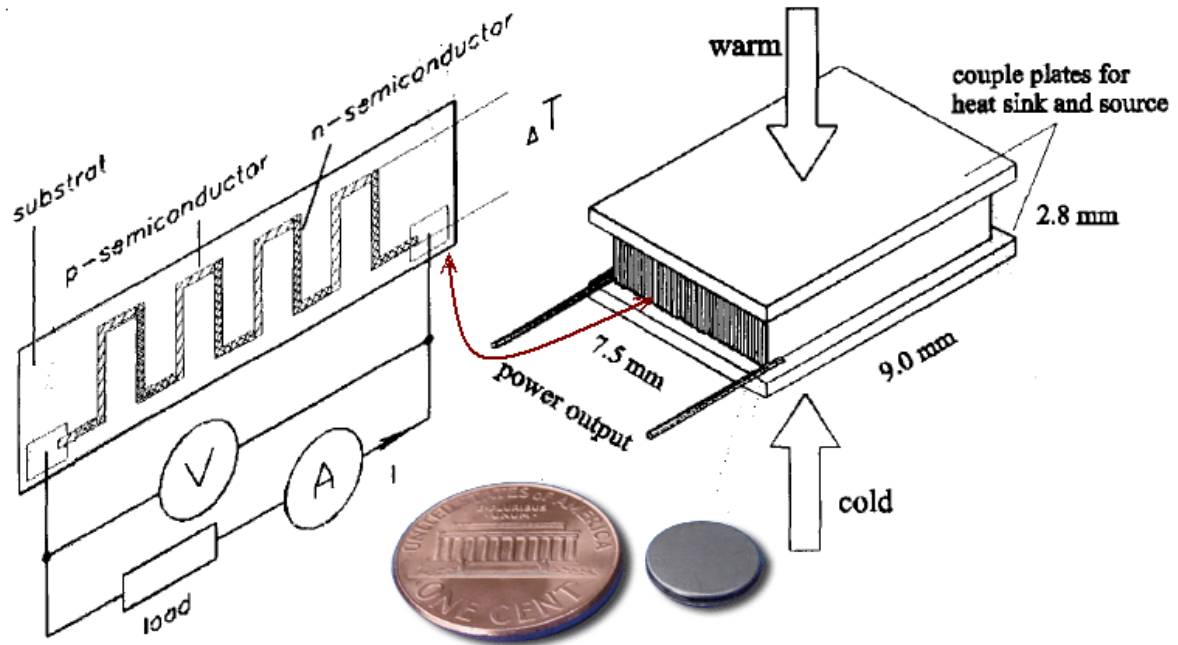


Figure 27 Construction of the LPTG in principle and the Thermo Life® button-type LPTG next to a penny. Image adapted from [90].

Stark et al [90] developed a low power thermoelectric generator (LPTG) consisting of a stack of 70 thin foil segments, each of them with a number of high sensitive thermocouples on it, which led to a series of 2250 thermocouples. The segments possessed an output voltage of about 8 mVK^{-1} . The stack was arranged between two thermal couple plates of ceramics for good thermal contacts to heat sink and source. The construction of the LPTG in principle is given in Figure 27. The device was introduced later in 2001 to the market by the company Thermo Life® Energy Corporation. The button-type LPTG also shown in Figure 27 has a surface of around 1 cm^2 and a height of about 3 mm and generates $30 \text{ }\mu\text{W}$ at 2,9 V under a temperature difference of only 5 K [91].

Thermopiles based on the deposition by sputtering of Bi_2Te_3 and subsequent dry-etch have been fabricated at Fraunhofer IPM in cooperation with Infineon [92]. The thermoelectric elements consist of n- and p-type semiconductor materials, which are separately produced and optimized on two different wafers. After sawing, the n- and p-parts are bonded

together to single devices. Using this wafer-based thin-film MEMS-like micro-structuring process, Micropelt today commercializes the MPG thermogenerators offering up to 100 thermoelectric leg pairs per mm^2 . As per Seebeck's law this translates into 1,4 V at a temperature difference of 10 °C. The smaller TEG (i.e. MPG-D651) measures 3,325 mm x 2,45 mm and around 1,1 mm of height. It can generate around 0,7 mW at 0,5 V under a temperature difference of 10 K [93]. Figure 28 presents the MPG-D651 TEG on top of the MPG-D751 TEG and a detailed view of the thermoelectric legs on silicon wafer.

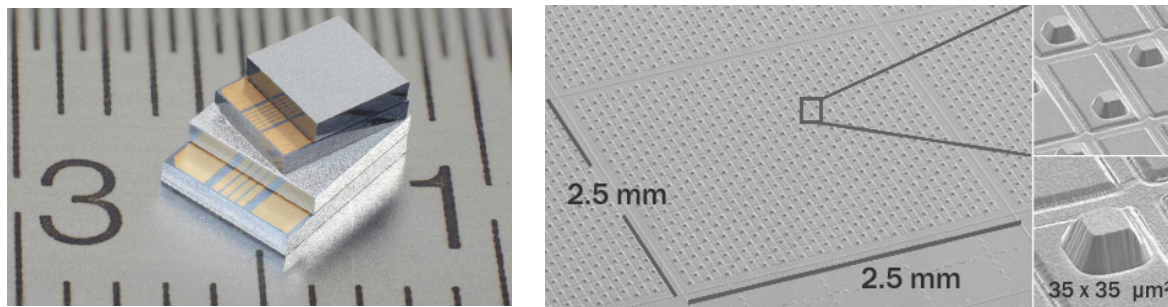


Figure 28 On the left the MPG-D651 and MPG-D751 proposed by Micropelt. On the right detailed view of a 2,5 mm x 2,5 mm wafer containing 578 thermoelectric couples [93].

The TE-Power NODE (60 mm x 25 mm x 30 mm) is the world's first, generic, fully integrated sensor node powered from waste heat. Micropelt manufactures this sensor node with a MPG-D751 TEG (4,2 mm x 3,2 mm), power management circuitry, and a Texas Instrument radio and micro-controller (CC2500 2,4 GHz; MSP430). The sensor node transmits every second whenever there is a temperature difference of 10 °C between heat source and ambient (3,5 °C effective temperature difference over the TEG). Sensor data provided include hot and cold side temperature of the TEG and output voltage [94].

Recently, thin film thermoelectric material has been integrated into the widely accepted copper pillar bumping process used in high-volume electronic packaging to achieve microscale power generation. This new thermoelectric technology, referred to as thermal copper pillar bump or “thermal bump” [95], was developed by Nextreme Thermal Solutions. Their eTEG HV14 (Figure 29 left) is capable of producing 9 mW of output power and an open circuit voltage of 0,3 V at a temperature difference of 50 K [96]. HV14 modules measuring just 1,8 mm x 1,5 mm can be configured electrically in series to produce higher voltage outputs.

In [97] the various steps in the development of a full-fledged TEG for human body applications is described. Due to its comparative advantages, such as lower thermal conductivity and ease of processing, over other materials, poly-SiGe was chosen to fabricate a surface micromachined thermopile for the device. For a wearable TEG made up of high-topography thermocouples the output power transferred to a matched external load is expected to be in excess of 2 μ W. According to the authors [98] the output performance can be further improved by mounting several thermopile chips together in the same wearable TEG, which is expected to fulfill the power consumption of miniaturized components in a typical wireless body sensor network. Figure 29 presents a photo of the surface micromachined poly-SiGe thermopile chips (on the center) and a photo of the wearable TEG (on the right), which is assembled from the thermopile chip and other components, such as a pin-featured radiator and a shock protection grid.

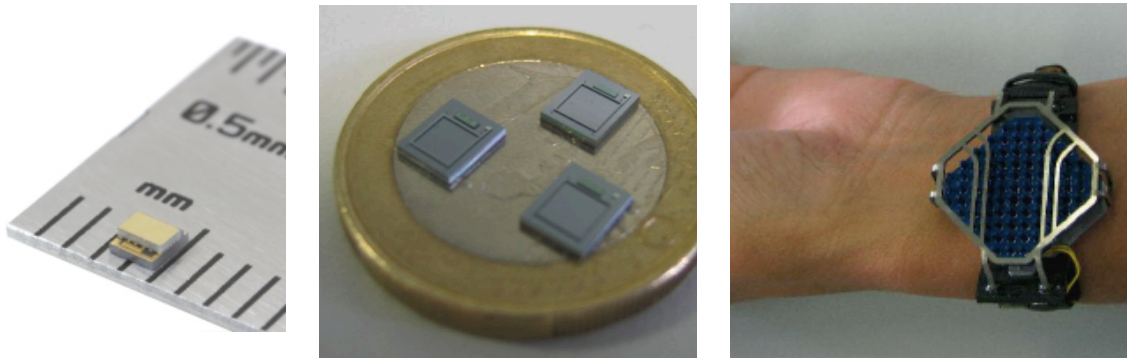


Figure 29 On the left the eTEG HV14 commercialized by Nextreme Thermal Solutions [96]. On the center a photo of the surface micromachined poly-SiGe thermopile chips and on the right a photo of a wearable TEG [98].

6. ENERGY CONSUMPTION OF COMMERCIAL HARDWARE PLATFORMS

6.1. INTRODUCTION

As presented in section 2, to achieve energetic sustainability in WSNs, sensor nodes cannot consume more energy than the one each can harvest. The math seems simple; the energy harvested by a sensor node minus the energy consumed by the sensor node cannot be less than zero.

In the previous sections one part of this problem (i.e. energy harvesting) was analyzed, by presenting different harvesting technologies along with several types of generators and their performance characteristics as energy sources. In this section, the other part (i.e. energy consumption) is considered so that the reader can have an idea of the energy values related to sensor nodes and better understand the problem of energetic sustainability in WSNs.

The current drawn by each of the components that forms a sensor node when in a determined state is usually provided by the component's supplier. Although an indicative

value, its usefulness regarding the overall energy consumption of the sensor node is very limited since that value depends not only on hardware platform features but also on how software manages hardware resources [99].

The general idea behind the energy consumption measurements carried out in the context of this MSc work, was to determine the energy consumed by each of the selected sensor nodes when performing pre-established, common tasks, like sleeping or transmitting. The chosen sensor nodes are some of the most widespread within the WSN community and represent the most common chipsets, as described later in Section 6.4. The tasks were chosen considering the weight that each one of them has in the lifetime of a sensor node and are also described later in Section 6.6.

Sensor data acquisition is one of the principal tasks of WSN platforms and an undoubted energy dissipation source [100]. However, the energy spent on those operations depends mostly on the type of used sensor(s) and on the application specificity. Therefore, sensing operations were not considered on these measurements.

Since many factors influence on the energy consumption, the obtained results are intended as an indication of the energy consumption under the given setup only. Nevertheless, they present a useful input to better understand the major contributors to the lifetime of a sensor node.

6.2. MEASUREMENT SETUP

The following setup was used to test the sensor nodes and an effort was made so that the testing conditions were the same for each of them. The measurements were made using the digital storage oscilloscope TEKTRONIX TDS2014B [101]. Results were acquired and exported to MS ExcelTM for further interpretation/analysis.

The oscilloscope provided three different graphical representations of the voltage drop over: a) a test resistor; b) the sensor node; and c) a trigger pin. Since there is a linear relationship between the voltage and current, the graphical representation of the voltage drop over the test resistor illustrated the current consumed by the sensor node.

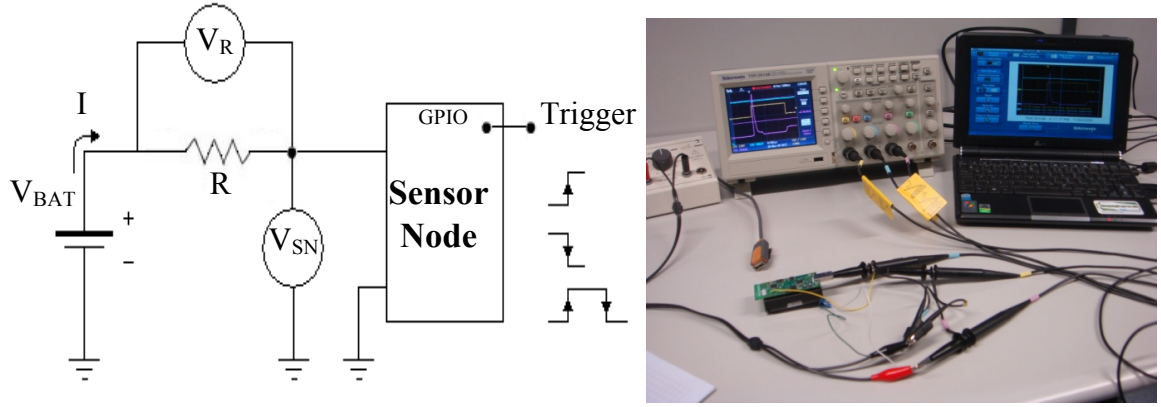


Figure 30 Schematic and picture of the measurement setup

The calculation of the current I was based on the well-known relation,

$$I = \frac{V_R}{R} \quad (18)$$

where V_R is the voltage drop over the test resistance and R is the test resistance value. By measuring at the power supply side, the test system observed the total current I consumed by the platform.

The voltage drop over the sensor node V_{SN} was also recorded, so that along with the value of the sampling interval used by the digital oscilloscope was possible to calculate the energy consumption and integrate such value to indirectly calculate the total energy consumed by each sensor node when performing the chosen task.

The selected value for the resistance was 5Ω so it wouldn't reduce much the effective voltage over the sensor node. Exceptionally, a value of 50Ω was used for the events where the current consumption was very low (e.g. sleeping), hence the voltage drop on the test resistance was negligible, in order to decrease the uncertainty in the measured values. For convenience a decade resistance box with an uncertainty of 1% was used.

As it was always necessary to synchronize event execution with data collection, a GPIO pin from the sensor node was used as the trigger source of the oscilloscope. In most operations the trigger pin was set and then cleared to mark the beginning and the end of an event, respectively, as shown in Figure 31a. In these cases, it was possible to calculate the total energy consumed by the sensor node when executing the chosen task by using only the data collected in-between the trigger events (rising and falling edges).

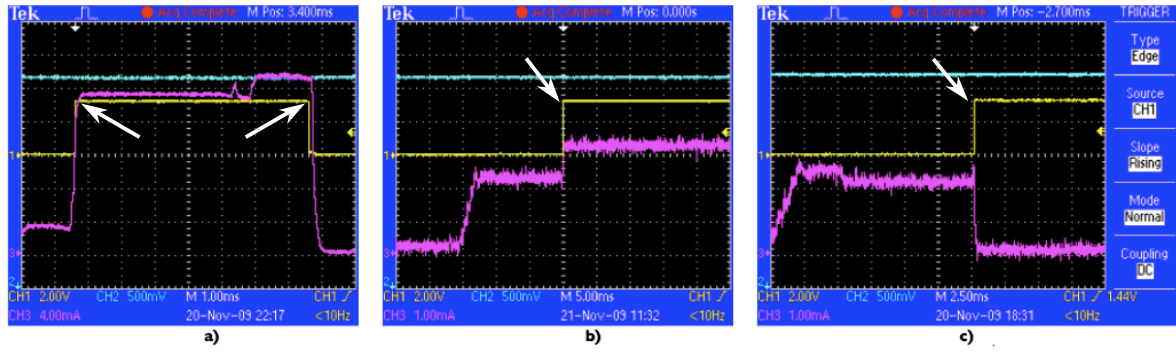


Figure 31 Synchronizing task execution with data collection when the chosen platform is: a) receiving a message; b) turning on a LED; c) booting. The yellow trace represents the trigger voltage, the blue trace the voltage drop over the sensor node and the pink trace the current consumed.





However, in order to keep the programs simple, in some tasks the trigger was used to mark only the beginning of the event (rising edge) (i.e. *SleepNoInterrupt* and *LEDTest* applications - Figure 31b) or the end of the event (falling edge) (i.e. *Booting* application - Figure 31c). In the first case, only the average power consumption was calculated, as the total energy consumption depends on the time that the sensor node is in the chosen state (e.g. the time chosen for the LED to be on). In the second case, the value calculated represents the energy consumed from the moment the platform was turned on until the trigger was set. The white arrows in Figure 31 identify the moments when the trigger occurs.

6.3. HARDWARE AND SOFTWARE

6.3.1. HARDWARE PLATFORMS UNDER TEST

Typically, sensor nodes are intended to be as small and inexpensive as possible, each equipped with at least a processing unit, a wireless communication interface, as well as sensors and/or actuators. The “mote” concept, originated at the University of California at Berkeley, has a broader adoption in the user and developer communities. The name was coined to indicate that they could be regarded as a sort of ‘smart dust’ (dictionary definition: mote = something, especially a bit of dust, that is so small it is almost impossible to see). It made sense to choose such disseminated designs for use in this setup as they represent the most common chipsets used in WSN platforms. Their main features are presented in Table 1. These platforms should be regarded as big form-factor prototypes for the much tinier versions that are expected in the coming years.

Table 1 WSN hardware platforms used in the measurements

Wireless Sensor Network Platforms				
Model	MICA2	MICAz	TelosB	Iris
				
Release year	2002	2004	2005	2007
Microcontroller				
Manufacturer	Atmel	Atmel	Texas Instruments	Atmel
Model	ATmega128L	ATmega128L	MSP430	ATmega1281
Processor performance	8-bit RISC	8-bit RISC	16-bit RISC	8-bit RISC
Program flash memory (kB)	128	128	48	128
RAM (kB)	4	4	10	8
Configuration EEPROM (kB)	4	4	16	4
Analog to digital converter	10 bit ADC	10 bit ADC	12 bit ADC	10 bit ADC
RF transceiver				
Chip	CC1000	CC2420	CC2420	AT86RF230
Radio frequency (MHz)	915	2400	2400	2400
Maximum data rate (kb/s)	38,4	250	250	250

The development of such devices started in 1998 with the WeC mote along with the development of an operating system, the TinyOS [1], which has since grown to involve thousands of academic and commercial developers as well as users worldwide.

6.3.2. OPERATING SYSTEM AND PROGRAMMING LANGUAGE

TinyOS is a free and open-source operating system specially designed for embedded systems such as sensor networks. It features a component-based architecture that enables rapid innovation and implementation while minimizing code size as required by the severe memory constraints inherent in WSNs [102]. It also differs from traditional operating system models in that events drive the behavior of the system. In this particular experiments, TinyOS v2.x was used.

nesC [103] is an extension to the C programming language designed to embody the structuring concepts and execution model of TinyOS. Applications are built in nesC by

linking components that interact by providing or using interfaces. An interface lists one or more functions, tagged as commands or events. Commands are used to start operations, while events are used to collect the results asynchronously. An example of an interface is shown in Figure 32.

```
(1) interface AMSend {
(2)   command error_t send (am_addr_t addr, message_t * msg, uint8_t
      len);
(3)   command error_t cancel ( message_t * msg );
(4)   event void sendDone ( message_t * msg, error_t error );
(5)   command uint8_t maxPayloadLength ();
(6)   command void * getPayload ( message_t * msg, uint8_t len );
(7)}
```

Figure 32 nesC Active Message interface.

A component providing an interface implements the commands it declares, whereas the one using the interface implements its events. Therefore, data may flow both ways between components connected through the same interface [104].

There are two types of components in nesC: modules and configurations. Modules provide the implementations of one or more interfaces. Configurations are used to wire other components together, connecting interfaces used by components to interfaces provided by others. Every nesC application is described by a top-level configuration that wires components [105].

6.4. EXPERIMENTAL ANALYSIS

The following programs were written using a pre-configured Xubuntu virtual machine [106] that runs in VMware player, since it was the fastest way to get started using TinyOS.

In some cases, the programs could be reduced in size and complexity, leading to an almost certainly lower energy consumption, if fewer checks were used. However, the idea was to approximate the programming methodology as close as possible to the one used in a real scenario. This led to the adoption of a defensive programming style, usually applied in large WSNs to decrease the possibility of a failure.

The programs represent a few tasks usually implemented in WSNs applications: booting, sleeping, setting a LED, and transmitting and receiving a message. A short introduction is provided for each of these programs, for better understanding of what was being measured and why.

6.4.1. BOOTING

In the first WSNs, sensor nodes were started once and remained in operation until their battery ran out. In addition, unless the source of energy was replenished, they could no longer fulfill their role. In other words, it did not matter the energy spent by the sensor node to boot because this was done only once when its battery was at full charge. However, the tendency is for WSNs to be powered mainly by energy harvesting [34]. Some authors go even further and idealize WSNs powered solely by energy harvesting which they refer to as WSN Powered by Ambient Energy Harvesting (WSN-HEAP) [8].

In these second types of WSNs, nodes have to automatically suspend the service completely when enough energy is not available to even remain in sleep mode. On the other hand they should be able to wakeup again when an adequate amount of energy has been harvested to support initialization. The booting program was therefore used to measure the energy needed by each of the sensor nodes to boot up.

The TinyOS 2.x boot sequence uses three interfaces: *Init*, for initializing component/hardware state; *Scheduler*, for initializing and running tasks; and *Boot*, for signaling that the system has successfully booted. In the applications page of the TinyOs Community Forum [107] a program called *PowerUp* is available to test that the build environment is functional and that an application correctly installs on a piece of hardware. It simply turns on LED0 on power up. In order to measure the energy required by each sensor node to boot, the program was modified so that when the system boots, instead of turning on LED0, it sets the trigger pin. A portion of the application code is shown below.

```
(1) implementation {
(2)   event void Boot.booted() {
(3)       // This event signals that the system has completed booting
(4)       //call Leds.led0On(); Original code commented
(5)       call Trigger.set();      //Stop the measurements
(6)   }
(7) }
```

Figure 33 Booting implementation

Figure 34 depicts the traces of the current consumed by each platform when booting. It is clear that TelosB uses up much less energy to boot than the others. In fact, the difference is so pronounced that in order to make its trace perceptible the figure had to be enlarged.

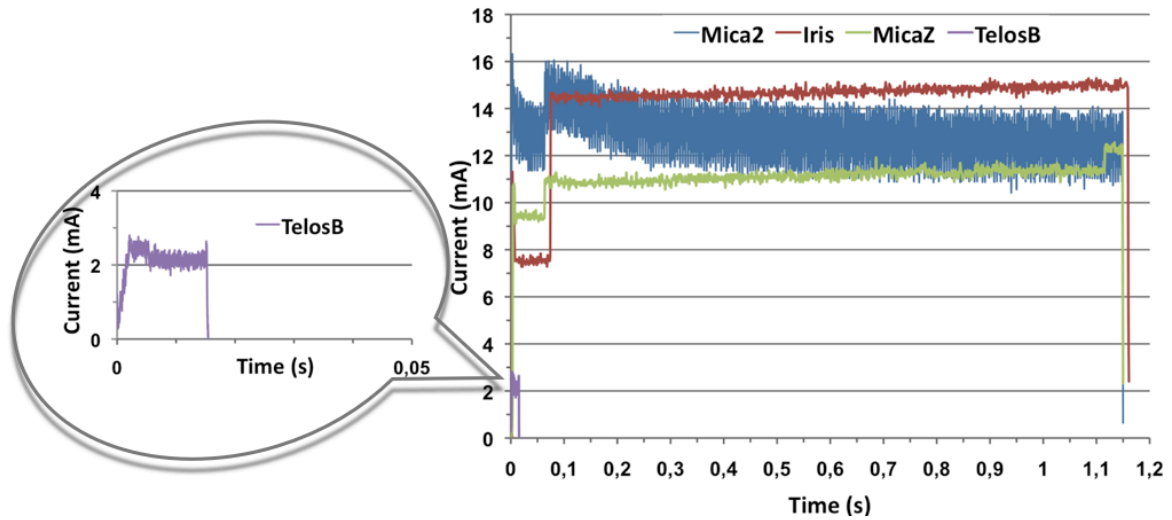


Figure 34 Traces of current consumption for each platform when booting

The performed calculations, presented in Table 2, revealed that the Iris is the one that consumes more energy when booting, approximately 53,38 mJ against the 0,103 mJ consumed by the TelosB. Note that for the calculation of the energy consumed when booting, only the values collected until the trigger was set (rising edge) were used.

Table 2 Energy spent by each sensor node to boot

	Mica2	MicaZ	TelosB	Iris
Energy spent in booting (mJ)	47,74	40,97	0,103	53,38

6.4.2. LOW POWER MODES

As sensor nodes spend most of their time sleeping, it was important to measure how much energy each expends when in that state. However, that is not as simple as it may look as processors usually have a wide spectrum of power states. For example, the MSP430 (present in the TelosB platform) has one active mode (issuing instructions) and five low-power modes. The low-power modes range from LPM0, which disables only the CPU and main system clock, to LPM4, which disables the CPU, all clocks, and the oscillator, expecting to be woken by an external interrupt source.

Manually choosing the lowest possible power state in which the microcontroller should be requires knowing a great deal about the power state of many subsystems and their peripherals. Therefore such decision was left to the OS (like an application programmer

would do), which is responsible for putting the processor into a low power state that can satisfy application requirements whenever the task queue is empty.

Two programs with different requirements were written for measuring the energy consumption of the sensor nodes when sleeping. The *SleepNoInterrupt* application does not use any timers to drive an interrupt service routine, so the platforms enter a low power state right after they have finished booting. In the case of the *SleepPeriodicInterrupt*, the system boots and before it enters a low power state a timer is set to fire periodically every few milliseconds and drive an interrupt service routine.

6.4.2.1. JUST SLEEPING

Once all initialization has completed the *Boot.booted()* event is signaled and TinyOS enters its core scheduling loop. The scheduler runs as long as there are tasks on the queue. As soon as it detects an empty queue, the scheduler puts the microcontroller into the lowest power state allowed by the active hardware resources.

The *SleepNoInterrupt* (SNI) application, sets the trigger after the system has booted and explicitly instructs the MCU to enter a low power state by calling the *McuSleep.sleep()* command. A fragment of the application code is shown below.

```
(1) implementation {
(2)   event void Boot.booted() {
(3)       call Trigger.set();      // Start the measurements
(4)       call McuSleep.sleep();
(5)   }
(6) }
```

Figure 35 *SleepNoInterrupt* implementation

The above application was installed and executed on all sensor nodes except on the Iris. In that particular case, the radio had to be turned off before doing any measurements otherwise the current drawn was around a few mA. Table 3 shows the average power (P_{avg}) consumed by each sensor node when sleeping without any interruptions.

Table 3 Average power consumed by each sensor node when sleeping without the use of any timer

	Mica2	MicaZ	TelosB	Iris
$P_{avg} (mW)$	0,2841	0,0456	0,0489	0,0327

To determine the energy consumption of the sensor nodes when sleeping with no interruptions (E_{SNI}), for a total time of t seconds, the following equation applies:

$$E_{SNI} = P_{avg} \cdot t \quad (19)$$

6.4.2.2. SLEEPING WITH PERIODIC INTERRUPTIONS

The *SleepPeriodicInterrupt* application adds a timer to the previous program simulating a scenario where a sensor node has to wake up from time to time to do some work. The aim was to verify if there was a significant increase in energy consumption caused by the periodic timer interruptions.

The following code uses an instance of the interface *Timer<TMilli>* named *Timer0*. The *<TMilli>* syntax simply supplies the generic *Timer* interface with the required timer precision. The dummy type *TMilli* represents milliseconds, that is, one second contains 1024 binary milliseconds. As in the previous application, the radio of the Iris had to be turned off before the measurements.

```
(1) implementation {
(2)   event void Boot.booted() {
(3)       call Trigger.set();           // Start the measurements
(4)       call Timer0.startPeriodic(t); // Fires every t (ms)
(5)       call McuSleep.sleep();
(6)   }
(7)   event void Timer0.fired() {
(8)       call Trigger.clr();           // Stop the measurements
(9)   }
(10) }
```

Figure 36 Implementation of the *SleepPeriodicInterrupt* application

After running the application, it was noticed that in addition to the expected current peaks due to timer interruptions and interrupt service routines handling, there were also smaller peaks in between, which were later related with the timer's reload event. Figure 37 shows the traces obtained for both the TelosB and Micaz when the periodic timer was set with the decimal values of 2048 and 384 respectively. These values were chosen so that it was possible to visualize (in the oscilloscope) the timer reload event associated to the 16-bit counter of TelosB and the 8-bit counter of Micaz.

The traces obtained for the Iris and Mica2 are similar to the traces presented for the MicaZ. Note that in the case of TelosB (illustration on the left), a vertical division represents a current ten times smaller than in the case of the remaining sensor nodes.

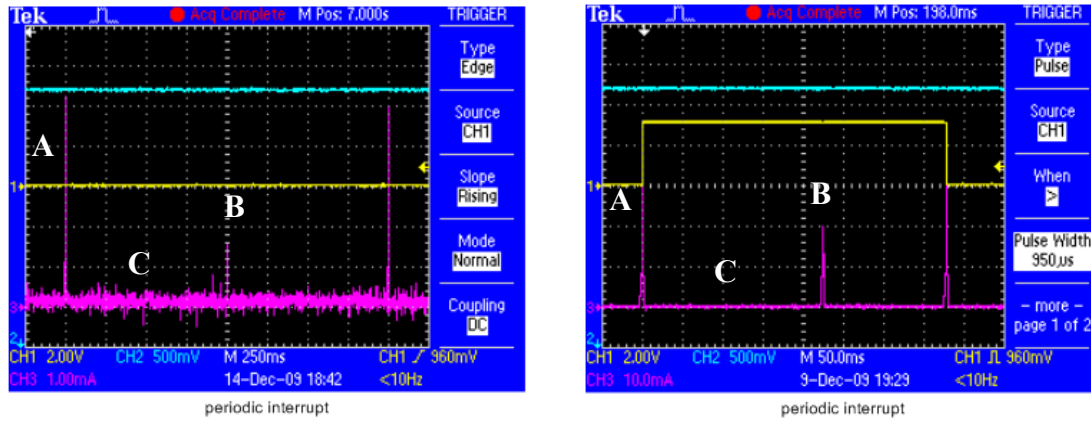


Figure 37 Traces obtained for TelosB and MicaZ for the *SleepPeriodicInterrupt* application

The events marked in Figure 37 were analyzed individually: “A” represents the timer’s interruption event characterized by its energy consumption E_{int} and duration t_{int} ; “B” corresponds to the timer’s reload event characterized again by its energy consumption E_{rld} and duration t_{rld} and also by its reload periodicity T_{rld} ; and “C” stands for the average power consumed P_{avg} when the platforms are sleeping with the timer running in the background. Table 4 presents the obtained results for the four platforms.

Table 4 Values obtained for each platform when sleeping with the use of a timer

		Mica2	MicaZ	TelosB	Iris
A	$E_{int} (mJ)$	0,0189	0,0140	0,0022	0,0178
	$t_{int} (ms)$	4,868	5,840	2,558	7,896
B	$E_{rld} (mJ)$	0,0167	0,0110	0,0008	0,0136
	$t_{rld} (ms)$	4,840	5,820	2,728	7,360
	$T_{rld} (ms)$	225	225	1000	225
C	$P_{avg} (mW)$	0,4516	0,0624	0,0499	0,0522

As expected, the average power consumed when the platforms are sleeping rises with the use of a timer. That increase is quite significant even if only the values of the average power presented in Tables 3 and 4 are compared: approximately 59%, 37% and 60% for Mica2, MicaZ and Iris, respectively. The exception is TelosB with a rise of only about 2% in its average power consumption.

In spite of that, to accurately determine the increase in energy consumption due to the use of a timer, the energy spent when the timer interrupts and when the timer reloads has also to be considered. The following equation was used to determine the energy consumption of

the sensor nodes when sleeping with periodic interruptions (E_{SPI}), for a total time of t seconds,

$$E_{SPI} = \frac{t}{T_{tmr}} \times (E_{int} + P_{avg} \cdot t_{slp} + n \cdot E_{rld}) + E_{int} \quad (20)$$

where:

T_{tmr} - is the period of the timer (s)

E_{int} - is the energy consumed due to the timer's interruption (mJ)

P_{avg} - is the average power consumed when sleeping with periodic interruptions (mW)

E_{rld} - is the energy consumed due to the timer's reload (mJ)

t_{slp} is the expended time between two interruptions (i.e. the timer's period T_{tmr}) minus the time spent by the timer's reload (t_{rld}) and interruption (t_{int}) events. This value is given as follows:

$$t_{slp} = T_{tmr} - t_{int} - n \cdot t_{rld} \quad (21)$$

In equations 20 and 21 n represents the number of reload events that occur in a timer's period. This value is given by the following equation, where T_{rld} is the timer's reload period.

$$n = \left\lfloor \frac{T_{tmr} - t_{int}}{T_{rld}} \right\rfloor \quad (22)$$

Table 5 presents the energy consumption of the sensor nodes for both the *SleepNoInterrupt* and *SleepPeriodicInterrupt* applications obtained by applying equations 19 and 20 respectively, for a total time t of 3600 s and an interruption (T_{tmr}) every 60 seconds. It is clear the increase in the energy consumption of the sensor nodes when in sleep state due to the use of the timer.

Table 5 Energy increase in the energy consumption of the platforms when in a sleep state due to the use of a timer ($t = 3600$ s and $T_{tmr} = 60$ s)

	Mica2	MicaZ	TelosB	Iris
E_{SNI} (mJ)	1022,76	164,16	176,04	117,72
E_{SPI} (mJ)	1861,60	398,05	182,54	403,54
Energy Increase	82,03%	142,48%	3,69%	242,79%

The rise in energy consumption is very substantial and can be related mainly to the energy expended by the timer to reload. With exception to the TelosB platform, the energy consumed when the timer reloads is very close to the one used when the timer interrupts (see Table 4), which it is not significant in a one-time occurrence. However, one must note that a reload event occurs every 225 milliseconds in the case of the Atmel's 8-bit counter and every 1 second in the case of the TI's 16-bit counter.

6.4.3. LEDs TEST

All tested sensor nodes have three different LEDs, which are typically used for program debugging. In some WSNs applications however, LEDs are set at specific points in the code to provide visual information for diagnose purposes (e.g. indication of a successful reception), in spite of the obvious increase in the energy consumption. This program is intended to evaluate the LEDs consumption.

```
...
(1) event void AMControl.stopDone(error_t err) {
(2)   call Trigger.set();      // Start the measurements
(3)   call Leds.led0On();      // Turn on LED 0
(4) }
...
```

Figure 38 LEDTest implementation

The *LedTest* program is similar to the one used for testing the sleep state. The difference is that when the radio-stop event fires, a command sets the chosen LED, as shown in Figure 38. The average power and current consumption of the platforms for each LED are resumed in Table 6.

Table 6 Consumption for each sensor node with each LED on

		Mica2	MicaZ	TelosB	Iris
LED 0	P(mW)	10,97	9,05	10,09	9,65
	I (mA)	3,44	2,83	3,16	3,02
LED 1	P(mW)	10,02	8,48	14,89	8,93
	I (mA)	3,14	2,65	4,67	2,79
LED 2	P(mW)	10,51	8,79	10,61	9,08
	I (mA)	3,29	2,75	3,32	2,84

The results are worthy of note as they show that each LED requires different current draw and the variances are in some cases very significant. As an example one can consider a simple case where a LED is on five seconds each minute to provide some kind of visual information. In such scenario choosing TelosB LED 1 instead of LED 0, represents an energy consumption of approximately more 35 J a day.

This means that in such energy constrained networks like WSNs even the slightest and apparently insignificant detail like choosing which LED to use, will influence the total lifetime of the sensor nodes and consequently the total lifetime of the WSN.

6.4.4. TRANSMITTING AND RECEIVING

Transmitting and receiving sensing information is one of the most energy consuming features of a WSN node. Three different programs were written to measure the energy spent by each sensor node to realize simple tasks like initializing the radio, building and sending a message and receiving a message.

6.4.4.1. INITIALIZING THE RADIO

The *RadioInit* program is used to measure the energy spent by the platforms when initializing the transceiver installed in each of them. The tested models were the TI's CC1000 used by Mica2, the TI's CC2420 used by both the Micaz and TelosB, and the Atmel's RF230 used by the IRIS.

```
(1) implementation {
(2)   event void Boot.booted() {
(3)       call Timer0.startOneShot(t); // Fires once in t (ms)
(4)   }
(5)   event void Timer0.fired() {
(6)       call Trigger.set();           // Start the measurements
(7)       call AMControl.start();       // Start the radio
(8)   }
(9)   event void AMControl.startDone(error_t err) {
(10)      if (err == SUCCESS) {
(11)          call Trigger.clr();       // Stop the measurements
(12)      }
(13)      else {
(14)          call AMControl.start(); //Try again to start the
radio
(15)      }
(16)  }
(17) ...
(18) }
```

Figure 39 Implementation of the *RadioInit* application

The program sets a one shot timer after the system has completed booting. When the timer fires, the trigger pin is set and the radio initialization is called. Next, when the radio startDone-event fires, the trigger pin is cleared, indicating the end of the measurements. The timer was used so that the measurements began only after the consumption had stabilized at a sleep-state level.

Figure 40 illustrates the traces of the current consumed by each platform to initialize the radio. As expected, the platforms using the CC2420 transceiver have similar traces, yet the MicaZ spends more energy than TelosB to do the same task. With respect to the remaining sensor nodes the traces show that the Iris initializes the radio faster than the others despite its consumption being similar to the TelosB. The results are presented in Table 7.

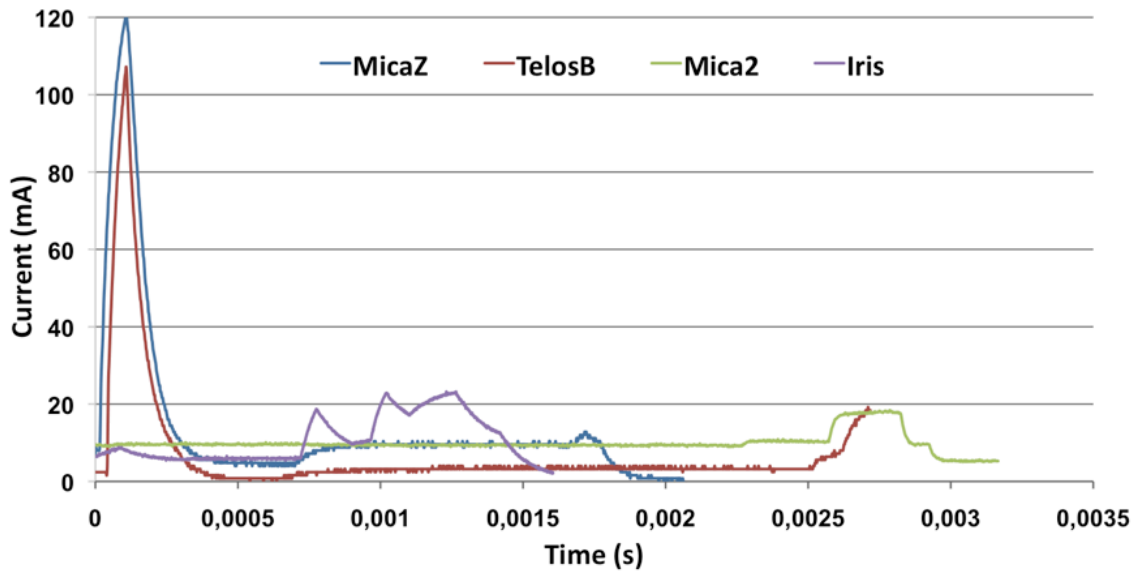


Figure 40 Traces of the current consumed by each of the sensor nodes when initializing the radio

Table 7 Energy consumed by each sensor node for initializing the radio

	E (mJ)			
	Mica2	MicaZ	TelosB	Iris
Initializing	0,101	0,094	0,063	0,055

6.4.4.2. SENDING A MESSAGE

The *Mote-mote radio communication* tutorial [107] introduces interfaces and components that support communications in TinyOS. All of these interfaces and components use a common message buffer abstraction, called *message_t*, which has the following structure.

```

(1) typedef nx_struct message_t {
(2)   nx_uint8_t header[sizeof(message_header_t)];
(3)   nx_uint8_t data[TOSH_DATA_LENGTH];
(4)   nx_uint8_t footer[sizeof(message_footer_t)];
(5)   nx_uint8_t metadata[sizeof(message_metadata_t)];
(6) } message_t;

```

Figure 41 Structure of the common message buffer abstraction called *message_t*

This format keeps the data (payload) at a fixed offset on a platform, avoiding a copy when a message is passed between two link layers. The header, footer, and metadata fields are all opaque and cannot be accessed directly. Instead, data-link layers provide access to the *message_t* fields through nesC interfaces. As some of these interfaces were used for implementing the *RadioSend* program, a brief explanation of each is given in the ensuing text.

The *Packet* interface provides the basic assessors for the *message_t* abstract data type. This interface makes available commands for clearing a message's contents, getting its payload length, and getting a pointer to its payload area. For sending a message or canceling a pending message send, the *Send* interface can be used. This interface also provides an event to indicate whether a message was sent successfully or not.

Since it is very common to have multiple services using the same radio to communicate, TinyOS provides the Active Message (AM) layer to multiplex access to the radio. The term AM type refers to the field used for multiplexing. To support the AM services additional interfaces named *AMPacket* and *AMSend* are available. The key difference between *AMSend* and *Send* is that *AMSend* takes a destination AM address in its send command.

The *RadioSend* program is based on the exercise proposed in the tutorial mentioned above. The exercise increments a counter, displays the counter's three least significant bits on the three LEDs, and sends a message over the radio. Some modifications were made so that it was feasible to only measure the energy spent by each sensor node on building and sending a pre-defined message called *RadioSendMsg*. The message sends both the node identification and the counter value over the radio. Rather than directly writing and reading the payload area of the *message_t* with this data, a structure was used to hold them and then use structure assignment to copy the data into the message payload area. The defined structure is shown below.

```

(1) typedef nx_struct RadioSendMsg {
(2)   nx_uint16_t nodeid;
(3)   nx_uint16_t counter;
(4) } RadioSendMsg;

```

Figure 42 Structure used to hold the node identification and the counter value

This syntax is similar to the one used to define a C structure with the difference of the `nx_` prefix on the keywords `struct` and `uint16_t`. The `nx_` prefix is specific to the `nesC` language and indicates that the `struct` and `uint16_t` are external types, which means they have the same representation on all platforms. The following code outlines the sending mechanism implementation of the *RadioSend* program.

```

(1) implementation {
(2)   uint16_t counter = 0;
(3)   message_t pkt;
(4)   bool busy = FALSE;
(5)   ...
(6)   event void Timer0.fired() {
(7)       counter++;
(8)       call Trigger.set();           // Start the measurements
(9)       if (!busy) {
(10)          RadioSendMsg* pointer = (RadioSendMsg*) (call
              Packet.getPayload(&pkt, sizeof(RadioSendMsg)));
(11)          pointer->nodeid = TOS_NODE_ID;
(12)          pointer->counter = counter;
(13)          if (call AMSend.send(AM_BROADCAST_ADDR, &pkt,
              sizeof(RadioSendMsg)) == SUCCESS) {
(14)              busy = TRUE;
(15)          }
(16)      }
(17) }
(18) event void AMSend.sendDone(message_t* msg, error_t err) {
(19)     if (&pkt == msg) {
(20)         call Trigger.clr();         // Stop the measurements
(21)         busy = FALSE;
(22)     }
(23) }
(24) ...
(25) }

```

Figure 43 Implementation of the *RadioSend* application

First, the program ensures that a message transmission is not in progress by checking the busy flag. Then it gets the packet's payload portion and casts it to a pointer to the previously declared *RadioSendMsg* external type. It then uses this pointer to initialize the packet's fields, and afterwards send the packet by calling *AMSend.send*. The packet is sent to all nodes in radio range by specifying the broadcast address (`AM_BROADCAST_ADDR`) as the destination address. The test against `SUCCESS` verifies that the AM layer accepted the message for transmission. If so, the busy flag is set to true. Finally, the *AMSend.sendDone* event signals whether the message was transmitted successfully or not. Another check ensures that the message buffer that was signaled is the

same as the local message buffer and if so, the measurements are stopped and the busy flag is cleared indicating that the message buffer can be reused.

Measurements were made for both the maximum and minimum transmission power of each sensor node. With exception to Mica2, the transmission power was chosen by setting the following makefile variables known as CFLAGS.

```
CFLAGS += -DCC2420_DEF_RFPOWER= power_level    (MicaZ and TelosB)
CFLAGS += -DRF230_DEF_RFPOWER= power_level    (Iris)
```

Figure 44 CFLAGS used to set the transmission power for different platforms

For the platforms with a CC2420 transceiver the maximum and minimum output power is 0 dBm and – 25 dBm, which were obtained by replacing the *power_level* parameter for the values 31 and 3, respectively. For the AT86RF230 transceiver the output power can be varied in 16 levels ranging from -17,2 dBm to 3 dBm, which correspond to a *power_level* parameter of 0 and 15 respectively.

In the case of Mica2 the transmission power was chosen by using the *setRFPower* command from the CC1000Control interface shown in Figure 45. The CC1000 output power is programmable in steps of 1 dB, ranging from -20 dBm to 5 dBm. The *power_level* parameter was set to 0x02 for the minimum output power and to 0xFF for the maximum output power. The obtained results are shown in Table 8.

```
call CC1000Control.setRFPower(power_level);
```

Figure 45 The *setRFPower* command for Mica2

Table 8 Energy consumed by each sensor node for sending a message

		E (mJ)			
		Mica2	MicaZ	TelosB	Iris
Sending	Maximum	1,700	0,584	0,467	0,123
	Minimum	0,985	0,553	0,446	0,108

6.4.4.3. RECEIVING A MESSAGE

Another interface had to be used so that the *RadioSendMsg* sent by a platform running the *RadioSend* application was received by another platform. The *Receive* interface is the one that provides an event for receiving messages. It also provides, for convenience, commands for getting a message's payload length and getting a pointer to a message's

payload area. Message reception is an event-driven process so there was no need to call any commands on the *Receive*. The code shown below is the implementation of the *Receive.receive* event handler.

```
(1) event message_t* Receive.receive(message_t* msg, void* payload,
    uint8_t len) {
(2)   if (len == sizeof(RadioSendMsg)) {
(3)       call Trigger.clr();           // Stop the measurements
(4)   }
(5)   return msg;
(6) }
```

Figure 46 Implementation of the *Receive.receive* event

The receive event handler performs some simple operations. It ensures that the length of the message is what was expected, and if so, calls the command that clears the trigger. In the case of the *RadioReceive* application the trigger was set as soon as the radio finished its initialization.

Table 9 Energy consumed by each sensor node for receiving a message

	E (mJ)			
	Mica2	MicaZ	TelosB	Iris
Receiving	0,829	0,693	0,438	0,153

6.4.5. SUMMARY

The energy measurements made for each platform are resumed in Table 10. Note that for the *SleepNoInterrupt* and *SleepPeriodicInterrupt* applications the values presented are for a total time of 3600 s, and that in the particular case of the *SleepPeriodicInterrupt*, an interruption occurs every 60 seconds.

Table 10 Summary of the energy measurements for each sensor node

	E (mJ)			
	Mica2	MicaZ	TelosB	Iris
Booting	47,74	40,97	0,103	53,58
Sleeping with no interruptions	1022,76	164,16	176,04	117,72
Sleeping with periodic Interruptions	1861,60	398,05	182,54	403,54
Initializing the radio	0,101	0,094	0,063	0,055
Receiving a message	0,829	0,693	0,438	0,153
Transmitting a message	1,700	0,584	0,467	0,123
Less consuming LED on for 1 s	10,02	8,48	10,09	8,93

From the table it is clear that the Iris, equipped with the AT86RF230 transceiver, is the less consuming sensor node when dealing with any of the different radio events. As to the sensor nodes using the CC2420 transceiver, once again they present similar energy consumption, yet MicaZ spends more energy than TelosB to do the same task.

As for the energy consumed during the sleeping with periodic interruptions, the most efficient sensor node is TelosB. The difference in consumption when compared with the second less consuming sensor node is more than half the energy. Note that as mentioned earlier TelosB uses a 16-bit counter while the others sensor nodes use a 8-bit counter.

For better understanding these numbers the following scenario will be considered. Each sensor node wakes up once every 60 seconds, initializes its radio, receives and transmits a message and in the end turns on its less consuming LED for one second. Table 11 presents the energy spent by each platform when performing this set of tasks, and the total energy spent by each of them during one hour, one day and one year.

Table 11 Total energy consumption of each sensor node in a simple scenario

	E (mJ)			
	Mica2	MicaZ	TelosB	Iris
Booting	47,74	40,97	0,103	53,58
Sleeping with periodic Interruptions	1861,60	398,05	182,54	403,54
Initializing the radio	6,06	5,64	3,78	3,30
Receiving a message	49,74	41,58	26,28	9,18
Transmitting a message	102	35,04	28,02	7,38
Less consuming LED	601,2	508,8	605,4	535,8
Total energy spent in 1-hour (mJ)	2668,34	1030,08	846,12	1012,58
Total energy spent in 1-day (J)	64,04	24,72	20,31	24,30
Total energy spent in 1-year (J)	23374,66	9023,50	7412,04	8870,20

Considering an energy source consisting in two AA batteries with a total energy of 20000 J, TelosB (ideally) would be capable of sustaining operation during 984 days. For an energy harvester to sustain the same operation for the same time, it would have to produce an average power of 235 μ W. If the LED wasn't used (normally it isn't) this value would decrease to 66,78 μ W, which is a very acceptable value for a today's harvester to achieve.

7. CONCLUSIONS AND FUTURE WORK

There are no doubts that WSNs have the potential to emerge as the intelligent choice for underlying communication infrastructures for many different applications [11]. However, for that to happen several steps have first to be fulfilled.

This thesis presented the concepts of *energy conservation* and *energy efficiency*, which together can reduce the *energy consumption* of a sensor node. Energy conservation techniques affect the energy consumption but are specific to the application. As a result, the influence they have in the energy consumption of a sensor node can only be assessed on a case-by-case basis. On the other hand, it is easier to evaluate how energy efficiency affects the energy consumed by a sensor node. The energy measurements presented show that not only it is important to choose the most efficient chipsets and components that form the sensor node but also study the efficiency of the all set. The concept of *energy harvesting* and several harvesting technologies were also presented along with many (feasible) options for energy generation. As each option has its own constraints, it is unlikely that one option can serve all application fields.

The work presented in this thesis implies that self-sustainable, large sensor nodes are today feasible, which means that current energy scavenging technologies are able to sustain the operation of wireless sensor networks. Such sensor nodes are characterized by their low energy consumption and their capability of harvesting from the surrounding environment the energy needed to operate perennially. The choice of harvesting principle will depend on the application and the environment in which it is used.

Everyone likes to use and take advantage of new technologies but few like to “see” it. This has lead to the assumption that sensor nodes have to be smaller and smaller, almost invisible, so they can be accepted. It is my opinion however, that such an assumption is not correct. It is true that certain applications (e.g. the ones related to the human body) demand for true MEMS devices, but it is also true that for most applications sensor nodes do not have to be necessarily micro; they just have to be sized accordingly to the application and environment where they will work. In other words, it does not matter if a sensor node is not microscale, as long as it can be pleasantly embedded in the application environment.

Research is still ongoing in order to reduce severely the size of large self-sustainable sensor nodes. Electrostatic and thermoelectric generators are leading this way, as they are both easily realizable as MEMS. Still, several difficulties have to be overcome before microgenerators can produce enough energy to sustain a sensor node. A solution underexplored, or at least poorly documented, is the combination of different types of microgenerators to provide energy to a sensor node.

The proliferation of these tiny self-sustainable sensor nodes will happen naturally after they became cheap. For this to happen more and more WSNs have to be deployed in real world applications. Some companies have already given an important push by commercializing kits for assessing the suitability of their generators on the customers’ application (by measuring the energy generated).

Future work should follow the direction of the utilization of these evaluation kits to determine with accuracy the energy that can be generated by commercially available energy-harvesting technologies in specific case-study applications, and then outline a framework that best represents the possible solutions.

References

- [1] HILL, J.; SZEWCZYK, R.; WOO, A.; HOLLAR, S.; CULLER, D.; PISTER, K. - System architecture directions for networked sensors. *SIGPLAN Notices*. ISSN 0362-1340. Vol. 35, n° 11, (2000), p. 93-104.
- [2] AKYILDIZ, I. F.; SU, W.; SANKARASUBRAMANIAM, Y.; CAYIRCI, E. - Wireless sensor networks: a survey. *Computer Networks*. ISSN 1389-1286. Vol. 38, n° 4, (2002), p. 393 - 422.
- [3] YICK, J.; MUKHERJEE, B.; GHOSAL, D. - Wireless sensor network survey. *Comput. Netw.*. ISSN 1389-1286. Vol. 52, n° 12, (2008), p. 2292-2330.
- [4] STANKOVIC, J. A. - When sensor and actuator networks cover the world. *ETRI Journal*. Vol. 30, n° 5, (2008), p. 627-633.
- [5] CALHOUN, B. H.; DALY, D. C.; VERMA, N.; FINCHELSTEIN, D. F.; WENTZLOFF, D. D.; WANG, A.; CHO, S.; CHANDRAKASAN, A. P. - Design considerations for ultra-low energy wireless microsensor nodes. *Computers, IEEE Transactions on*. ISSN 0018-9340. Vol. 54, n° 6, (2005), p. 727-740.
- [6] KANSAL, A.; HSU, J.; ZAHEDI, S.; SRIVASTAVA, M. B. - Power management in energy harvesting sensor networks. *Trans. on Embedded Computing Sys.*. ISSN 1539-9087. Vol. 6, n° 4, (2007), p. 32.
- [7] ANASTASI, G.; CONTI, M.; DI FRANCESCO, M.; PASSARELLA, A. - Energy conservation in wireless sensor networks: a survey. *Ad Hoc Netw.*. ISSN 1570-8705. Vol. 7, n° 3, (2009), p. 537-568.
- [8] SEAH, W.; EU, Z. A.; TAN, H. - Wireless sensor networks powered by ambient energy harvesting (wsn-heap) - survey and challenges. In *Wireless Communication, Vehicular Technology, Information Theory and Aerospace & Electronic Systems Technology, 2009. Wireless VITAE 2009. 1st International Conference on*. (2009), p. 1-5.
- [9] FETCENKO, M. A.; OVSHINSKY, S. R.; REICHMAN, B.; YOUNG, K.; FIERRO, C.; KOCH, J.; ZALLEN, A.; MAYS, W.; OUCHI, T. - Recent advances in nimbh battery technology. *Journal of Power Sources*. ISSN 0378-7753. Vol. 165, n° 2, (2007), p. 544 - 551.
- [10] PARADISO, J. A.; STARNER, T. - Energy scavenging for mobile and wireless electronics. *IEEE Pervasive Computing*. ISSN 1536-1268. Vol. 4, n° 1, (2005), p. 18-27.
- [11] ALVES, M.; BACCOUR, N.; KOUBAA, A.; SEVERINO, R.; DINI, G.; PEREIRA, N.; SÁ, R.; SAVINO, I.; SOUSA, P. G. - Quality-of-service in wireless sensor networks: state-of-the-art and future directions. CISTER - Research Centre in Real-Time Computing Systems. 2009.

- [12] ROUNDY, S.; STEINGART, D.; FRECHETTE, L.; WRIGHT, P.; RABAEY, J. - Power sources for wireless sensor networks. *Wireless Sensor Networks*, (2004), p. 1-17.
- [13] THOMAS, J. P.; QIDWAI, M. A.; KELLOGG, J. C. - Energy scavenging for small-scale unmanned systems. *Journal of Power Sources*. ISSN 0378-7753. Vol. 159, n° 2, (2006), p. 1494-1509.
- [14] HANDE, A.; POLK, T.; WALKER, W.; BHATIA, D. - Indoor solar energy harvesting for sensor network router nodes. *Microprocess. Microsyst.*. ISSN 0141-9331. Vol. 31, n° 6, (2007), p. 420-432.
- [15] WANG, W. S.; O'DONNELL, T.; RIBETTO, L.; O'FLYNN, B.; HAYES, M.; O'MATHUNA, C. - Energy harvesting embedded wireless sensor system for building environment applications. In *Wireless Communication, Vehicular Technology, Information Theory and Aerospace & Electronic Systems Technology, 2009. Wireless VITAE 2009. 1st International Conference on*. (2009), p. 36-41.
- [16] MITCHESON, P. D.; YEATMAN, E. M.; RAO, G. K.; HOLMES, A. S.; GREEN, T. C. - Energy harvesting from human and machine motion for wireless electronic devices. *Proceedings of the IEEE*. ISSN 0018-9219. Vol. 96, n° 9, (2008), p. 1457-1486.
- [17] RENAUD, M.; FIORINI, P.; VAN SCHAIJK, R.; VAN HOOFF, C. - Harvesting energy from the motion of human limbs: the design and analysis of an impact-based piezoelectric generator. *Smart Material Structures*. Vol. 18, n° 3, (2009), p. 035001.
- [18] LEONOV, V.; TORFS, T.; FIORINI, P.; VAN HOOFF, C. - Thermoelectric converters of human warmth for self-powered wireless sensor nodes. *Sensors Journal, IEEE*. Vol. 7, n° 5, (2007), p. 650-657.
- [19] WANG, Z.; LEONOV, V.; FIORINI, P.; VAN HOOFF, C. - Micromachined thermopiles for energy scavenging on human body. *Solid-State Sensors, Actuators and Microsystems Conference, 2007. TRANSDUCERS 2007*. (2007), p. 911-914.
- [20] CHOU, P. H.; PARK, C. - Energy-efficient platform designs for real-world wireless sensing applications. In *ICCAD '05: Proceedings of the 2005 IEEE/ACM International conference on Computer-aided design*. San Jose, CA, (2005), p. 913-920.
- [21] MORAIS, R.; MATOS, S.; FERNANDES, M.; VALENTE, A.; SOARES, S.; FERREIRA, P.; REIS, M. - Sun, wind and water flow as energy supply for small stationary data acquisition platforms. *Computers and Electronics in Agriculture*. ISSN 0168-1699. Vol. 64, n° 2, (2008), p. 120-132.
- [22] BHALERAO, S. A.; CHAUDHARY, A. V.; DESHMUKH, R. B.; PATRIKAR, R. M. - Powering wireless sensor nodes using ambient rf energy. *Systems, Man and Cybernetics, 2006. SMC '06. IEEE International Conference on*. Vol. 4, (2006), p. 2695-2700.
- [23] BOUCHOUICHA, D.; DUPONT, F.; LATRACH, M.; VENTURA, L. - Ambient rf energy harvesting. (2010), p. 652-656.

- [24] HOLMES, A. S.; HONG, G.; PULLEN, K. R.; BUFFARD, K. R. - Axial-flow microturbine with electromagnetic generator: design, cfd simulation, and prototype demonstration. *Micro Electro Mechanical Systems, 2004. 17th IEEE International Conference on. (MEMS)*. (2004), p. 568-571.
- [25] PARK, C.; CHOU, P. H. - Ambimax: autonomous energy harvesting platform for multi-supply wireless sensor nodes. *SECON '06, 3rd Annual IEEE Communications Society on Sensor and Ad Hoc Communications and Networks*. Vol. 1, (2006), p. 168-177.
- [26] BOGLIOLO, A.; LATTANZI, E.; ACQUAVIVA, A. - Energetic sustainability of environmentally powered wireless sensor networks. In *PE-WASUN '06: Proceedings of the 3rd ACM international workshop on Performance evaluation of wireless ad hoc, sensor and ubiquitous networks*. Terromolinos, Spain. (2006), p. 149-152.
- [27] CARSON, J. A., ed. - *Solar cell research progress*. New York: Nova Science Publishers, 2008. ISBN 1-60456-030-4.
- [28] ZHANG, P.; SADLER, C. M.; LYON, S. A.; MARTONOSI, M. - Hardware design experiences in zebranet. In *SenSys '04: Proceedings of the 2nd international conference on Embedded networked sensor systems*. Baltimore, MD, USA, (2004), p. 227-238.
- [29] GREEN, M. A. - Third generation photovoltaics: solar cells for 2020 and beyond. *Physica E: Low-Dimensional Systems and Nanostructures*. Vol. 14, n° (1-2), (2002), p. 65-70.
- [30] *Horiba*. [Online]. 1996. Available at: <http://www.horiba.com/scientific/products/ellipsometers/application-notes/photovoltaics/>.
- [31] CONIBEER, G. - Third-generation photovoltaics. *Materials Today*. ISSN 1369-7021. Vol. 10, n° 11, (2007), p. 42-50.
- [32] KOTTER, D. K.; NOVACK, S. D.; SLAFER, D. W.; PINHERO, P. - Solar nantenna electromagnetic collectors. (2008), p. 54016-1--54016-7.
- [33] *Panasonic solar cells technical handbook*. [Online]. 1998. [Lastchecked 05 October 2010]. Available at: <http://downloads.solarbotics.com/PDF/sunceramcat.pdf>.
- [34] RAGHUNATHAN, V.; CHOU, P. H. - Design and power management of energy harvesting embedded systems. In *ISLPED '06: Proceedings of the 2006 international symposium on Low power electronics and design*. Tegernsee, Bavaria, Germany. (2006), p. 369-374.
- [35] DONDI, D.; BRUNELLI, D.; BENINI, L.; PAVAN, P.; BERTACCHINI, A.; LARCHER, L. - Photovoltaic cell modeling for solar energy powered sensor networks. In *IWASI 2007: 2nd International Workshop on Advances in Sensors and Interface*. (2007), p. 1-6.
- [36] ESRAM, T.; CHAPMAN, P. L. - Comparison of photovoltaic array maximum power point tracking techniques. *Energy Conversion, IEEE Transactions on*. ISSN 0885-8969. Vol. 22, n° 2, (2007), p. 439-449.

- [37] SIMJEE, F.; CHOU, P. H. - Everlast: long-life, supercapacitor-operated wireless sensor node. In *ISLPED '06: Proceedings of the 2006 international symposium on Low power electronics and design*. Tegernsee, Bavaria, Germany. (2006), p. 197-202.
- [38] RAGHUNATHAN, V.; KANSAL, A.; HSU, J.; FRIEDMAN, J.; SRIVASTAVA, M. - Design considerations for solar energy harvesting wireless embedded systems. In *IPSN '05: Proceedings of the 4th international symposium on Information processing in sensor networks*. Los Angeles, California. (2005), p. 64.
- [39] JIANG, X.; POLASTRE, J.; CULLER, D. - Perpetual environmentally powered sensor networks. In *IPSN '05: Proceedings of the 4th international symposium on Information processing in sensor networks*. Los Angeles, California, n° 65, (2005).
- [40] ROUNDY, S.; WRIGHT, P. K.; RABAEY, J. - A study of low level vibrations as a power source for wireless sensor nodes. *Computer Communications*. Vol. 26, n° 11, (2003), p. 1131-1144.
- [41] STARNER, T.; PARADISO, J. A. - Human generated power for mobile electronics. In *Low Power Electronics Design*. (2004), p. 1-35.
- [42] BEEBY, S. P.; TUDOR, M. J.; WHITE, N. M. - Energy harvesting vibration sources for microsystems applications. *Measurement Science and Technology*. Vol. 17, n° 12, (2006), p. R175-R195.
- [43] MITCHESON, P. D.; GREEN, T. C.; YEATMAN, E. M.; HOLMES, A. S. - Architectures for vibration-driven micropower generators. *Microelectromechanical Systems, Journal of*. Vol. 13, n° 3, (2004), p. 429-440.
- [44] S. J. Roundy - Energy scavenging for wireless sensor nodes with a focus on vibration to electricity conversion. University of California, Berkeley, 2003. PhD thesis.
- [45] VULLERS, R. J. M.; VAN SCHAIJK, R.; DOMS, I.; HOOFF, C. V.; MERTENS, R. - Micropower energy harvesting. *Solid-State Electronics*. ISSN 0038-1101. Vol. 53, n° 7, (2009), p. 684 - 693.
- [46] ARNOLD, D. P. - Review of microscale magnetic power generation. *Magnetics, IEEE Transactions on*. ISSN 0018-9464. Vol. 43, n° 11, (2007), p. 3940 -3951.
- [47] ROUNDY, S.; WRIGHT, P. K.; PISTER, K. S. J. - Micro-electrostatic vibration-to-electricity converters. *ASME Conference Proceedings*. (2002), p. 487-496.
- [48] ANTON, S. R.; SODANO, H. A. - A review of power harvesting using piezoelectric materials (2003-2006). *Smart Materials and Structures*. Vol. 16, n° 3, (2007), p. R1-R21.
- [49] SAADON, S.; SIDEK, O. - A review of vibration-based mems piezoelectric energy harvesters. *Energy Conversion and Management*. ISSN 0196-8904. Vol. 52, n° 1, (2011), p. 500-504.
- [50] AMIRTHARAJAH, R.; CHANDRAKASAN, A. P.; CH, A. P. - Self-powered signal processing using vibration-based power generation. *IEEE Journal of Solid-State Circuits*. Vol. 33, (1998), p. 687-695.

- [51] Electric wristwatch with generator. HAYAKAWA, M., U.S. Patent 5 001 685. March 1991.
- [52] WILLIAMS, C. B.; YATES, R. B. - Analysis of a micro-electric generator for microsystems. In *Proceedings of the 8th International Conference on Solid-State Sensors and Actuators Eurosensors IX*. Vol. 1. , (1996), p. 369-372.
- [53] SHEARWOOD, C.; YATES, R. B. - Development of an electromagnetic micro-generator. *Electronics Letters*. Vol. 33, n° 22, (1997), p. 1883-1884.
- [54] LI, W. J.; LEONG, P. H. W.; HONG, T. C. H.; WONG, H. Y.; CHAN, G. M. H. - Infrared signal transmission by a laser-micromachined vibration-induced power generator. In *Proceedings of the 43rd IEEE Midwest Symposium on Circuits and Systems*. (2000), p. 236-239.
- [55] CHING, N. N. H.; WONG, H. Y.; LI, W. J.; LEONG, P. H. W.; WEN, Z. - A laser-micromachined multi-modal resonating power transducer for wireless sensing systems. *Sensors and Actuators A: Physical*. Vol. 97-98, (2002), p. 685-690.
- [56] EL-HAMI, M.; GLYNNE-JONES, P.; WHITE, N. M.; HILL, M.; BEEBY, S.; JAMES, E.; BROWN, A. D.; ROSS, J. N. - Design and fabrication of a new vibration-based electromechanical power generator. *Sensors and Actuators A: Physical*. ISSN 0924-4247. Vol. 92, n° 1-3, (2001), p. 335-342.
- [57] GLYNNE-JONES, P.; TUDOR, M. J.; BEEBY, S. P.; WHITE, N. M. - An electromagnetic, vibration-powered generator for intelligent sensor systems. *Sensors and Actuators A: Physical*. ISSN 0924-4247. Vol. 110, n° 1-3, (2004), p. 344-349.
- [58] JAMES, E. P.; TUDOR, M. J.; BEEBY, S. P.; HARRIS, N. R.; GLYNNE-JONES, P.; ROSS, J. N.; WHITE, N. M. - An investigation of self-powered systems for condition monitoring applications. *Sensors and Actuators A: Physical*. ISSN 0924-4247. Vol. 110, n° 1-3, (2004), p. 171-176.
- [59] TORAH, R.; BEEBY, S. P.; TUDOR, M. J.; O'DONNELL, T.; ROY, S. - Development of a cantilever beam generator employing vibration energy harvestin. In *The 6th Int. Workshop on Micro and Nanotechnology for Power Generation and Energy Conversion Applications (PowerMEMS 2006)*. (2006), p. 181-184.
- [60] MUR MIRANDA, J. O. - Electrostatic vibration-to-electric energy conversion. Department of Electrical Engineering and Computer Science, Massachusetts Institute of Technology, February 2004. PhD thesis.
- [61] MENINGER, S.; MUR MIRANDA, J. O.; AMIRTHARAJAH, R.; CHANDRAKASAN, A. P.; LANG, J. H. - Vibration-to-electric energy conversion. *IEEE Transactions On Very Large Scale Integration (VLSI) Systems*. Vol. 9, (2001), p. 64-76.
- [62] MENINGER, S.; MUR MIRANDA, J. O.; AMIRTHARAJAH, R.; CHANDRAKASAN, A. P.; LANG, J. H. - Vibration-to-electric energy conversion. *Low Power Electronics and Design, 1999. Proceedings. 1999 International Symposium on*, (1999), p. 48-53.

- [63] AMIRTHARAJAH, R.; MENINGER, S.; MUR-MIRANDA, J. O.; CHANDRAKASAN, A.; LANG, J. H. - A micropower programmable dsp powered using a mems-based vibration-to-electric energy converter. *Solid-State Circuits Conference, 2000. Digest of Technical Papers. ISSCC. 2000 IEEE International*, (2000), p. 362-363.
- [64] TASHIRO, R.; KABEI, N.; KATAYAMA, K.; ISHIZUKA, Y.; TSUBOI, F.; TSUCHIYA, K. - Development of an electrostatic generator that harnesses the motion of a living body : use of a resonant phenomenon. *JSME international journal. Series C, Mechanical systems, machine elements and manufacturing*. ISSN 13447653. Vol. 43, n° 4, (2000), p. 916-922.
- [65] TASHIRO, R.; KABEI, N.; KATAYAMA, K.; TSUBOI, E.; TSUCHIYA, K. - Development of an electrostatic generator for a cardiac pacemaker that harnesses the ventricular wall motion. *Journal of Artificial Organs*. ISSN 1434-7229. Vol. 5, (2002), p. 0239-0245.
- [66] MIYAZAKI, M.; TANAKA, H.; ONO, G.; NAGANO, T.; OHKUBO, N.; KAWAHARA, T.; YANO, K. - Electric-energy generation using variable-capacitive resonator for power-free lsi: efficiency analysis and fundamental experiment. In *ISLPED '03: Proceedings of the 2003 international symposium on Low power electronics and design*. Seoul, Korea. (2003), p. 193-198.
- [67] DESPESSE, G.; CHAILLOUT, J. J.; JAGER, T.; LÉGER, J. M.; VASSILEV, A.; BASROUR, S.; CHARLOT, B. - High damping electrostatic system for vibration energy scavenging. In *sOc-EUSAI '05: Proceedings of the 2005 joint conference on Smart objects and ambient intelligence*. Grenoble, France, (2005), p. 283-286.
- [68] APC, INTERNATIONAL LTD - *Piezoelectric ceramics: principles and applications*. Mackeyville: APC International Ltd., 2002. ISBN 0-9718744-0-9.
- [69] SODANO, H. A.; PARK, G.; INMAN, D. J. - A review of power harvesting using piezoelectric materials. *Shock and Vibration Digest*. Vol. 36, n° 3, (2004), p. 197-206.
- [70] BAKER, J.; ROUNDY, S.; WRIGHT, P. - Alternative geometries for increasing power density in vibration energy scavenging for wireless sensor networks. In *Proc. 3rd Int. Energy Conversion Engineering Conf.*, (2005), p. 959-970.
- [71] RENAUD, M.; KARAKAYA, K.; STERKEN, T.; FIORINI, P.; HOOF, C. V.; PUERS, R. - Fabrication, modelling and characterization of mems piezoelectric vibration harvesters. *Sensors and Actuators A: Physical*. ISSN 0924-4247. Vol. 145-146, (2008), p. 380 - 386.
- [72] ROUNDY, S.; WRIGHT, P. K. - A piezoelectric vibration based generator for wireless electronics. *Smart Materials and Structures*. Vol. 13, n° 5, (2004), p. 1131.
- [73] NG, T.; LIAO, W. - Feasibility study of a self-powered piezoelectric sensor. *Smart Structures and Materials 2004: Smart Electronics, MEMS, BioMEMS, and Nanotechnology*. Vol. 5389, n° 1, (2004), p. 377-388.

- [74] NG, T.; LIAO, W. - Sensitivity analysis and energy harvesting for a self-powered piezoelectric sensor. *Journal of Intelligent Material Systems and Structures*. Vol. 16, n° 10, (2005), p. 785-797.
- [75] SNYDER, D. S. - *Vibrating transducer power supply for use in abnormal tire condition warning systems*. [Online]. 1983. Available at: <http://www.freepatentsonline.com/4384482.html>.
- [76] SEGAL, D.; BRANSKY, I. - Testing of a piezoelectric generator for in-flight electrical powering of electrical guidance systems. *Ferroelectrics*. Vol. 202, n° 1, (1997), p. 81-85.
- [77] CHURCHILL, D. L.; HAMEL, M. J.; TOWNSEND, C. P.; ARMS, S. W. - Strain energy harvesting for wireless sensor networks. In *Society of Photo-Optical Instrumentation Engineers (SPIE) Conference Series*. Vol. 5055. (2003), p. 319-327.
- [78] ARMS, S. W.; TOWNSEND, C. P.; CHURCHILL, D. L.; GALBREATH, J. H.; MUNDELL, S. W. - Power management for energy harvesting wireless sensors. *Smart Structures and Materials 2005: Smart Electronics, MEMS, BioMEMS, and Nanotechnology*. Vol. 5763, n° 1, (2005), p. 267-275.
- [79] DU PLESSIS, A. J.; HUIGSLOOT, M. J.; DISCENZO, F. D. - Resonant packaged piezoelectric power harvester for machinery health monitoring. *Smart Structures and Materials 2005: Industrial and Commercial Applications of Smart Structures Technologies*. Vol. 5762, n° 1, (2005), p. 224-235.
- [80] DISCENZO, F. M.; LOPARO, K. A.; CASSAR, H.; CHUNG, D. - Machinery condition monitoring using wireless self-powered sensor nodes. *Proc. 24th International Modal Analysis Conference*, (2006).
- [81] CAMMARANO, A.; BURROW, S. G.; BARTON, D. A. W.; CARRELLA, A.; CLARE, L. R. - Tuning a resonant energy harvester using a generalized electrical load. *Smart Materials and Structures*. Vol. 19, n° 5, (2010), p. 055003.
- [82] SNYDER, G. J. - Thermoelectric energy harvesting. In PRIYA, S.; INMAN, D. J., ed. - *Energy harvesting technologies*. New York: Springer US. 2009. p. 325-336.
- [83] MATSUBARA, K. - Development of a high efficient thermoelectric stack for a waste exhaust heat recovery of vehicles. *Thermoelectrics, 2002. Proceedings ICT '02. Twenty-First International Conference on*. (2002), p. 418-423.
- [84] SNYDER, G. J. - Small thermoelectric generators. *The Electrochemical Society Interface*. Vol. 17, n° 3, (2008), p. 54-56.
- [85] IMEC - *Micropower generation and storage*. [Online]. 2007. [Lastchecked 3 October 2010]. Available at: <http://www.imec.be/ScientificReport/SR2007/html/1384155.html>.
- [86] KISHI, M.; NEMOTO, H.; HAMAO, T.; YAMAMOTO, M.; SUDOU, S.; MANDAI, M.; YAMAMOTO, S. - Micro thermoelectric modules and their application to wristwatches as an energy source. *Thermoelectrics, 1999. Eighteenth International Conference on*. (1999), p. 301-307.

- [87] DALOLA, S.; FERRARI, M.; FERRARI, V.; GUIZZETTI, M.; MARIOLI, D.; TARONI, A. - Characterization of thermoelectric modules for powering autonomous sensors. *Instrumentation and Measurement, IEEE Transactions on*. ISSN 0018-9456. Vol. 58, n° 1, (2009), p. 99-107.
- [88] MAGILL, P. A. - *Thermal harvesting and storage: a heavenly match*. [Online]. 2010. Available at: http://www.nextreme.com/pages/learning_center/articles.shtml.
- [89] SNYDER, G. J.; URSELL, T. S. - Thermoelectric efficiency and compatibility. *Phys. Rev. Lett.*. Vol. 91, n° 14, (2003), p. 148301.
- [90] STARK, I.; STORDEUR, M. - New micro thermoelectric devices based on bismuth telluride-type thin solid films. *Thermoelectrics, 1999. Eighteenth International Conference on*. (1999), p. 465 -472.
- [91] *Thermo life® technical data*. [Online]. 2005. [Lastchecked 05 October 2010]. Available at: http://www.poweredbythermolife.com/pdf/Thermo_LifeTM_Technical_Data.pdf.
- [92] BOTTNER, H.; NURNUS, J.; GAVRIKOV, A.; KUHNER, G.; JAGLE, M.; KUNZEL, C.; EBERHARD, D.; PLESCHER, G.; SCHUBERT, A.; SCHLERETH, K.-H. - New thermoelectric components using microsystem technologies. *Microelectromechanical Systems, Journal of*. ISSN 1057-7157. Vol. 13, n° 3, (2004), p. 414-420.
- [93] *Thin film thermogenerators*. [Online]. 2006. [Lastchecked 05 October 2010]. Available at: http://www.micropelt.com/down/datasheet_mpg_d651_d751.pdf.
- [94] *Te-power node, self-powered, wireless sensor node & thermoharvesting explorer*. [Online]. 2009. [Lastchecked 05 October 2010]. Available at: http://www.micropelt.com/down/datasheet_te_power_node.pdf.
- [95] *The thermal copper pillar bump*. [Online]. 2008. [Lastchecked 05 October 2010]. Available at: http://www.nextreme.com/media/pdf/whitepapers/Nextreme_Thermal_Bump_White_Paper_Jan08.pdf.
- [96] *Eteg hv14 power generator*. [Online]. 2010. [Lastchecked 5 October 2010]. Available at: http://www.nextreme.com/media/pdf/techspecs/Nextreme_eTEG_HV14_Data_Brief.pdf.
- [97] WANG, Z.; LEONOV, V.; FIORINI, P.; HOOFF, C. V. - Realization of a wearable miniaturized thermoelectric generator for human body applications. *Sensors and Actuators A: Physical*. ISSN 0924-4247. Vol. 156, n° 1, (2009), p. 95 - 102.
- [98] WANG, Z.; FIORINI, P.; LEONOV, V.; HOOFF, C. V. - Characterization and optimization of polycrystalline si 70% ge 30% for surface micromachined thermopiles in human body applications. *Journal of Micromechanics and Microengineering*. Vol. 19, n° 9, (2009), p. 094011.
- [99] BARBONI, L.; VALLE, M. - Experimental analysis of wireless sensor nodes current consumption. In *SENSORCOMM '08: Proceedings of the 2008 Second International Conference on Sensor Technologies and Applications*, (2008), p. 401-406.

- [100] DLUGOSZ, R.; INIEWSKI, K. - Flexible architecture of ultra-low-power current-mode interleaved successive approximation analog-to-digital converter for wireless sensor networks. *VLSI Des.*. ISSN 1065-514X. Vol. 2007, n° 2, (2007), p. 1-13.
- [101] Tektronix - *Tds1000b and tds2000b series digital storage oscilloscope user manual*. [Online]. 2009. Available at: <http://www.tek.com/downloads/>.
- [102] *Tinyos documentation wiki*. [Online]. 2010. Available at: http://docs.tinyos.net/index.php/Main_Page.
- [103] GAY, D.; LEVIS, P.; VON BEHREN, R.; WELSH, M.; BREWER, E.; CULLER, D. - The nesc language: a holistic approach to networked embedded systems. In *PLDI '03: Proceedings of the ACM SIGPLAN 2003 conference on Programming language design and implementation*. San Diego, California, USA. (2003), p. 1-11.
- [104] MOTTOLA, L.; PICCO, G. P. - *Programming wireless sensor networks: fundamental concepts and state-of-the-art*. [Online]. 2008. Available at: <http://citeseerx.ist.psu.edu/viewdoc/download?doi=10.1.1.148.2779&rep=rep1&type=pdf>.
- [105] LEVIS, P.; GAY, D. - *Tinyos programming*. [Online]. 2009. [Lastchecked 14 October 2010]. Available at: <http://csl.stanford.edu/~pal/pubs/tos-programming-web.pdf>.
- [106] *Xubuntos virtual machine image*. [Online]. Available at: <http://sing.stanford.edu/tinyos/dists/xubuntos-2.1-vm.tar.gz>.
- [107] *Tinyos 2.0.2 documentation*. [Online]. Available at: <http://www.tinyos.net/tinyos-2.x/doc/>.

Appendix A. Technical Report



Technical Report

Quality-of-Service in Wireless Sensor Networks: state-of-the-art and future directions

**Mário Alves, Nouha Baccour, Anis Koubaa, Ricardo Severino
Gianluca Dini, Nuno Pereira, Rui Sá, Ida Savino, Paulo
Grandra de Sousa**

HURRAY-TR-091108

Version: 0

Date: 11-11-2009

Quality-of-Service in Wireless Sensor Networks: state-of-the-art and future directions

Mário alves, Nouha Baccour, Anis Koubaa, Ricardo Severino, Gianluca Dini, Nuno Pereira, Rui Sá, Ida Savino, Paulo Grandra de Sousa

IPP-HURRAY!

Polytechnic Institute of Porto (ISEP-IPP)

Rua Dr. António Bernardino de Almeida, 431

4200-072 Porto

Portugal

Tel.: +351.22.8340509, Fax: +351.22.8340509

E-mail:

<http://www.hurray.isep.ipp.pt>

Abstract

Wireless sensor networks (WSNs) are one of today's most prominent instantiations of the ubiquitous computing paradigm. In order to achieve high levels of integration, WSNs need to be conceived considering requirements beyond the mere system's functionality. While Quality-of-Service (QoS) is traditionally associated with bit/data rate, network throughput, message delay and bit/packet error rate, we believe that this concept is too strict, in the sense that these properties alone do not reflect the overall quality-of-service provided to the user/application. Other non-functional properties such as scalability, security or energy sustainability must also be considered in the system design. This paper identifies the most important non-functional properties that affect the overall quality of the service provided to the users, outlining their relevance, state-of-the-art and future research directions. Key words: Wireless Sensor Networks, Quality-of-Service, Non-Functional Properties, Cooperating Objects, Scalability, Reliability, Timeliness, Mobility, Heterogeneity, Security, Energy-Sustainability.

Quality-of-Service in Wireless Sensor Networks: state-of-the-art and future directions

Mário Alves*

CISTER/ISEP, Polytechnic Institute of Porto, Portugal

Nouha Baccour¹

ReDCAD Research Unit, National School of Engineers of Sfax, Tunisia

Anis Koubâa²

CISTER/ISEP, Polytechnic Institute of Porto, Portugal

Ricardo Severino

CISTER/ISEP, Polytechnic Institute of Porto, Portugal

Gianluca Dini

University of Pisa, Italy

Nuno Pereira

CISTER/ISEP, Polytechnic Institute of Porto, Portugal

Rui Sá

MSc candidate, ECE Department, ISEP/IPP, Polytechnic Institute of Porto, Portugal

Ida Savino³

ELSAG DATAMAT, Italy

Paulo Sousa

*Corresponding author

Email addresses: `mjf@isep.ipp.pt` (Mário Alves), `nabr@isep.ipp.pt` (Nouha Baccour), `aska@isep.ipp.pt` (Anis Koubâa), `rars@isep.ipp.pt` (Ricardo Severino), `gianluca.dini@ing.unipi.it` (Gianluca Dini), `nap@isep.ipp.pt` (Nuno Pereira), `1980168@isep.ipp.pt` (Rui Sá), `Ida.Savino@elsagdatamat.com` (Ida Savino), `pag@isep.ipp.pt` (Paulo Sousa)

¹also with CISTER/ISEP, Polytechnic Institute of Porto, Porto, Portugal

²also with the Al-Imam Mohamed bin Saud University, Riyadh, Saudi Arabia

³formely with the University of Pisa, Italy

Abstract

Wireless sensor networks (WSNs) are one of today's most prominent instantiations of the ubiquitous computing paradigm. In order to achieve high levels of integration, WSNs need to be conceived considering requirements beyond the mere system's functionality. While Quality-of-Service (QoS) is traditionally associated with bit/data rate, network throughput, message delay and bit/packet error rate, we believe that this concept is too strict, in the sense that these properties alone do not reflect the overall quality-of-service provided to the user/application. Other non-functional properties such as scalability, security or energy sustainability must also be considered in the system design. This paper identifies the most important non-functional properties that affect the overall quality of the service provided to the users, outlining their relevance, state-of-the-art and future research directions.

Key words: Wireless Sensor Networks, Quality-of-Service, Non-Functional Properties, Cooperating Objects, Scalability, Reliability, Timeliness, Mobility, Heterogeneity, Security, Energy-Sustainability.

1. Introduction

Today, we can find computing capabilities in everyday physical objects as diverse as mobile phones, digital personal assistants, gaming platforms, household appliances or cars, just to name a few examples. From the computational perspective, these devices are often called embedded computing systems, as their computing capabilities are just a component of the whole system. With over 99% of all microprocessors produced today being used in embedded computing systems [1], we can witness the tremendous relevance of these systems.

The computing capability of these embedded devices is usually "hidden" from users, but they are interacting with them and with the physical environment. While today these devices interact with the physical environment at unprecedented levels, an even more dramatic change is yet to come, when these (mostly) isolated islands of computing intelligence will be seamlessly

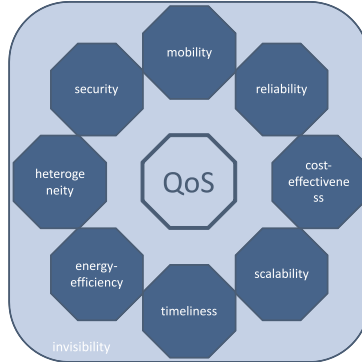


Figure 1: Holistic view of QoS [2]

cooperating for achieving common goals. Road vehicles will interact between them and with fixed infrastructures; humans and machines will coexist in smart computing environments; the Internet will penetrate the physical world via wireless sensor/actuator networks; every single “object” will be electronically and remotely identifiable, monitorable and controllable.

Wireless sensor networks (WSNs) are one of today’s most prominent instantiations of this ubiquitous computing paradigm. In order to achieve these high levels of integration, WSNs need to be conceived considering requirements beyond the mere system’s functionality. Properties concerning the quality of the system are also of primary importance.

In this paper, we focus on the most relevant properties of WSNs that, although not affecting their functionality, affect their behavior or performance. These are the so-called Non-Functional Properties (NFP) and include scalability, reliability, robustness, timeliness or security. By employing a broader (than the traditional one) view of Quality-of-Service (QoS), we refer to them as QoS properties.

QoS has been traditionally defined as a set of traffic characteristics for a network service (such as an Internet phone call) [3]. These characteristics may include performance-oriented as well as non-performance-oriented criteria. The ITU-T (International Telecommunication Union) has created two groups of QoS criteria for this purpose [4]. The performance-oriented group includes parameters such as set-up delay, throughput, jitter, or probability of dropping. The non-performance-oriented group defines the parameters cost, priority and level of service. These do not directly affect performance of communications, but are concerned with related matters. Traditional QoS

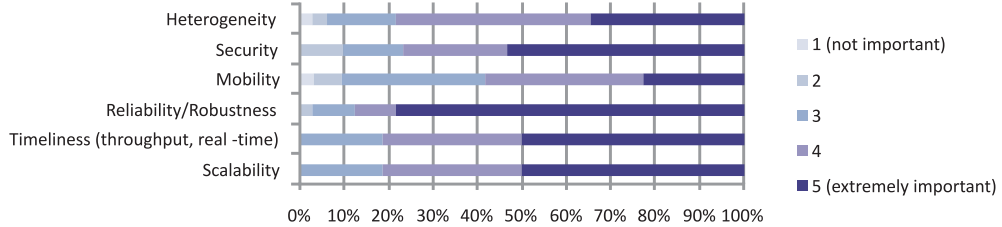


Figure 2: Survey: Non Functional Properties [7]

criteria provide a view of service parameters that is very independent and are thus limited in the way they reflect the *overall* QoS provided to the user/application.

We believe that WSN calls for a broader perspective of QoS. Each WSN application/task (which can be rather diverse [5]) must be correct, secure, produced “on time” and with the smallest energy consumption possible. WSNs are expected to be highly heterogeneous besides being cost-effective, maintainable and scalable. They must also be as much “invisible” to their users/environment as possible, to be seamlessly accepted and used at large-scale [6]. Therefore, QoS should be seen at and addressed in a more extensive and holistic perspective, instantiated in a wider range of properties (as illustrated in Figure 1), namely heterogeneity, energy-sustainability, timeliness, scalability, reliability, mobility, security, cost-effectiveness and invisibility.

The relevance of these NFP can be inferred from the results of a recent survey carried out by the CONET consortium. Figure 2 shows that, with exception to heterogeneity and mobility, all these NFPs were considered of top importance (rank 5) for at least by 50% of the interviewees. Furthermore, around 80% of the answers for every property ranked it as at least 4, except for mobility which had around 60%. One can also note that there is high interest in reliability/robustness issues since that property had 80% of the answers ranking it as 5, featuring its importance for system development. Power efficiency and energy harvesting, which we fit into the context of “Energy Sustainability”, have been considered separately (chart not shown here) and both were considered very or extremely important (4 and 5) by over 80% of the interviewees.

This paper attempts to organize the research area and contribute to a more integrated view of QoS. While not providing concrete solutions for

this problem, we selected the most relevant QoS criteria and overview each one. The paper discusses the QoS criteria individually, their relevance and provides an introduction to the research efforts developed up to now.

Invisibility and Cost-Effectiveness are considered to be more subjective and transversal aspects, thus are not explicitly addressed in this paper. The term “Invisibility” is based on Mark Weisers vision [6] - “the best computer is a quiet, invisible servant”. In our context, the idea is that if WSN systems/components are to be embedded in the environment in a ubiquitous large-scale fashion, they should be as much invisible and environmentally friendly (e.g. avoiding “buying new is cheaper than maintaining/repairing/recharging”, or use recyclable materials and sustainable systems that are ecologically friendly). “Cost-Effectiveness” encompasses issues such as system design/development, hardware (e.g. cost/node), deployment and commissioning, exploration, maintenance and decommissioning.

This paper was written in synergy with the first edition of the CONET Roadmap [7] and also with [2]. The CONET Roadmap includes a complete and comprehensive survey on the current state and future directions of research, practice, technology and applications of Cooperating Objects systems. To the authors’ best knowledge, there were no publications specifically addressing this topic so far.

The remainder of this paper elaborates on the previously mentioned QoS properties in WSNs. Section 2 introduces relevant concepts, terminology and relevance of QoS attributes. Section 3 presents the state-of-the-art of research works, practice and technology related to QoS. Section 4 presents gaps, trends and future research directions. In Section 5, we present and analyse the results of a survey regarding the timeline for achieving tangible results on the research challenges presented in Section 4. Some general conclusions are drawn in Section 6.

2. Description and Relevance

2.1. Scalability

Wireless Sensor Network (WSN) systems may involve different entities, such as network nodes (for serving as sensors/actuators, routers/ gateways and/or sinks/controllers), machines (e.g. roller belt, mobile robot, fridge, traffic light) or other agents (e.g. humans, plants, animals, microscopic organisms). Depending on the deployment characteristics such as the application, the environment or the users, a WSN system scale may dynamically

change with time. The term “scale” may refer to the number of nodes in the field (fewer or more nodes in the overall system), spatial density (fewer or more nodes in a restricted area of the system), or the dimension of the geographical region under coverage (smaller or wider, 2D or 3D). The ability of a system to easily/transparently adapt itself to these dynamic changes in scale is named *scalability*.

Scalability might be of a great importance for most WSN applications. For instance, in an environmental monitoring application, the network may need up to thousands of nodes in order to cover the whole area, depending on the required sensing information granularity (more sensor density leads to richer information, but also to more information to transmit and process) and on the transmission range of the sensor nodes. In such a case, the deployed network protocols must scale well with the number of nodes in a region, to continually ensure the correct behavior of the application. In addition, the system should adapt itself to these scale changes in a transparent way, i.e. without requiring (or with a minimum) user intervention.

Although a very large number of processors and sensors can operate in parallel and hence the processing and sensing capabilities increase linearly with the number of WSN nodes, the communication capability unfortunately does not. Due to unreliability of the radio link quality, message collisions and to the multihop nature of communications, QoS can be severely affected by the increase in the network scale. Therefore, WSN communication protocols and mechanisms must encompass scalability. Medium Access Control (MAC) and routing mechanisms must be scalable, otherwise problems such as uncontrolled routing and medium access delays as well as overflow of routing tables may occur. Scalability must also be taken into consideration for achieving efficient data processing, aggregation, storage and querying in WSNs, especially when large amounts of data are involved.

2.2. Timeliness

The timing behaviour in WSNs is becoming increasingly important, mainly due to the growing tendency for a very tight integration and interaction between embedded computing devices and the physical environment, via sensing and actuating actions [8]. Such “cyber-physical” systems require a rethinking in the usual computing and networking concepts [9], and given that the computing entities closely interact with their environment, timeliness is of increasing importance [10]. *Timeliness* represents the timing behaviour of

a system, both in terms of computations and communications, encompassing issues such as message transmission delay (how long does it take for a message to be transmitted from source to destination, task execution time, task and message priority, network bandwidth/throughput, etc.

Some WSN applications, or some specific tasks within an application, might impose to be finished within a certain time limit (deadline). These are usually referred to as “real-time” applications/tasks and require real-time computation (requiring real-time operating systems and programming languages) and real-time communications (requiring real-time communication protocols). For instance, in a WSN application there might be a task that is to detect a certain event (e.g. gas leak) in a certain region and transmit that information to a remote sink within at most 10 seconds. Note that the timing behaviour of WSN hardware, such as sensors/actuators devices, signal conditioning circuits and analogue-to-digital converters, must also be considered due to its impact in monitoring/control loops.

A fundamental difficulty in designing WSN systems with real-time requirements results from design principles that are usually antagonist to “traditional” real-time systems. “Traditional” real-time systems rely on the over-allocation of resources (due to the pessimism of the analysis, e.g. Worst-Case Execution Time), usually reducing their ability to tackle the dynamic behaviour of the physical phenomena. On the other hand, WSN systems based on unattended resource-constrained nodes, must optimize resource utilization and heavily depend on the dynamic nature of their environment. An example is tracking the motion and evolution of a fluid (e.g. gas leak), where the computational and communication demands change in time and space, according to the propagation of that fluid.

2.3. *Reliability/Robustness*

Robustness refers to the fact that a component or a system performs well not only under ordinary conditions, but also under abnormal conditions that violate its designers’ assumptions. Both hardware and software system components must be robust to be resistant and adaptive to sudden and/or long-term changes. An algorithm/protocol (e.g. for routing, localization, mobility) is robust if it continues operating correctly despite abnormalities (e.g. in inputs, calculations) or despite the change of its operational conditions or its network/system structure.

On the other hand, *Reliability* is the ability of a system or component to perform its required functions under predefined conditions for a speci-

fied period of time. This is especially important in WSNs, since it may be extremely difficult or even impossible to access them again once they are deployed. In such applications, nodes are expected to live as long as possible. To achieve these high levels of reliability, WSNs must be robust and support fault-tolerance mechanisms.

In addition, depending on the application and environment characteristics and requirements, WSN hardware (e.g. sensors, actuators) must be resistant to potentially harsh environmental conditions [11] [12] [13] [14] such as vibration/mechanical impacts, high and/or low temperature, water/humidity/moisture, dust or Radio-Frequency (RF) and Electromagnetic Interference (EMI) sources. Moreover, WSN nodes resource limitations and the multi-hop nature of the communication worsen the situation. As a consequence, considering robustness and reliability becomes a must in the design process of WSNs to overcome the impact of these harsh operational conditions, thus mitigating maintenance actions and maximizing system lifetime.

2.4. Mobility

Mobility will be a key issue in WSNs as at least some nodes/agents are likely to be physically or logically moving relatively to each other. Physical mobility mainly refers to the changes of the entity's geographical locations during time, such as the movement of vehicles, animals, humans. Logical mobility refers to the dynamic changes in the network topology such as adding or removing new entities to/from the system.

Mobility can be classified according to the type of mobile entity into three classes: (1) *Node mobility*: (mobile nodes, node clusters, routers and gateways), (2) *Sink Mobility*: (data sinks may be moving, either on purpose (e.g. data mules) or due to the application requirements), (3) *Event Mobility*: (which means that the events physically move from one location to another, such as in event detection/tracking). Mobility can also be classified according to other aspects (e.g. mobility speed, intra/inter-cell, etc.; please refer to [7] (Section 3.3.5) for further details).

Mobility support significantly increases the capabilities of a WSN system, namely: to repair or extend the network connectivity [15] [16], to balance energy consumption, such as rotating routers closer to the sink, to adapt to dynamic stimulus changes, such as collecting information when a sudden incident occurs, or to improve the lifetime of WSNs with mobile data collectors ("data mules"). However, in many application scenarios it is not enough that the WSN protocol supports joining and leaving of nodes, since this process

might lead to inadmissible network inaccessibility times (unbounded message delays or message losses). Mobility support in WSNs is therefore a rather heterogeneous and challenging topic.

2.5. Security

Given the interactive and pervasive nature of WSNs, security is one of the key points for their acceptance outside the research community. In fact, a security breach in such systems can result in severe privacy violations and physical side effects, including property damage, injury and even death.

Security in WSNs is a more difficult long-term problem than is today in desktop and enterprise computing. In fact, such objects that are in spatial proximity cooperate among themselves in order to jointly execute a given task. It follows that there is no central, trusted authority that mediates interaction among them. Furthermore, WSNs use wireless communication in order to simplify deployment and increase reconfigurability. So, unlike a traditional network, an adversary with a simple radio receiver/transmitter can easily eavesdrop as well as inject/modify packets in a wireless network.

Cost reasons cause devices to have limitations in terms of energy consumption, computation, storage, and communication capabilities. This leads to constraints on the types of security solutions that can be applied. To further worsen this scenario, devices often lack adequate physical/hardware support to protection and tamper-resistance. This, together with the fact that WSNs can be deployed over a large, unattended, possibly hostile area, implies that each device can be tampered with by a malicious subject.

Finally, the drive to provide richer functionalities, increased customizability and flexible reconfigurability of WSNs requires the ability to dynamically download software on them [17] [18]. In fact, traditional systems have been designed to perform a fixed set of predefined functionalities in a well-known operating environment. Hence, their functionality is not expected to change during the system lifetime. This design approach can no longer be pursued in the vast majority of applications. In order to be cost-effective and operational over time, WSNs must be reconfigurable for becoming customizable to different operating environments and adaptable to changing operating conditions. However, the need for reconfigurability acts against security as it introduces new sources of vulnerability. Downloading malicious software (including viruses, worms, and Trojan horses) is by far the instrument of choice in launching security logical attacks. The magnitude of this problem will

only worsen with the rapid increase in the software content of embedded systems.

2.6. Heterogeneity

WSN systems will inherently be composed of heterogeneous components, therefore heterogeneity must be appropriately considered both pre-run-time (at design time) and during system operation (e.g. for system management and maintenance). In the context of this paper, heterogeneity is considered in a broad perspective and at different levels, namely:

- *heterogeneity in networking hardware/software*: sensor/actuator-level nodes (different motes, RFID, MEMS) and communication protocols, higher-level nodes (e.g. gateways) and communication protocols, system and network planning/management;
- *heterogeneity in embedded system nodes hardware/software architecture* : sensors and sensor boards, design diversity, calibration, operating systems and programming languages for resource-constrained networked embedded systems, middleware;
- *heterogeneity in cyber/pervasive/host computing devices*: HMIs (in general), wearable computers, mobile phones, PDAs, HMDs, mobile robots, transportation vehicles and other industrial (or other) machinery;
- *heterogeneity in applications/services/user-perspective*: many applications/services may be provided by the same networking infrastructure, different human users, eventually with different roles.

The integration of heterogeneous Cooperating Objects featuring different embedded information processing and communication capabilities has a huge number of application possibilities. Furthermore, WSNs featuring heterogeneous hardware offer the additional advantage of exploiting the complementarities and specialisation of each object. Nevertheless, it must be highlighted that system design/management complexity grows (even more than linearly) with heterogeneity.

2.7. Energy Sustainability

Particularly in larger-scale WSNs, most of the nodes must be energetically self-sustainable, as maintenance actions such as battery recharge/replacement may not be feasible or at least not convenient. Current WSN nodes rely on small batteries with a very restricted energy budget. Moreover, batteries with reasonable form factor and cost do not yield the lifetime required by most applications, despite recent technological advances [19].

Energy-efficiency has been a major focus of research since the dawn of the WSN paradigm and witnessed significant advancements over the last decade. Energy efficiency can be defined as the ratio of the amount of work done to the amount of energy consumed. Thus, using less energy to perform the same amount of work or performing more work from the same energy input can be defined as an *efficiency gain*. However, efficiency alone is not enough to reduce energy consumption. This is why several techniques have been proposed to maximize the lifetime of battery-powered WSN nodes. These techniques aim at energy conservation, which can be defined as reducing energy consumption through a reduction in the amount of work done. Conservation schemes leave the ratio of the amount of work done to energy consumption unchanged and so do not affect efficiency.

Efficiency and conservation, even in combination, prolong the lifetime of a WSN system, but cannot turn it “perpetual”. Therefore, energy must be collected from the surrounding environment in order to supplement or even replace batteries [20][21]. The process of extracting energy from the ambient environment and converting it into consumable electrical energy is generally known as energy harvesting (or energy scavenging). Energy harvesting, along with energy efficiency and energy conservation, are the available means to enable nodes self-sustainability and to prolong system lifetime, and can all be framed within the broader concept of “Energetic Sustainability”.

3. State of the art

3.1. Scalability

Although the new paradigm of WSNs was coined over one decade ago and lots of research has been done in this area, real-world WSNs applications are still of insignificant number and particularly of insignificant scale. To our best knowledge, real (academic-driven and temporary) WSN deployments were only up to a few hundred (e.g. VigilNet, [22]) to one thousand

nodes (ExScal, [23]). Reasons for the non-existence of large-scale applications include the lack of standards and mature and cost-effective technologies for WSNs. Some considerations about the current state of research in scalability-related aspects are presented next.

A typical strategy for supporting WSN scalability relies on the use of hierarchical (or tiered) network architectures, e.g. cluster-based (e.g. [24], [25] or [26]), hexagonal ([27]) or heterogenous-protocols (e.g. [28], [29]). The underlying philosophy in these communication architectures is to have a more powerful (e.g. higher energy capacity, radio coverage and bit rate) network technologies working as a backbone for less powerful (sub)networks at the sensor/actuator level.

In [30], the authors proposed the use of a two-tiered WSN architecture for structural health monitoring. This is a GSM-like architecture that divides the monitored area into several clusters. Each cluster is managed by a local master that handles the communication using a TDMA-like protocol inside the cluster. This approach lacks scalability inside each cluster due to the TDMA inherent limitations. Also, this architecture is entirely dependent on the presence of a local master to ensure communications, which is not suitable for WSNs. In fact, for a large-scale network, this architecture is unpractical since the number of local master's increases linearly with the number of deployed nodes, resulting in a significant increase of the overall cost.

In [29], the authors proposed using a gateway as a portal where every WSN node is identified by an IP address, allowing direct and individual access. However, there is no mobility support and the handling of very large networks may become a difficult task. In [31], the authors proposed a multiple-tiered architecture relying on a IEEE 802.11/WiFi-based backbone and a IEEE 802.15.4/ZigBee-based sensor/actuator network. Though there is a concern on supporting QoS in IEEE 802.15.4/ZigBee-based WSNs, especially on supporting both best-effort and real-time traffic, there are still many open issues, specially on the interoperability with the backbone network.

Some commercial solutions are available (e.g. from Digi, ScatterWeb, SensiNode and CrossBow) to interface WSNs to IP/Internet, therefore fostering scalability. However, QoS properties (such as timeliness) are basically neglected. The IETF 6LoWPAN group is driving IPv6 over IEEE 802.15.4, aiming at scaling up Internet into the "smart objects" level. This solution might be interesting for WSN applications with scalability and interoperability requirements, provided that 6LoWPAN supports the required levels of

QoS.

Recent findings on wireless dominance-based MAC protocols (like the one used in the Controller Area Network [32]) provide unprecedented advantages for WSNs, since aggregate computations can be performed with a complexity that is independent of the number of sensing nodes [33].

3.2. Timeliness

Real-time issues have only recently drawn attention from the “wireless sensor networks” scientific community [10]. However, the timing behaviour of WSNs will be of increasing importance for many applications: real world processes and phenomena often require real-time data acquisition and processing [8]. Some examples include mission critical applications, such as early warning systems for natural disasters or contamination (forest fires, earthquakes, tsunamis, radiation, etc.), critical infrastructures monitoring (e.g. bridges, tunnels, energy grid) or support for emergency interventions (firemen, doctors at a hospital etc.).

In this context, it is crucial that WSN resources are predicted in advance, to support the prospective applications with a pre-defined timeliness. Thus, it is mandatory to have adequate methodologies to dimension network resources in such a way that the system behaves as expected [10]. However, the provision of timeliness guarantees has always been considered as very challenging due to the usually severe limitations of WSN nodes, such as the ones related to their energy, computational and communication capabilities, in addition to the large-scale nature of WSNs. So, adequate mechanisms must be devised for dimensioning WSN resources in order to guarantee a minimum timeliness performance. Actually, the evaluation of the performance limits of WSNs is a crucial task, particularly when the network is expected to operate under worst-case conditions [34].

Real-time communications over sensor networks are mostly achieved through deterministic routing and MAC (Medium Access Control) protocols. Most of the MAC protocols developed to support deadline requirement in the context of WSN are designed around some TDMA-based scheme. Indeed, TDMA protocols have very appealing characteristics for this context, such as being inherently collision-free, having the possibility of scheduling transmit/receive times, and consequently being very power efficient.

Common to all TDMA-based protocols is the requirement that nodes have the same time reference. This is a notably difficult problem, that has been addressed in a number of ways. The simplest approach is to use some type of

global clock. This can be achieved, for example, using GPS. However, GPS requires power hungry receivers, and does not perform well indoors. The synchronization problem was also tackled using distributed algorithms that distribute/exchange clock information. There are several such time synchronization schemes in the research literature, where some of the most salient of these, providing good accuracy, are RBS [35], TPSN [36] or FTSP [37]. Notably, the work in [38] is the only practical synchronization strategy that does not require nodes to construct a hierarchical organization, but it can take an unbounded number of broadcasts to achieve synchronization.

Some examples of TDMA-based MAC protocols are TRAMA [39], RT-Link [40], PEDAMACS [41], or I-EDF [42]. This last work ([42]) is interesting in that it implements the EDF algorithm when accessing the medium. It is based on the assumption that all nodes know the traffic on the other nodes that compete for the medium and all these nodes execute the EDF scheduling algorithm. Unfortunately, this algorithm is based on the assumption that a node knows the arrival time of messages on other nodes, thus nodes be placed in static cells, and channel assignment needs to be carefully handled to avoid interference between neighbor cells. The Dual-mode real-time MAC protocol [43] is similar to I-EDF in the respect that it is also based on a cellular structure, where each cell has a different channel. This MAC protocol ([43]) has two modes: protected and unprotected. The unprotected mode is used while no collisions are detected, after which the protected mode is started. The protected mode is a typical TDMA scheme.

The MAC layer in IEEE 802.15.4 [44] has several operating modes. For the purpose of this section (supporting messages with deadline requirements in wireless ad-hoc networks) the most interesting mode is the beacon-enabled mode, where nodes organize themselves in a Personal Area Network (PAN), and a coordinator (called the PAN coordinator) organizes channel access and data transmissions in a structure called the superframe. A thorough review of IEEE 802.15.4 in the context of supporting messages with deadline requirements in WSN can be found in [45]. The GTS allocation mechanism was also subject of several studies that address the throughput and delay guarantees provided by this mechanism [46], and energy/delay trade-offs [47]. To overcome the maximum limit of seven GTS allowed, in [48] the authors propose i-Game, an implicit GTS allocation mechanism that enables the use of a GTS by several nodes.

At the routing layer, timeliness has been addressed by several works (e.g. [49, 50, 51, 52]). Other works have also employed hierarchical network/topological

models such as hexagonal, grid or cluster-tree (e.g. [53], [54], [27], [28], [55]).

3.3. Reliability/Robustness

There are different fault-management techniques for "traditional" distributed systems [56]: 1) *fault prevention*, to avoid or prevent faults; 2) *fault detection*, to use different metrics to collect symptoms of possible faults; 3) *fault isolation*, to correlate different types of fault indications received from the network, and propose various fault hypotheses; 4) *fault identification*, to test each of the proposed hypotheses in order to precisely localize and identify faults; 5) *fault recovery*, to treat faults, i.e., reverse their adverse effects.

Most fault avoidance techniques in WSNs operate in the network layer by adding redundancy in routing paths and sometimes enabling load balancing and congestion control. Some proposals are GRAB [57], Node-Disjoint Multipath [58], and Braided Multipath [58]. Fault prevention techniques prevent faults from happening by (1) ensuring full network coverage and connectivity at the design and deployment stages as proposed in [59] [60] [61], (2) constantly monitoring network status and triggering reactive actions if deemed necessary, or (3) enforcing redundancy in the data delivery path, hoping that at least one of the paths will survive.

Network monitoring, as in traditional distributed systems, provides a fundamental support for efficient fault detection and identification, either in passive (observing the traffic already present in the network to infer network condition) or active (probes injected into the network or relying on reports from the nodes) modes. Monitored network parameters include: (1) Node Status, concerning node's energy level, e.g. eScan [62] or energy map [63]; (2) Link Quality, enabling higher level protocols to adapt by changing routing structures as in [12]; (3) Congestion Level, by observing the buffer length as proposed in [64] and in CODA [65]; (4) Packet Loss, to be used as an indicator of faults, e.g. PSFQ [66] and GARUDA [67].

Upon detecting abnormal situations, fault isolation and identification will diagnose the causes. For instance, when a sink does not hear from a particular part of the routing tree, it is unknown whether it is due to failure of a key routing node, or failure of all nodes in a region. Sympathy [68] determines whether the cause of failure is in node health, bad connectivity/connection, or at the sink by, using an empirical decision tree.

Faults can be recovered independently of applications, like CODA [65]. However, this type of application-independent recovery does not differentiate between important (e.g., a new report) and unimportant packets (e.g.,

redundant reports, control packets). On the other hand, application aware fault tolerant protocols try to achieve application specified metrics (e.g., the percentage of distinct packets delivered), which requires the nodes to analyze packets and take different actions based on packet types.

There are different proposals for ensuring reliability in data collection in upstream communications, according to the data collection mode (raw or aggregated data). ESRT [64], PERG [69] and TAG [70] are some examples. Also, for downstream communications, other techniques were already proposed in the literature. PSFQ [66], GARUDA [67], and ReACT [71] are among the most popular.

In order to provide a higher level solution for fault-tolerance, fault-management frameworks with complete management infrastructures and information models have been also proposed (e.g. Digest [72], SNMS [73], AgletBus [74], MANNA [75]), which can be complemented with previous discussed approaches to achieve better performance.

3.4. *Mobility*

Mobility management has long been addressed for different types of computer networks, such as IP-based [76, 77], MANETs [78] or cellular [79] networks. Nevertheless, WSN characteristics such as scale (number of nodes and coverage area), node resource constraints and the fact that WSNs are usually supposed to detect/track physical phenomena, impose a rethinking of the mobility management paradigm.

In most WSNs literature, topology dynamics results mainly from nodes failure rather than from the mobility of nodes (sensors or sinks), i.e. WSN nodes (and the physical topology) are assumed to be static during runtime. Most WSN architectures/protocols support joining and leaving of nodes (e.g. ZigBee). Nevertheless, they react to topological changes by dropping the broken paths and computing new ones, thus resulting in network inaccessibility times that lead to message delay/loss. Although several WSN architectures have explored the use of mobility for data collection (e.g. [80]), target tracking (e.g. [81]) or repairing network connectivity (e.g. [82, 16]), no guarantees are given on timely data delivery. Some other works on mobility in WSNs (e.g. [83, 84]) reflect incomplete results.

Mobility scenario generation models enable to test mobility in WSNs. They are often based on stochastic models [85], taking into account mobility parameters such as speed, movement direction, radio propagation models

and presence of obstacles. BonnMotion [86] is an example of a tool to create and analyze mobility scenarios that can feed several network simulators.

Mobility support greatly impacts WSN lower protocol layers design and particularly MAC and routing mechanisms, for two main reasons: first, mobility involves topological changes that may affect algorithms that need to tune some parameters according to the density of nodes in the contention area. Second, MAC algorithms based on medium reservation may fail in case of mobility, since the reservation procedures usually assume static nodes. For instance, algorithms based on the Request-To-Send/Clear-To-Send (RTS/CTS) handshake for medium reservation may fail because either the corresponding nodes move outside the mutual coverage range after the handshake or external nodes get into the contention area and start transmitting without being aware of the medium reservation. Nevertheless, some MAC algorithms can self-adapt to topological changes resulting from nodes mobility (e.g. [87, 88]), but at the expense of higher energy consumption and medium access delay.

Generally speaking, many routing algorithms are able to cope with topology dynamics resulting from nodes mobility. However, most of them react to topology variations by dropping the broken paths and computing new ones from scratch, thus incurring in performance degradation. In particular, mobility may strongly affect cluster-based algorithms, due to the high cost of maintaining the cluster-architecture over a set of mobile nodes. Some routing algorithms specifically designed for networks with slow mobile nodes (e.g. GAF [89], TTDD [90]) attempt to estimate the nodes trajectories. The SPIN [91] family of protocols seems well-suited for environments where the sensors are mobile, since forwarding decisions are based on local neighbourhood information.

Another relevant issue is how well WSN nodes are able to estimate radio link quality, since usually handoff is performed when the current radio link quality is over passed by the link quality of an adjacent cell or cluster. The problem is that radio links cannot be identified just as "good" or "bad". There is a "transitional region" that leads to very variable quality and symmetry properties and is not adequately characterized by current link quality estimators [92].

3.5. Security

On the communication side, low power and low bit rate wireless networks suitable for WSN systems are the focus of an industrial consortium [93], IEEE

standard [94], and research community [95]. These proposals address multiple embedded devices and control of them from authenticated principals. They also propose solutions for preventing usage of the WSN by external principals. While ZigBee and IEEE 802.15.4 took the stance that cryptographic hardware support is needed (e.g. CC2420), TinySec has shown that with sufficient engineering effort, it is possible to encrypt and authenticate all communications entirely in software, without special hardware, at a cost of 5 – 10% performance loss [95]. TinySec has also proven that the advantages introduced by cryptographic hardware support are limited with respect to its costs both financial and in terms of increased power consumption.

In all these secure communication proposals a crucial problem is how devices can establish a shared secret cryptographic key. This is the classical *key agreement problem* that has been extensively investigated in general networks. This problem becomes non trivial in WSNs for the following reasons. The public-key agreement schemes used in general networks (e.g., Diffie-Hellman) are not suitable for wireless sensor networks due to the limited computational abilities of sensor nodes. Furthermore, pre-distribution of secret keys for all pairs of nodes is not viable due to the large amount of memory this requires when the network size is large. Finally, resorting to centralized trusted third-party (e.g., Kerberos) is not suitable for WSN due to the communication overhead it would cause.

The main approaches to pair-wise key establishment in WSNs are based on pre-deployment. All these approaches move from the observation that, in the most general case, WSN deployment is a random process and thus deterministically predicting the set of neighbors is not possible. In order to solve this problem Eschenauer and Gligor propose a random key pre-distribution scheme and show that, by adjusting the parameters of the scheme, key-establishment probability can be sufficiently great, nodes can set up keys with sufficiently many nodes, and the network becomes fully connected [96]. The main weakness of this approach is that an attacker who compromises a sufficiently number of nodes could reconstruct the key set and break the scheme. In LEAP+, Zhu *et al.* assume that a sensor node is able to resist an attack for a short period of time (say several seconds) when captured by an adversary and propose a scheme in which a shared secret is pre-deployed in every node [97]. The disadvantage of this scheme is that newly deployed nodes cannot establish a secure channel with those already deployed.

Recently, Malan *et al.* have shown that a purely software implementation of the Diffie-Hellman key establishment based on Elliptic Curve Cryptogra-

phy (ECC) over \mathbb{F}_{2^p} for sensor nodes on 8-bit, 7.3828 MHz MICA2 mote is indeed feasible [98].

In-network processing is a fundamental technique for elaborating the wealth of data provided by WSNs in an efficient and scalable way. In order to efficiently support this technique while guaranteeing security, pair-wise security is not adequate because it would ensue too many pair-wise encryptions and decryptions. Thus, it is more convenient to organize sensor nodes in a *group* and distribute a *group key* to all group members which use it to encrypt and decrypt messages. The challenge here consists in securely and efficiently revoking and distributing group keys upon joining and leaving of nodes [99]. Several group key management systems have been proposed so far aimed at reducing the overhead of group key management [97, 100, 101]. Younis *et al.* suggest a dynamic combinatorial grouping strategy [101]. Zhu *et al.* group neighbouring sensor nodes and iteratively merge groups up to establish network-wide shared key [97]. S2RP provides a dynamic, scalable and efficient group rekeying by integrating in a novel way two basic mechanisms, namely Logical Key Hierarchy [102] and Lamport's one time passwords [103].

A related problem is *authenticated broadcast*, a fundamental security service that enables a sender to broadcast critical data and/or commands to sensor nodes in an authenticated way. Due to the resource constraints on WSN nodes, traditional broadcast authentication techniques based on digital signatures are not viable. Perrig *et al.* developed μ TESLA for broadcast authentication in WSNs based on symmetric cryptography, which removes the dependence on public key cryptography [104]. Several multi-level μ TESLA schemes have been later proposed to extend the capability of the original μ TESLA protocol. A relevant example is reported in [105].

3.6. Heterogeneity

Almost no work has been tackling heterogeneity in WSNs. In our perspective, one of the most important reasons is that the number of WSN deployments so far is almost insignificant, particularly concerning real-world applications.

WSN nodes currently span over a large range of types, from MEMS (MicroElectroMEchanical Systems, e.g. for accelerometers), passive RFIDs (Radio-Frequency Identifiers, e.g. for inventory), active RFIDs (e.g. for toll charge), "general-purpose" motes (e.g. Mica, Telos, FireFly) to more powerful nodes for routing/gateway or processing/control (e.g. iMote, SunSPOT, Stargate). The integration of Radio-frequency Identifier (RFID) technology

with Wireless Sensor Networks has been accepted to provide a symbiotic solution that leads to improved system performance. The growing convergence between WSN and RFID nodes technology (particularly active RFIDs, whose computation and communications modules are battery-powered) has been turning the frontier between these heterogeneous technologies increasingly undefined.

Also, different types of sensors and sensor boards may be used for measuring different physical parameters, adding complexity to the WSN system (e.g. calibration). "Design diversity", i.e. using heterogeneous components to perform the same task (e.g. measuring the same physical parameter with two different types of sensors or performing the same computation using two different processors), is usually required in critical applications. Different operating systems and programming languages (particularly for resource-constrained networked embedded systems) might also be required. Also middleware (e.g. for security or fault tolerance) might be quite heterogeneous. Solutions for supporting these different levels of heterogeneity have not been achieved yet, particularly for large-scale systems.

Communication protocols might also be heterogeneous, both in horizontal and vertical perspectives. Some solutions are available for achieving interoperability between sensor/actuator-level network protocols in process control and automation industry (e.g. PROFIBUS, ASi, FF, HART, DeviceNet, ModBus), in automotive systems (e.g. CAN, FlexRay, TTP, LIN, MOST) or in building automation (e.g. EIB/KNX, LonWorks, HomePlug). The interoperability between these and higher-level networks, such as the Internet has also been achieved through adequate gateway-like devices. However, the large-scale nature of emerging networked embedded systems impose new networking architectures based on wireless communications, both at the sensor/actuator-level (e.g. IEEE 802.15.4, ZigBee, IEEE 802.15.6 (Body Sensor Networks), 6LoWPAN, Bluetooth Low Power, ISA SP100 or WirelessHART) and at backbone levels (e.g. WiFi/WiGig, WiMAX). Tangible results on this interoperability between wireless protocols are not available yet.

3.7. Energy sustainability

Several techniques regarding sensor networks have been proposed to maximize the lifetime of battery-powered wireless sensor nodes. In [106] the authors identify three main enabling techniques used for energy conservation

in wireless sensor networks: duty cycling, data driven, and mobility. The design principles behind them and their features are presented in the referred survey, however for a complete set of networking protocols the reader is referred to [107]. While all these techniques optimize and adapt energy usage to maximize the lifetime of energy reservoirs, the lifetime remains bounded and finite. Thus, further enhancements have to be done, especially regarding energy harvesting, to accomplish perpetual operation [108][109].

A comprehensive review of the many possible sources of energy that could potentially be harnessed is given in [110]. Among the currently most feasible are photonic, mechanical and thermal differentials. Solar-energy harvesting is based on the well-known principle of photovoltaic conversion, which provides high power densities, making it the best-suited choice to power wireless outdoor applications (e.g. ZebraNet, Trio, SHiMmer, etc.). A solution to power indoor routers was proposed in [111]. This approach revealed several weaknesses that enhance the need for further research on this area. In [112] several motes are reviewed and AmbiMax is presented as a new solution that uses both a solar panel and a wind generator to charge a supercapacitor based energy storage system. The need for multiple power sources is mentioned in [113] and a well successful approach is exploited in the multi-powered platform for precision agriculture proposed in [114]. In the cited example, besides a solar panel and a wind turbine, a small size hydrogenerator has been introduced as a way to harvest the energy of water-flow in irrigation pipes.

Mechanical energy from vibrations or movements is present almost everywhere and it can be transformed into useful electrical power by any kind of electromechanical transduction. Piezoelectric, electrostatic, and electromagnetic devices have been widely investigated and several companies now offer commercially miniature mechanical harvesters delivering sufficient power for sensor operating in an industrial environment [115]. However, researchers have not yet overcome difficulties encountered for body-powered applications [116], which require MEMS devices.

Temperature differences between various objects (natural and industrial) are also freely available within the environment. Manufacturing applications, where heat is a by-product of the manufacturing process, are typically ideal applications for thermal energy harvesting. Several companies (e.g. Micro-pelt, Nextreme and Thermolife) are already commercializing thermoelectric generators that can exploit those scenarios. Despite their high cost and low efficiency, due to their reliability and absence of moving parts, there has been

a growing interest in the generation of power from body heat [117], as a means to power wearable devices. Further research is needed on nanostructured materials and multilayers, in order to optimize thermoelectric properties [118], as well as on miniaturization using micromachining [119].

4. Roadmap

4.1. Scalability

From the very beginning of WSN research, the scientific community has been aware of the importance of building scalable systems. Although there were some research efforts where WSNs of a few hundreds (e.g. [22]) to one thousand nodes ([23]) were deployed, WSN with tens or hundreds of thousands of nodes are still a vision.

Hierarchical (multiple-tiered, clustered) architectures are a well-known and proven principle to make computer networks scale, bringing advantages such as: the communication latency increases very slowly with distance (timeliness), the cost per node is approximately the same as the one of the cheapest nodes (cost-efficiency) and it is easy to manage “sleep schedules” for nodes (energy-efficiency). Though eventually leading to more complex network architectures, the multiple-tiered architectural solution that we dubbed “heterogenous-protocols” seems the most promising for supporting scalability without compromising other QoS metrics (e.g. throughput, delay, reliability). In this case, the communication architecture is composed of a more powerful (e.g. higher energy capacity, radio coverage and bit rate) network technologies serving as a backbone to less powerful (sub)networks at the sensor/actuator level. Communication technologies such as the ones referred in Section 3.6 must be explored as potential candidates for these architectures.

Algorithms such as MAC, routing, data processing/aggregation and congestion control have been developed to operate as far as possible at different network scales, especially envisaging large scale systems. However, existing approaches are still far away from the desired scalability, so requiring further investigation. New algorithms might be either designed from scratch or based on (adapting) already available ones. Just as an example, dominance-based MAC protocols for WSNs may be explored in a way that the time complexity in the computation of aggregate quantities becomes independent of the number of nodes [33].

Larger scale may also mean more information sinks, depending on the application. While this can lead to a more complex design and system

architecture (e.g. concerning routing), it might also be beneficial in some other perspectives. The existence of multiple geographically distributed sinks might ease the load balancing task, reducing the amount of “bottlenecks” in the WSN. A multiple-tiered architecture may be seen as a particular case of “multiple sinks”, since data converges to separate “sink” nodes that may act as gateways to a higher level network.

4.2. Timeliness

As already referred the “big” challenge in large-scale WSN systems is to optimize all QoS properties simultaneously, knowing a priori that some (most) of them are contradictory. In what concerns “Timeliness”, we point to the following research directions:

- *explore hierarchical network architectures and models*, particularly trying to merge interesting features from more “mesh-like” (probabilistic MAC/routing, but more flexible, scalable and redundant) and more “clustered-like” approaches (deterministic MAC/routing, but less flexible and redundant, synchronization is complex), to grab the “best of both worlds”;
- *design protocols and algorithms in an optimized cross-layered approach*; analyse trade-offs in terms of flexibility and interoperability, since the software structure becomes more difficult to update and maintain; for example, explore how prioritized MAC schemes can be used to compute aggregated computations, in a way that time-complexity becomes independent of the number of nodes;
- *consider timeliness (and real-time) both at the node level (hardware and software) and at the network level*; the timing performance of a WSN depends on node hardware design, on the operating system (if any), programming language and style, as well as on the network protocol; in this line, investigate existing operating systems (OSs) for resource-constrained embedded systems, specially the most widely used (e.g. TinyOS and Contiki) in a way to support real-time features (pre-emption, priority inheritance mechanism) existing in other OSs (e.g. nano-RK and ERIKA);
- *investigate whether the classical approaches of embedded real-time systems still apply* (such as formal WCET analysis, synchronous lan-

guages), despite their strong resource limitations, or if more probabilistic-oriented approaches must be followed; these probabilistic models must consider the peculiarities of resource-constrained devices, particularly considering the probability of transmission errors (e.g. radio link quality must be correctly estimated) and thus of message retransmissions; one approach is to associate a confidence level with each guaranteed delay bound to *quantify the uncertainty* on the guaranteed delay bound;

- *design innovative MAC mechanisms for improving timeliness, reliability and energy-efficiency* (e.g. for mitigating the hidden-node problem, to avoid “idle/waste” times during nodes power on; using scheduling techniques for nodes efficiently sharing TDMA slots), guaranteeing an optimal trade-off between flexibility and complexity;
- *investigate on distributed and dynamic resource allocation schemes* for synchronized WSNs, where resources (e.g. bandwidth and memory) must be adequately allocated depending of the physical/logical network changes (e.g. a critical event); centralized adaptive synchronization induces a significant amount of computation and communication overheads, which may be unsuitable for WSNs.
- *build appropriate system planning and network dimensioning tools* to be able to achieve optimal trade-offs between QoS properties, particularly for timeliness;

4.3. Reliability/Robustness

As outlined in section 3.3, WSN hardware must be designed to be resistant to harsh environmental and usage conditions and no to harm the flora, fauna or the ecological structure of the environment (e.g. batteries), hence this aspect must be taken into consideration. The increasing tendency for miniaturization, instantiated in technologies such as RFID (Radio-Frequency Identification), MEMS (Microelectromechanical Systems) or SoC/NoC (Systems/Networks on Chip) and for reduction of cost per node should not compromise (or at least at a reduced level) hardware robustness. Actually, the trends for integrating sensing, processing, memory, communication and mechanical functionalities in a single chip may even be explored to improve hardware robustness.

Common practices for robust software/algorithms can be allied with a careful resource management for improved system robustness and in general

to higher reliability, e.g.: 1) writing “generic” code that can accommodate a wide range of situations and thereby avoid having to insert extra code into it just to handle special cases (code added just for special cases is often buggier than other code, and stability problems can become particularly frequent and/or severe from the interactions among several such sections of code); 2) using formal techniques, such as fuzz testing, to test algorithms since this type of testing involves invalid or unexpected inputs/stimulus; 3) providing each application with its own memory area and prevent it from interfering with the memory areas of other applications or of the kernel.

Although the fault-tolerance techniques enumerated in section 3.3 are promising in terms of robustness and energy efficiency, further research is needed to address the scalability and network dynamics in designing fault-tolerant mechanisms. Some interesting topics to address in the future are:

- when faults occur in WSNs, MAC and routing protocols must accommodate the formation of new links and routes to the destination, transport protocols must adaptively decide how to retransmit, and application layer protocols must determine which part of the missing data is critical and what level of loss is tolerable; therefore, multiple levels of redundancy may be needed and a cross-layer approach exploring the interactions among different protocol layers is desirable.
- the mechanisms presented in 3.3 only consider reliability (logical correctness) of data delivery as a performance metric; trade-offs with other QoS metrics must be considered as well;
- the presence of faults in WSNs introduces uncertainty into standard operations such as answering queries, as data should not be extracted in a purely best-effort manner, but be produced with a clearly defined formal meaning; for instance, if only a subset of the sensor readings satisfies the application query, the network only reports part of the readings filtered by the query; however, the sink does not know whether the remaining reports were not received due to network faults or because results were filtered by the query; if a metric is defined to indicate the completeness of the returned answer, the sink would be better informed; therefore, it is essential to develop informative quality metrics for sensor applications (network semantics).

Most fault management techniques in WSNs have been integrated with

application requirements [120]. Design of a generic fault management technique for WSNs must take into account a wide variety of applications with diverse needs, different sources of faults, and various network configurations. In addition, scalability, mobility, and timeliness may also have to be considered.

4.4. Mobility

Most network protocols support joining and leaving of nodes. Nevertheless, they react to topological changes by dropping the broken paths and computing new ones, thus resulting in network inaccessibility times that lead to message delays and losses. Although some WSN architectures have explored the use of mobile data collectors (data mules), which collect data from the sensor nodes and deliver it to the sinks, there are no guarantees on timely data delivery. In contrast, critical applications such as patient monitoring, factory automation or intelligent transportation systems require strict bounds on latency and guaranteed data delivery. In this context, coordination among mobile nodes is required, thus an important challenge is how a WSN can compute, in a distributed way, the path that a mobile node should follow. This path can be updated depending on the changes of the environment (e.g. mobility of observers, other WSNs or the phenomenon).

Mobility may be particularly difficult to support in cluster-based WSN architectures, due to the cost for maintaining clusters with a set of mobile nodes. Therefore, mobility management mechanisms for cluster-based WSNs must be carefully designed. MAC and routing protocols must also be adaptive to dynamic changes resulting from mobility, as they must transparently readapt to node number and density changes.

Mobility management mechanisms must be designed based on realistic (real-world) models, derived from real-world data. Mobility speed, obstacles, radio link quality and propagation models, network scale, network density and network partitioning are important factors that must be considered. For instance, an efficient mobility management mechanism greatly depends on how far the nodes are able to estimate radio link quality (usually handoff is performed when the current radio link quality is overpassed by the link quality of an adjacent cell or cluster). Recent studies show that radio links cannot be identified just as “good” or “bad”. There is a “transitional region” that can lead to very variable quality and symmetry properties, which is yet to be fully and adequately characterized.

Mobility models and benchmarks should be used to evaluate communication protocols and middleware approaches. While most simulation tools for WSNs lack mobility support (eventually due to the lack of protocols with mobility support), future simulators for WSN systems should encompass mobility support and be based on the previously referred realistic models.

The design of a mobility management mechanism fully depends on the existence or not of a localization mechanism (this may impact routing decisions as well). Location information may be quite beneficial for better mobility support, but may also have a negative impact on network management, energy-efficiency and cost. Consequently, localization mechanisms that are scalable, distributed, accurate, cost-effective and energy-efficient must be devised.

In summary, future research should focus on supporting transparent, seamless, energy-efficient, real-time and reliable mobility management mechanisms in WSNs.

4.5. Security

The topics addressed in Section 3.5 have achieved important results but they have not yet reached an adequate level of maturity. Actually, we need a secure and efficient key distribution mechanism that is resilient to node compromise, allows incremental deployment and scales to large networks. In this context, we expect to see research in more efficient public-key schemes, e.g., elliptic curves, hardware support for public-key cryptography [121], and efficiently and securely engineering elliptic curve cryptography for real world implementation [122].

The deployment of WSN in unattended, often hostile, environments makes it easier for an adversary to gain physical (not only logical) access to these devices. An adversary can physically capture an object, tamper with it, and have it behave maliciously. The compromise of even a single node may be sufficient to completely compromise the whole routing service [123]. Completely preventing this risk by means of tamper-resistant hardware does not seem viable because strong tamper-resistance is too expensive and not always absolutely safe. Thus the challenge is to build networks that can operate correctly even in the presence of several compromised nodes, at least up to a certain threshold. A possible direction consists in tolerating compromised nodes by exploiting the network redundancy and the knowledge of the physical environment. Interesting results have been achieved both in the context

of secure routing [124] and secure aggregation [125], but this remains a continuing overall challenge.

Another direction consists on program integrity verification, a technique enables to remotely verify the integrity of the program residing in each device whenever the device joins the network or has experienced a long service blockage. Software-based approaches to program integrity verification have been proposed for sensor networks [126, 127]. However, these approaches provide security under the assumption of a limited adversary. More research is thus necessary to overcome these limitations. In addition, efficient hardware support for integrity verification could be useful in order to make the integrity verification procedure more difficult to simulate and to indissolubly link the execution of such a procedure with the node under verification.

"Traditional" network QoS and network security have been considered as separate entities and research in these areas have largely proceeded independently. However, security impacts overall QoS and it is therefore essential to consider both security and QoS together when designing protocols for ad hoc environments as one impacts the other. The research community has recently acknowledged this gap. Some initial and promising results have been obtained [128, 129] but the topic is still in its infancy.

WSNs are more ubiquitous and pervasive than the Internet and therefore they tend to be a more invasive from the user privacy point of view. The Zigbee consortium [93] and the IEEE 802.15.4 [94] propose solutions aimed at preventing an unauthorized principal from accessing the WSN. However, these solutions reflect the perspective of a network administrator. A key challenge is to provide solutions that reflect the standpoint of the user, the ultimate owner of such a private information. The main challenges here are security and usability. On the one hand we need mechanisms that allow a user to retain control on who has access to his/her information. On the other hand, these mechanisms must be usable by a normal computer-illiterate user. From this standpoint, Johnson and Stajano have made a preliminary work in the smart-home context [130]. However, more research is necessary.

4.6. Heterogeneity

As can be inferred from section 3.6, WSN research must tackle heterogeneity almost from scratch. New classes of resource-constrained embedded system devices should be clearly identified, defining frontiers between nodes with different characteristics and capabilities (e.g. motes, RFIDs, MEMS).

As technology rapidly evolves, tending for miniaturization, these frontiers are increasingly harder to define, bringing enormous challenges ahead.

WSN applications may require sensor/actuator nodes to measure different physical parameters, implying heterogeneous sensing technology. Also, the same physical quantity may be required to be measured by many WSN nodes (for reliability purposes, or just because there is the need to extract the minimum/average/maximum value of that parameter in a certain region), or even by different types of sensors (“design diversity” for redundancy or accuracy purposes). The quantity and diversity of these sensing technologies will bring important challenges (e.g. for hardware design, hardware abstraction layers design, calibration).

Another challenge is how to tackle the interoperability between sensor/actuator-level communication protocols. From past experience, there will be no “single” standard for sensor/actuator-level communication protocols. Wireless protocols such as IEEE 802.15.4, IEEE 802.15.6, ZigBee, 6LoWPAN, Bluetooth Low Power, ISA SP100 or WirelessHART might need to interoperate between them and also with wired ones. Vertical integration of networks at different hierarchical levels will also be a major challenge. Higher bandwidth and more robust wired (e.g. ATM, Switched Ethernet) and wireless (e.g. WiFi/WiGig, WiMAX, UWB) networks will have to interoperate with sensor/actuator-level networks. Guaranteeing end-to-end QoS brings even more complexity into WSN protocol design, i.e. satisfying throughput, delay, reliability, security, energy-efficiency requirements across different network tiers is not straightforward. Moreover, network planning/management tools must tackle these heterogeneous systems in an efficient and straightforward fashion.

Heterogeneity in WSN systems is also instantiated at the operating systems and programming language levels. Operating systems such as TinyOS, Contiki, Mantis, nano-RK, ERIKA have been around for some time, each of them with specific characteristics. So, it is likely that future WSN systems (particularly at large-scale) might comprise computing devices running more than one operating systems, leading to additional design complexity. The same applies to programming languages/environments (e.g. nesC, C, JAVA) and simulation/debugging tools.

Hosting/client equipment and HMIs are also likely to be quite heterogeneous. Wearable computing equipments are likely to be used in a panoply of WSN applications (e.g. HMDs for industrial maintenance or mobile phones in participatory/urban sensing). Other equipment, such as database servers,

video-surveillance cameras, monitoring/control computers (industrial PCs, PLCs, RCs) mobile robots or transportation vehicles, industrial machinery (welding/painting/assembly robots, machine-tools, roller belts, cranes) will rise the level of heterogeneity to unprecedented levels.

WSN systems will probably have to support several applications and services, imposing different QoS requirements which might dynamically change depending on spatiotemporal issues (e.g. WSN system for building automation may control security/access control, fire/smoke alarm systems, HVAC system, lights, doors, blinds, lifts/escalators, each of these with particular/dynamic requirements). Therefore, mechanisms such routing/MAC, admission control and scheduling, security, fault-tolerance or data aggregation must be designed to encompass such heterogeneous applications and services. The diversity of users (culture, technical skills) of a WSN system is also a challenge for system designers, namely in what concerns HMIs, safety and security requirements. Semantics should be further explored to ease the users role.

4.7. Energy sustainability

Energy sources are ubiquitous in the environment [20][111], so it is reasonable to consider that the energy required to permanently operate a WSN can be obtained through energy harvesting. There are currently several methods to harness energy from some of those sources. Nevertheless, some others are neglected, mostly due to challenges raised by the low energy density or feasibility of the energy harvesting method (e.g. ambient RF energy). All those sources have in common their random nature, a characteristic that still dictates the undesirable use of energy reservoirs, typically rechargeable batteries or, more recently, ultracapacitors [112]. Based on the above remarks, several approaches have to be exploited simultaneously, so that a system continues to operate perennially.

As the power levels achieved by miniature harvesters are usually low, wireless sensor nodes must be prepared to harvest energy from all the available energy sources surrounding it, in order to suffice nodes' power requirements. Moreover, in contrast to approaches that only attempt to minimize the energy consumption of each node, software (e.g. algorithms, protocols) design must also concern on adapting node-level system parameters (e.g. duty-cycling, transmission power, sensing reliability, etc) such that a maximal efficiency is obtained while respecting the energetic sustainability of the node.

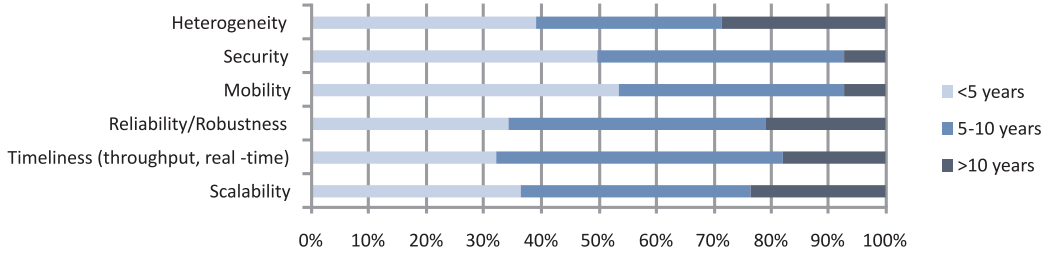


Figure 3: Survey: Non Functional Properties

Finally, another important issue is that nodes deployed in different places will probably have different harvesting opportunities. This means that it is absolutely necessary to align the workload allocation with the energy availability of each individual node. For that, network solutions and protocols such as MAC and routing will have to be redesigned, so they can deal with such changeable nodes and maintain the desired QoS.

5. Timeline

Non-functional properties (NFPs) are considered to be of paramount importance to Cooperating Objects and Wireless Sensor Network systems. This is reflected by the market analysis presented in [7] (Chapter 5) and also by the answers to a recent survey (CONET questionnaire filled by academics and industrialists). As already referred, heterogeneity, timeliness, reliability/robustness, mobility, security and heterogeneity are quality-of-service (QoS) properties that must be observed in all WSN systems and fulfilled for each particular application in both individual and integrated perspectives. Mobility is probably the only exception, in the sense that only some WSN applications will require mobility support.

Figure (3) (*source*: [7], Section 6.2.3) reflects the answers in what concerns how long it will take to get effective solutions for each NFP. The current state-of-the-art and state-of-technology reveals a strong immaturity and a clear lack of solutions (protocols, software/hardware architectures, technology) in respect to these NFPs. Current real-world applications and even research-oriented test-beds exist in a relatively small number and feature just up to some hundreds of sensor/actuator nodes. Market studies (e.g. On World) forecast mass deployments of WSN systems (sensor/actuator networks, pervasive Internet, smart environments) at a global scale, but this

seems to be a vision that will see the light only in more than one decade.

Research on improving the timeliness, security and reliability/robustness of WSN systems are still at a very early stage, particularly for the latter. Scalability is being considered by researchers (e.g. algorithms, methodologies, protocols), but results are still either incomplete, immature and/or yet to be validated through large-scale real-world applications. Almost no work exists on supporting mobility (nodes, node clusters) in WSNs. While successful results are not obtained using homogeneous WSN systems, it will be hard (almost impossible) to support high levels of heterogeneity, such as the coexistence and interoperability between heterogeneous hardware platforms, network protocols, operating systems, middleware and applications.

Power Efficiency and Energy Harvesting (which we fit into “Energy Sustainability”) have been considered separately ([7], Section 6.2.1). For the former, a major breakthrough is expected in a short to medium term, because of the importance of this issue for the massive adoption of WSN technology and systems. Energy Harvesting seems to be a harder problem that will require more time to find solutions that can be widely used.

Even more difficult is to fulfil and balance all these NFP/QoS properties at the same time, i.e. in a holistic perspective, since most of them are contradictory (i.e. improving one of them may harm the others). While a minimum level of maturity in each NFP must be reached, a bigger challenge is to devise system/network dimensioning methodologies and tools that are able to support system designers on balancing these properties in a way that system/application requirements are met. This is why we preclude that mature solutions to fulfil these QoS properties in a holistic fashion might only be achieved in a decade or so.

6. Conclusion

As people increasingly depend on embedded computing systems, the quality of their service (QoS) is also of growing importance, particularly for Wireless Sensor Network (WSN) applications where humans, fauna, flora, the environment or any valuable good may be severely affected by their behavior.

However, the provision of QoS in WSNs is very challenging due to the following problems: (1) the usually severe limitations of WSN nodes (e.g. energy, computational and communication capabilities and security); (2) the harsh nature of the environments (impacting e.g. node lifetime, communication reliability); (3) the large-scale nature of most WSNs (impacting e.g.

timeliness, reliability, security); (4) the high interdependency between QoS properties (as they are often contradictory).

This paper aimed at identifying the most important non-functional properties that affect the overall quality of the service provided to the users - scalability, heterogeneity, timeliness, reliability, security, mobility and energy sustainability - outlining their relevance, state-of-the-art and future research directions.

The bigger challenge seems to be how to achieve an optimal trade-off between QoS metrics, according to the QoS requirements imposed by each application. We envision that the solution is to conceive models, methodologies and tools for network and system planning and dimensioning, based on (multicriteria) optimization techniques. System designers must have software tools for automatically setting each and every property, parameter and mechanism of the system, trying to fulfill and balance all QoS properties. We preclude that this will only be possible in a decade or so. Enough maturity must first be achieved in each individual QoS property before holistic solutions may see the light.

References

- [1] J. Turley, "Embedded processors by the numbers," <http://www.embedded.com/1999/9905/9905turley.htm>, 1999.
- [2] M. Alves, "The wireless sensor networks standards and cots landscape: can we get qos and "calm technology"?" Tutorial at EWSN'09. [Online]. Available: <http://www.hurray.isep.ipp.pt/ART-WiSe>
- [3] W. Stallings, *Data and computer communications (5th ed.)*. Upper Saddle River, NJ, USA: Prentice-Hall, Inc., 1997.
- [4] J. Irvine and D. Harle, *Data Communications and Networks: An Engineering Approach*. John Wiley and Sons, Ltd, 2001.
- [5] B. Raman and K. Chebrolu, "Sensor networks: a critique of "sensor networks" from a systems perspective," *SIGCOMM Comput. Commun. Rev.*, vol. 38, no. 3, pp. 75–78, 2008.
- [6] M. D. Weiser, "The Computer for the 21st Century," *Scientific American*, vol. 265, no. 3, pp. 94–104, Sep. 1991.

- [7] P. Marron et al., Ed., *Cooperating Objects Roadmap 2009*, 1st ed. Logos Verlag, 2009.
- [8] J. Stankovic, I. Lee, A. Mok, and R. Rajkumar, "Opportunities and obligations for physical computing systems," *IEEE Computer*, vol. 38, no. 11, pp. 25–33, 2005.
- [9] E. A. Lee, "Cyber-physical systems - are computing foundations adequate?" in *Position Paper for NSF Workshop On Cyber-Physical Systems: Research Motivation, Techniques and Roadmap*, October 2006.
- [10] J. A. Stankovic, T. Abdelzaher, C. Lu, L. Sha, and J. Hou, "Real-Time Communication and Coordination in Embedded Sensor Networks," *Proceedings of the IEEE*, vol. 91, no. 7, pp. 1002–1022, 2003.
- [11] J. Zhao and R. Govindan, "Understanding packet delivery performance in dense wireless sensor networks," in *SenSys '03: Proceedings of the 1st international conference on Embedded networked sensor systems*. New York, NY, USA: ACM, 2003, pp. 1–13.
- [12] A. Woo, T. Tong, and D. Culler, "Taming the underlying challenges of reliable multihop routing in sensor networks," in *SenSys '03: Proceedings of the 1st international conference on Embedded networked sensor systems*. New York, NY, USA: ACM, 2003, pp. 14–27.
- [13] G. Zhou, T. He, S. Krishnamurthy, and J. A. Stankovic, "Impact of radio irregularity on wireless sensor networks," in *MobiSys '04: Proceedings of the 2nd international conference on Mobile systems, applications, and services*. New York, NY, USA: ACM, 2004, pp. 125–138.
- [14] A. Cerpa, J. L. Wong, L. Kuang, M. Potkonjak, and D. Estrin, "Statistical model of lossy links in wireless sensor networks," in *IPSN '05: Proceedings of the 4th international symposium on Information processing in sensor networks*. Piscataway, NJ, USA: IEEE Press, 2005, p. 11.
- [15] C. Chen and J. Ma, "Mobile enabled large scale wireless sensor networks," *Advanced Communication Technology, 2006. ICACT 2006. The 8th International Conference*, vol. 1, pp. 333–338, Feb. 2006.
- [16] B. Liu, P. Brass, O. Dousse, P. Nain, and D. Towsley, "Mobility improves coverage of sensor networks," in *MobiHoc '05: Proceedings of the 6th ACM international symposium on Mobile ad hoc networking and computing*. New York, NY, USA: ACM, 2005, pp. 300–308.

- [17] S. Ravi, A. Raghunathan, P. Kocher, and S. Hattangady, "Security in embedded systems: Design challenges," *Trans. on Embedded Computing Sys.*, vol. 3, no. 3, pp. 461–491, 2004.
- [18] S. Ravi, A. Raghunathan, and S. Chakradhar, "Tamper resistance mechanisms for secure, embedded systems," in *VLSID '04: Proceedings of the 17th International Conference on VLSI Design*. Washington, DC, USA: IEEE Computer Society, 2004, p. 605.
- [19] M. Fetcenko, S. Ovshinsky, B. Reichman, K. Young, C. Fierro, J. Koch, A. Zallen, W. Mays, and T. Ouchi, "Recent advances in nimh battery technology," *Journal of Power Sources*, vol. 165, no. 2, pp. 544 – 551, 2007, iBA - HBC 2006 - Selected papers from the INTERNATIONAL BATTERY ASSOCIATION & HAWAII BATTERY CONFERENCE 2006 Waikoloa, Hawaii, USA 9-12 January 2006. [Online]. Available: <http://www.sciencedirect.com/science/article/B6TH1-4MCW9T7-4/2/3d16368ff78e3c7b5bf30a61b9d91602>
- [20] J. A. Paradiso and T. Starner, "Energy scavenging for mobile and wireless electronics," *IEEE Pervasive Computing*, vol. 4, no. 1, pp. 18–27, 2005.
- [21] J. P. Thomas, M. A. Qidwai, and J. C. Kellogg, "Energy scavenging for small-scale unmanned systems," *Journal of Power Sources*, vol. 159, no. 2, pp. 1494 – 1509, 2006. [Online]. Available: <http://www.sciencedirect.com/science/article/B6TH1-4JBGJ45-6/2/ba83614ecb29098a9af8acdf590da792>
- [22] T. He, S. Krishnamurthy, J. Stankovic, T. Abdelzaher, L. Luo, R. Stoleru, T. Yan, L. Gu, G. Zhou, J. Hui, and B. Krogh, "VigilNet: An integrated sensor network system for energy-efficient surveillance," *ACM Transactions on Sensor Networks*, vol. 2, no. 1, pp. 1–38, February 2006.
- [23] A. Arora, R. Ramnath, E. Ertin, P. Sinha, S. Bapat, V. Naik, V. Kulathurmani, H. Zhang, H. Cao, M. Sridharan, N. Seddon, C. Anderson, T. Herman, N. Trivedi, C. Zhang, R. Shah, S. Kulkarni, M. Aramugam, and L. Wang, "Exscal: Elements of an extreme scale wireless sensor network," in *RTCSA '05: Proc. of the 11th IEEE International Conference on Embedded and Real-Time Computing Systems and Applications*, 2005, pp. 102–108.
- [24] Zigbee-Alliance, "Zigbee specification," <http://www.zigbee.org/>, 2005.

- [25] G. Gupta and M. Younis, "Fault-tolerant clustering of wireless sensor networks," in *WCNC '03: IEEE Wireless Communication and Networks Conference*. IEEE Press, 2003.
- [26] W. Heinzelman, A. Chandrakasan, and H. Balakrishnan, "Energy-efficient communication protocols for wireless microsensor networks," in *Proc. Hawaaiian Int'l Conf. on Systems Science*, 2000.
- [27] K. S. Prabh and T. Abdelzaher, "On scheduling and real-time capacity of hexagonal wireless sensor networks," in *ECRTS '07: Proc. of the 19th Euromicro Conference on Real-Time Systems*. IEEE Press, Los Alamitos, CA, 2007, pp. 136–145.
- [28] A. Koubaa, M. Alves, and E. Tovar, "Modeling and worst-case dimensioning of cluster-tree wireless sensor networks," in *RTSS'06: Proc. of the 27th IEEE Real-Time Systems Symposium*. IEEE Press, 2006, pp. 412–421.
- [29] O. Gnawali, K.-Y. Jang, J. Paek, M. Vieira, R. Govindan, B. Greenstein, A. Joki, D. Estrin, and E. Kohler, "The tenet architecture for tiered sensor networks," in *SenSys '06: Proceedings of the 4th international conference on Embedded networked sensor systems*. New York, NY, USA: ACM, 2006, pp. 153–166.
- [30] V. A. Kottapalli, A. S. Kiremidjian, J. P. Lynch, E. Carryer, T. W. Kenny, K. H. Law, and Y. Lei, "Two-tiered wireless sensor network architecture for structural health monitoring," in *SPIE '03: Proc. of 10th Annual International Symposium on Smart Structures and Materials*, 2003, pp. 8–19.
- [31] J. Leal, A. Cunha, M. Alves, and A. Koubaa, "On a IEEE 802.15.4/ZigBee to IEEE 802.11 gateway for the ART-WiSe architecture," in *ETFA '07: Work-in-Progress session of the 12th IEEE Conference on Emerging Technologies and Factory Automation*. IEEE Press, 2007.
- [32] R. B. GmbH, Stuttgart, "CAN specification, ver. 2.0," <http://www.semiconductors.bosch.de/pdf/can2spec.pdf>, 1991.
- [33] B. Andersson, N. Pereira, W. Elmenreich, E. Tovar, F. Pacheco, and N. Cruz, "A scalable and efficient approach for obtaining measurements in CAN-Based control systems," *IEEE Transactions on Industrial Informatics*, vol. 4, no. 2, pp. 80–91, 2008.
- [34] Z. Hu and B. Li, "Fundamental performance limits of wireless sensor networks," in *in Ad Hoc and Sensor*. Nova Science Publishers, 2004.

- [35] J. Elson, L. Girod, and D. Estrin, “Fine-grained network time synchronization using reference broadcasts,” in *Proceedings of 5th symposium on Operating systems design and implementation (OSDI’02)*, Boston, MA, USA, Dec. 2002, pp. 147–163.
- [36] S. Ganeriwal, R. Kumar, and M. B. Srivastava, “Timing-sync protocol for sensor networks,” in *Proceedings of 1st international conference on Embedded networked sensor systems (SenSys’03)*, Los Angeles, California, USA, Nov. 2003, pp. 138–149.
- [37] M. Maróti, B. Kusy, G. Simon, and A. Lédeczi, “The flooding time synchronization protocol,” in *Proceedings of 2nd international conference on Embedded networked sensor systems (SenSys’04)*, Baltimore, MD, USA, Nov. 2004, pp. 39–499.
- [38] G. Werner-Allen, G. Tewari, A. Patel, M. Welsh, and R. Nagpal, “Firefly-inspired sensor network synchronicity with realistic radio effects,” in *3rd international conference on Embedded networked sensor systems (SenSys’05)*, 2005, pp. 142 – 153.
- [39] V. Rajendran, K. Obraczka, and J. J. Garcia-Luna-Aceves, “Energy-efficient, collision-free medium access control for wireless sensor networks,” in *Proceedings of 1st international conference on Embedded networked sensor systems (SenSys’03)*, Los Angeles, California, USA, Nov. 2003, pp. 181–192.
- [40] A. Rowe, R. Mangharam, and R. Rajkumar, “RT-Link: A time-synchronized link protocol for energy- constrained multi-hop wireless networks,” in *Proceedings of the 3rd Annual IEEE Communications Society on Sensor and Ad Hoc Communications and Networks (SECON ’06)*, Reston, VA, USA, Sep. 2006, pp. 402–411.
- [41] A. P. Sinem Coleri and P. Varaiya, “PEDAMACS: Power efficient and delay aware medium access protocol for sensor networks,” *IEEE Transactions on Mobile Computing*, vol. 5, no. 7, pp. 920–930, 2006.
- [42] M. Caccamo and L. Y. Zhang, “An implicit prioritized access protocol for wireless sensor networks,” in *Proceedings of the 23rd IEEE Real-Time Syst. Symp. (RTSS’02)*, Austin, TX, USA, Dec. 2002, pp. 39–48.
- [43] T. Watteyne, I. Augé-Blum, and S. Ubéda, “Dual-mode real-time mac protocol for wireless sensor networks: a validation/simulation approach,” in *1st international conference on Integrated internet ad hoc and sensor networks InterSense’06*. New York, NY, USA: ACM, 2006, p. 2.

- [44] IEEE, "IEEE standard for information technology - telecommunications and information exchange between systems - local and metropolitan area networks - specific requirements - part 14.4: Wireless medium access control (MAC) and physical layer (PHY) specifications for low rate wireless personal area networks (LR-WPANs)," October, 2003.
- [45] A. Koubâa, M. Alves, and E. Tovar, "IEEE 802.15.4: a federating communication protocol for time-sensitive wireless sensor networks," IPP-HURRAY! Research Group, Institute Polytechnic Porto, Porto, Portugal, Tech. Rep. HURRAY-TR-060202, 2006.
- [46] A. Koubâa, M. Alves, and E. Tovar, "GTS allocation analysis in IEEE 802.15.4 for real-time wireless sensor networks," in *Proceedings of 14th International Workshop on Parallel and Distributed Real-Time Systems (WP-DRTS'06)*, Rhodes Island, Greece, Apr. 2006.
- [47] A. Koubâa, M. Alves, and E. Tovar, "Energy/delay trade-off of the GTS allocation mechanism in IEEE 802.15.4 for wireless sensor networks," *International Journal of Communication Systems*, vol. 20, no. 7, pp. 791–808, Jul. 2007.
- [48] A. Koubâa, M. Alves, and E. Tovar, "i-GAME: An implicit gts allocation mechanism in ieee 802.15.4," in *Proceedings of 18th Euromicro Conference on Real-Time Systems (ECRTS'06)*, Dresden, Germany, Jul. 2006.
- [49] T. He, J. A. Stankovic, C. Lu, and T. Abdelzaher, "Speed: a stateless protocol for real-time communication in sensor networks," in *Distributed Computing Systems, 2003. Proceedings. 23rd International Conference on*, 2003, pp. 46–55.
- [50] K. Akkaya and M. Younis, "An energy-aware qos routing protocol for wireless sensor networks," in *Distributed Computing Systems Workshops, 2003. Proceedings. 23rd International Conference on*, May 2003, pp. 710–715.
- [51] E. Felemban, C.-G. Lee, E. Ekici, R. Boder, and S. Vural, "Probabilistic qos guarantee in reliability and timeliness domains in wireless sensor networks," in *INFOCOM 2005. 24th Annual Joint Conference of the IEEE Computer and Communications Societies. Proceedings IEEE*, vol. 4, March 2005, pp. 2646–2657 vol. 4.
- [52] H. Li, P. Shenoy, and K. Ramamritham, "Scheduling messages with deadlines in multi-hop real-time sensor networks," in *11th IEEE Real Time and*

Embedded Technology and Applications Symposium RTAS'05, 2005, pp. 415 – 425.

- [53] T. Abdelzaher, K. S. Prabh, and R. Kiran, “On real-time capacity limits of multihop wireless sensor networks,” in *RTSS' 04: Proc. of the 25th IEEE Real-Time Systems Symposium*. IEEE Press, Los Alamitos, CA, 2004.
- [54] J. Gibson, G. Xie, and Y. Xiao, “Performance limits of fair-access in sensor networks with linear and selected grid topologies,” in *GLOBECOM '07: 50th IEEE Global Communications Conference Ad Hoc and Sensor Networking Symposium*, 2007.
- [55] P. Jurcik, R. Severino, A. Koubâa, M. Alves, and E. Tovar, “Real-time communications over cluster-tree sensor networks with mobile sink behaviour,” in *RTCSA '08: Proc. of the 14th IEEE International Conference on Embedded and Real-Time Computing Systems and Applications*, 2008.
- [56] A. S. Tanenbaum and M. V. Steen, *Distributed Systems: Principles and Paradigms*. Upper Saddle River, NJ, USA: Prentice Hall PTR, 2001.
- [57] F. Y. G. Zhong, “Gradient broadcast: A robust data delivery protocol for large scale sensor networks,” *ACM Wireless Networks (WINET)*, vol. 11, pp. 285–298, 2005.
- [58] D. Ganesan, R. Govindan, S. Shenker, and D. Estrin, “Highly-resilient, energy-efficient multipath routing in wireless sensor networks,” *SIGMOBILE Mob. Comput. Commun. Rev.*, vol. 5, no. 4, pp. 11–25, 2001.
- [59] S. Meguerdichian, F. Koushanfar, M. Potkonjak, and M. Srivastava, “Coverage problems in wireless ad-hoc sensor networks,” *INFOCOM 2001. Twentieth Annual Joint Conference of the IEEE Computer and Communications Societies. Proceedings. IEEE*, vol. 3, pp. 1380–1387 vol.3, 2001.
- [60] F. Xue and P. R. Kumar, “The number of neighbors needed for connectivity of wireless networks,” *Wirel. Netw.*, vol. 10, no. 2, pp. 169–181, 2004.
- [61] V. Isler, S. Kannan, and K. Daniilidis, “Sampling based sensor-network deployment,” *Intelligent Robots and Systems, 2004. (IROS 2004). Proceedings. 2004 IEEE/RSJ International Conference on*, vol. 2, pp. 1780–1785 vol.2, Sept.-2 Oct. 2004.
- [62] Y. Zhao, R. Govindan, and D. Estrin, “Residual energy scan for monitoring sensor networks,” *Wireless Communications and Networking Conference, 2002. WCNC2002. 2002 IEEE*, vol. 1, pp. 356–362 vol.1, Mar 2002.

- [63] R. A. F. Mini, A. A. F. Loureiro, and B. Nath, "The distinctive design characteristic of a wireless sensor network: the energy map," *Computer Communications*, vol. 27, no. 10, pp. 935 – 945, 2004, protocol Engineering for Wired and Wireless Networks. [Online]. Available: <http://www.sciencedirect.com/science/article/B6TYP-4BMY15B-2/2/9acdbb590e792dea4a44b6eb48360ff2>
- [64] Y. Sankarasubramaniam, Özgür B. Akan, and I. F. Akyildiz, "Esrt: event-to-sink reliable transport in wireless sensor networks," in *MobiHoc '03: Proceedings of the 4th ACM international symposium on Mobile ad hoc networking & computing*. New York, NY, USA: ACM, 2003, pp. 177–188.
- [65] C.-Y. Wan, S. B. Eisenman, and A. T. Campbell, "Coda: congestion detection and avoidance in sensor networks," in *SenSys '03: Proceedings of the 1st international conference on Embedded networked sensor systems*. New York, NY, USA: ACM, 2003, pp. 266–279.
- [66] C. yih Wan, A. T. Campbell, and L. Krishnamurthy, "Pump-slowly, fetch-quickly (psfq) : A reliable transport protocol for sensor networks," *IEEE Journal on Selected Areas in Communications*, vol. 23, pp. 862–872, 2005.
- [67] S.-J. Park, R. Vedantham, R. Sivakumar, and I. F. Akyildiz, "A scalable approach for reliable downstream data delivery in wireless sensor networks," in *MobiHoc '04: Proceedings of the 5th ACM international symposium on Mobile ad hoc networking and computing*. New York, NY, USA: ACM, 2004, pp. 78–89.
- [68] N. Ramanathan, K. Chang, R. Kapur, L. Girod, E. Kohler, and D. Estrin, "Sympathy for the sensor network debugger," in *SenSys '05: Proceedings of the 3rd international conference on Embedded networked sensor systems*. New York, NY, USA: ACM, 2005, pp. 255–267.
- [69] Q. Han, I. Lazaridis, S. Mehrotra, and N. Venkatasubramanian, "Sensor data collection with expected reliability guarantees," in *PERCOMW '05: Proceedings of the Third IEEE International Conference on Pervasive Computing and Communications Workshops*. Washington, DC, USA: IEEE Computer Society, 2005, pp. 374–378.
- [70] J. Considine, F. Li, G. Kollios, and J. Byers, "Approximate aggregation techniques for sensor databases," in *ICDE '04: Proceedings of the 20th International Conference on Data Engineering*. Washington, DC, USA: IEEE Computer Society, 2004, p. 449.

- [71] V. Rajendran, K. Obraczka, Y. Yi, S.-J. Lee, K. Tang, and M. Gerla, "Combining source- and localized recovery to achieve reliable multicast in multi-hop ad hoc networks," in *NETWORKING 2004, Networking Technologies, Services, and Protocols; Performance of Computer and Communication Networks; Mobile and Wireless Communication, Third International IFIP-TC6 Networking Conference, Athens, Greece, May 9-14, 2004, Proceedings*, ser. Lecture Notes in Computer Science, vol. 3042. Springer, 2004. [Online]. Available: citeseer.ist.psu.edu/704792.html
- [72] J. Zhao, R. Govindan, and D. Estrin, "Computing aggregates for monitoring wireless sensor networks," *Sensor Network Protocols and Applications, 2003. Proceedings of the First IEEE. 2003 IEEE International Workshop on*, pp. 139–148, May 2003.
- [73] G. Tolle and D. Culler, "Design of an application-cooperative management system for wireless sensor networks," *Wireless Sensor Networks, 2005. Proceedings of the Second European Workshop on*, pp. 121–132, Jan.-2 Feb. 2005.
- [74] J.-J. Lim, D. Kiskis, and K. Shin, "System support for management of networked low-power sensors," *Network Operations and Management Symposium, 2006. NOMS 2006. 10th IEEE/IFIP*, pp. 436–447, April 2006.
- [75] L. Ruiz, J. Nogueira, and A. Loureiro, "Manna: a management architecture for wireless sensor networks," *Communications Magazine, IEEE*, vol. 41, no. 2, pp. 116–125, Feb 2003.
- [76] D. Saha, A. Mukherjee, I. Misra, M. Chakraborty, and N. Subhash, "Mobility support in ip: a survey of related protocols," *Communications Magazine, IEEE*, vol. 18, no. 6, pp. 34–40, 2004.
- [77] A. T. Campbell, "Comparison of ip micromobility protocols," *Wireless Communication, IEEE*, vol. 9, pp. 72–82, Feb 2002.
- [78] F. Abduljalil and S. Bodhe, "A survey of integrating ip mobility protocols and mobile ad hoc networks," *Communications Surveys & Tutoriale, IEEE*, vol. 9, no. 1, pp. 14–30, 2007.
- [79] T.-Y. Wu, C.-Y. Huang, and H.-C. Chao, "A survey of mobile ip in cellular and mobile ad-hoc network environments," *Ad Hoc Networks, IEEE*, vol. 3, no. 3, pp. 351–370, May 2005.

- [80] M. Laibowitz and J. A. Paradiso, "Parasitic mobility for pervasive sensor networks," in *in Proc. 3rd Ann. Conf. Pervasive Computing (Pervasive 2005)*, Springer-Verlag, 2005. 29. A.S. Holmes et al., *??Axial-Flow Microturbine with Electromagnetic Generator: Design, CFD Simulation, and Prototype Demonstration,???* *Proc. 17th IEEE Int??l Micro Electro.* Springer-Verlag, 2005, pp. 255–278.
- [81] Y. Zou and K. Chakrabarty, "Distributed mobility management for target tracking in mobile sensor networks," *Transactions on Mobile Computing, IEEE*, vol. 6, no. 8, pp. 872–887, June 2007.
- [82] P. Corke, S. Hrabar, R. Peterson, D. Rus, S. Saripalli, and G. Sukhatme, "Autonomous deployment and repair of a sensor network using an unmanned aerial vehicle," in *in IEEE International Conference on Robotics and Automation*, 2004, pp. 3602–3609.
- [83] A. Muneeb, V. Thiemo, and U. Z. Afzal, "Mobility management in sensor networks," in *Proceedings of Workshops Proceeding of 2nd IEEE International Conference on Distributed Computing in Sensor Systems (DCOSS'06)*, San Francisco, California, 2006, p. 10, pages 131-140.
- [84] T. Sun, N.-C. Liang, L.-J. Chen, P.-C. Chen, and M. Gerla, "Evaluating mobility support in zigbee networks," in *EUC*, 2007, pp. 87–100.
- [85] T. Camp, J. Boleng, and V. Davies, "A survey of mobility models for ad hoc network research," *Wireless Communications and Mobile Computing (WCMC): Special issue on Mobile Ad Hoc Networking: Research, Trends and Applications*, vol. 2, pp. 483–502, 2002.
- [86] *BonnMotion - a mobility scenario generation and analysis tool*, University of Bonn, 2005, <http://www.cs.uni-bonn.de/IV/bomonet/BonnMotion.htm>.
- [87] V. Rajendran, K. Obraczka, and J. Garcia-Luna-Aceves, "Energy-Efficient, Collision-Free Medium Access Control for Wireless Sensor Networks," *Wireless Networks*, vol. 12, no. 1, pp. 63–78, 2006.
- [88] I. Chlamtac, A. Faragó, and H. Zhang, "Time-spread multiple-access (tsma) protocols for multihop mobile radio networks," *IEEE/ACM Trans. Netw.*, vol. 5, no. 6, pp. 804–812, 1997.
- [89] Y. Xu, J. Heidemann, and D. Estrin, "Geography-informed energy conservation for ad hoc routing," in *Proceedings of the ACM/IEEE International Conference on Mobile Computing and Networking*, USC/Information

- Sciences Institute. Rome, Italy: ACM, July 2001, pp. 70–84. [Online]. Available: <http://www.isi.edu/johnh/PAPERS/Xu01a.html>
- [90] H. Luo, F. Ye, J. Cheng, S. Lu, and L. Zhang, “Ttdd: two-tier data dissemination in large-scale wireless sensor networks,” *Wirel. Netw.*, vol. 11, no. 1-2, pp. 161–175, 2005.
 - [91] W. R. Heinzelman, J. Kulik, and H. Balakrishnan, “Adaptive protocols for information dissemination in wireless sensor networks,” in *MobiCom ’99: Proceedings of the 5th annual ACM/IEEE international conference on Mobile computing and networking*. New York, NY, USA: ACM, 1999, pp. 174–185.
 - [92] N. Baccour, A. Kouba, M. Jama, H. Youssef, M. Zuniga, and M. Alves, “A Comparative Simulation Study of Link Quality Estimators in Wireless Sensor Networks,” in *17th IEEE/ACM International Symposium on Modelling, Analysis and Simulation of Computer and Telecommunication Systems (MASCOTS’09)*, London, UK, 2009, pp. 21–23.
 - [93] “Zigbee alliance website, online at: <http://www.zigbee.org/en/index.asp>.”
 - [94] LAN/MAN Standards Committee of the IEEE Computer Society, *IEEE Standard for Information technology – Telecommunications and information exchange between systems – Local and metropolitan area networks – Specific requirements – Part 15.4: Wireless Medium Access Control (MAC) and Physical Layer (PHY) Specifications for Low Rate Wireless Personal Area Networks (LR-WPANs)*, Sep. 2006, revision of 2006.
 - [95] C. Karlof, N. Sastry, and D. Wagner, “Tinysec: a link layer security architecture for wireless sensor networks,” in *SenSys ’04: Proceedings of the 2nd international conference on Embedded networked sensor systems*. New York, NY, USA: ACM Press, 2004, pp. 162–175. [Online]. Available: <http://dx.doi.org/10.1145/1031495.1031515>
 - [96] L. Eschenauer and V. D. Gligor, “A key-management scheme for distributed sensor networks,” in *CCS ’02: Proceedings of the 9th ACM conference on Computer and communications security*. New York, NY, USA: ACM, 2002, pp. 41–47.
 - [97] S. Zhu, S. Setia, and S. Jajodia, “Leap+: Efficient security mechanisms for large-scale distributed sensor networks,” *ACM Trans. Sen. Netw.*, vol. 2, no. 4, pp. 500–528, 2006.

- [98] D. J. Malan, M. Welsh, and M. D. Smith, "Implementing public-key infrastructure for sensor networks," *ACM Transactions on Sensor Networks*, vol. 4, no. 4, pp. 1–23, 2008.
- [99] H. Chan, V. D. Gligor, A. Perrig, and G. Muralidharan, "On the distribution and revocation of cryptographic keys in sensor networks," *IEEE Trans. Dependable Secur. Comput.*, vol. 2, no. 3, pp. 233–247, 2005.
- [100] G. Dini and I. M. Savino, "S2rp: a secure and scalable rekeying protocol for wireless sensor networks," *Mobile Adhoc and Sensor Systems (MASS), 2006 IEEE International Conference on*, pp. 457–466, Oct. 2006.
- [101] K. Ghumman, "Location-aware combinatorial key management scheme for clustered sensor networks," *IEEE Transactions on Parallel and Distributed Systems*, vol. 17, no. 8, pp. 865–882, 2006, senior Member-Mohamed F. Younis and Senior Member-Mohamed Eltoweissy.
- [102] S. Rafaeli and D. Hutchison, "A Survey of Key Management for Secure Group Communication," *ACM Computing Surveys*, vol. 35, no. 3, pp. 309–329, September 2003.
- [103] L. Lamport, "Password authentication with insecure communication," *Communications of the ACM*, vol. 24, no. 11, pp. 770–772, November 1981.
- [104] A. Perrig, R. Szewczyk, V. Wen, D. Culler, and D. j. Tygar, "SPINS: Security protocols for sensor networks," in *Proceedings of the Seventh Annual International Conference on Mobile Computing and Networks*, Rome, Italy, July 16–21 2001, pp. 189–199.
- [105] D. Liu and P. Ning, "Multilevel μ tesla: Broadcast authentication for distributed sensor networks," *ACM Transaction on Embedded Computing Systems*, vol. 3, no. 4, pp. 800–836, 2004.
- [106] G. Anastasi, M. Conti, M. D. Francesco, and A. Passarella, "Energy conservation in wireless sensor networks: A survey," *Ad Hoc Netw.*, vol. 7, no. 3, pp. 537–568, 2009.
- [107] J. Yick, B. Mukherjee, and D. Ghosal, "Wireless sensor network survey," *Comput. Netw.*, vol. 52, no. 12, pp. 2292–2330, 2008.
- [108] V. Raghunathan, A. Kansal, J. Hsu, J. Friedman, and M. Srivastava, "Design considerations for solar energy harvesting wireless embedded systems," in *IPSN '05: Proceedings of the 4th international symposium on Information*

- processing in sensor networks*. Piscataway, NJ, USA: IEEE Press, 2005, p. 64.
- [109] A. Kansal, J. Hsu, S. Zahedi, and M. B. Srivastava, "Power management in energy harvesting sensor networks," *Trans. on Embedded Computing Sys.*, vol. 6, no. 4, p. 32, 2007.
 - [110] S. Roundy, D. Steingart, L. Frechette, P. Wright, and J. Rabaey, "Power sources for wireless sensor networks," *Wireless Sensor Networks*, pp. 1–17, 2004//. [Online]. Available: <http://www.springerlink.com/content/b0utgm8ahnphl13l>
 - [111] A. Hande, T. Polk, W. Walker, and D. Bhatia, "Indoor solar energy harvesting for sensor network router nodes," *Microprocess. Microsyst.*, vol. 31, no. 6, pp. 420–432, 2007.
 - [112] C. Park and P. Chou, "Ambimax: Autonomous energy harvesting platform for multi-supply wireless sensor nodes," vol. 1, Sept. 2006, pp. 168–177.
 - [113] P. H. Chou and C. Park, "Energy-efficient platform designs for real-world wireless sensing applications," in *ICCAD '05: Proceedings of the 2005 IEEE/ACM International conference on Computer-aided design*. Washington, DC, USA: IEEE Computer Society, 2005, pp. 913–920.
 - [114] R. Morais, S. G. Matos, M. A. Fernandes, A. L. G. Valente, S. F. S. P. Soares, P. J. S. G. Ferreira, and M. J. C. S. Reis, "Sun, wind and water flow as energy supply for small stationary data acquisition platforms," *Comput. Electron. Agric.*, vol. 64, no. 2, pp. 120–132, 2008.
 - [115] P. Mitcheson, E. Yeatman, G. Rao, A. Holmes, and T. Green, "Energy harvesting from human and machine motion for wireless electronic devices," *Proceedings of the IEEE*, vol. 96, no. 9, pp. 1457–1486, Sept. 2008.
 - [116] M. Renaud, P. Fiorini, R. van Schaijk, and C. van Hoof, "Harvesting energy from the motion of human limbs: the design and analysis of an impact-based piezoelectric generator," *Smart Material Structures*, vol. 18, no. 3, pp. 035 001–+, Mar. 2009.
 - [117] V. Leonov, T. Torfs, P. Fiorini, and C. Van Hoof, "Thermoelectric converters of human warmth for self-powered wireless sensor nodes," *Sensors Journal, IEEE*, vol. 7, no. 5, pp. 650–657, 2007. [Online]. Available: http://ieeexplore.ieee.org/xpls/abs_all.jsp?arnumber=4154682

- [118] G. J. Snyder and E. S. Toberer, "Complex thermoelectric materials," *Nature Materials*, vol. 7, pp. 105–114, Feb. 2008.
- [119] Z. Wang, V. Leonov, P. Fiorini, and C. Van Hoof, "Micromachined thermopiles for energy scavenging on human body," June 2007, pp. 911–914.
- [120] L. Paradis and Q. Han, "A survey of fault management in wireless sensor networks," *J. Netw. Syst. Manage.*, vol. 15, no. 2, pp. 171–190, 2007.
- [121] R. Roman, C. Alcaraz, and J. Lopez, "A survey of cryptographic primitives and implementations for hardware-constrained sensor network nodes," *Mob. Netw. Appl.*, vol. 12, no. 4, pp. 231–244, 2007.
- [122] A. Cilardo, L. Coppolino, N. Mazzocca, and L. Romano, "Elliptic curve cryptography engineering," *Proceedings of the IEEE*, vol. 94, no. 2, pp. 395–406, Feb. 2006.
- [123] C. Karlof and D. Wagner, "Secure routing in wireless sensor networks: Attacks and countermeasures," in *In First IEEE International Workshop on Sensor Network Protocols and Applications*, 2003, pp. 113–127.
- [124] J. Deng, R. Han, and S. Mishra, "Insens: Intrusion-tolerant routing for wireless sensor networks," *Computer Communications*, vol. 29, no. 2, pp. 216–230, January 2006.
- [125] B. Przydatek, D. Song, and A. Perrig, "Sia: secure information aggregation in sensor networks," in *SenSys '03: Proceedings of the 1st international conference on Embedded networked sensor systems*. New York, NY, USA: ACM, 2003, pp. 255–265.
- [126] T. Park and K. G. Shin, "Soft tamper-proofing via program integrity verification in wireless sensor networks," *Mobile Computing, IEEE Transactions on*, vol. 4, no. 3, pp. 297–309, 2005. [Online]. Available: http://ieeexplore.ieee.org/xpls/abs_all.jsp?arnumber=1413187
- [127] A. Seshadri, M. Luk, A. Perrig, L. van Doorn, and P. Khosla, "Scuba: Secure code update by attestation in sensor networks," in *WiSe '06: Proceedings of the 5th ACM workshop on Wireless security*. New York, NY, USA: ACM, 2006, pp. 85–94.
- [128] Z. Shen and J. P. Thomas, "Security and qos self-optimization in mobile ad hoc networks," *IEEE Transactions on Mobile Computing*, vol. 7, no. 9, pp. 1138–1151, 2008.

- [129] T. Pazynyuk, J. Li, G. S. Oreku, and L. Pan, “Qos as means of providing wsns security,” in *ICN '08: Proceedings of the Seventh International Conference on Networking (icn 2008)*. Washington, DC, USA: IEEE Computer Society, 2008, pp. 66–71.
- [130] M. Johnson and F. Stajano, “Usability of security management: Defining the permissions of guests,” in *Proceedings of the 14th Security Protocols Workshop*, Cambridge (UK), 2006.